FACTORS LEADING TO THE FORMATION OF ARC CLOUD COMPLEXES

Mark John Welshinger
and
Kenneth C. Brundidge

Texas A&M University
College Station, Texas

Prepared for George C. Marshall Space Flight Center

under Contract NAG8-043

ABSTRACT

Factors leading to the formation of arc cloud complexes

A total of 12 mesoscale convective systems (MCSs) were investigated. The duration of the gust front, produced by each MCS, was used to classify the MCSs. Category 1 MCSs were defined as ones that produced a gust front and the gust front lasted for more than 6 h. There were seven category 1 MCSs in the sample. Category 2 MCSs were defined as ones that produced a gust front and the gust front lasted for 6 h or less. There were four category 2 MCSs. The MCS of Case 12 was not categorized because the precipitation characteristics were similar to a squall line, rather than an MCS. All of the category 1 MCSs produced arc cloud complexes (ACCs), while only one of the category 2 MCSs produced an ACC. To determine if there were any differences in the characteristics between the MCSs of the two categories, composite analyses were accomplished. The analyses showed that there were significant differences in the characteristics of category 1 and 2 MCSs. Category 1 MCSs, on average, had higher thunderstorm heights, greater precipitation intensities, colder cloud top temperatures and produced larger magnitudes of surface divergence than category 2 MCSs. It was deduced that the more pronounced characteristics of category 1 MCSs played an important role in the conversion of an MCS to an ACC.

ACKNOWLEDGMENTS

The authors thank Dr. Aylmer H. Thompson, whose helpful comments aided tremendously in the preparation of this report. Mrs. Jacquelyn V. Strong typed the manuscript.

The National Aeronautics and Space Administration sponsored this research through Contract NAG8-043 under the auspices of the Atmospheric Sciences Division, Space Sciences Laboratory, Marshall Space Flight Center. Special thanks are extended to Mr. Paul Meyer for his assistance in procuring satellite images and other data through the McIDAS system at the Marshall Space Flight Center.

TABLE OF CONTENTS

LIST OF TABLES

LIST OF FIGURES

LIST OF FIGURES (Continued)

LIST OF FIGURES (Continued)

CHAPTER I

INTRODUCTION

Since the launch of the first operational weather satellite in February 1966 (Schnapf, 1982), satellite observations and interpretation have become increasingly important in the areas of weather research and operational forecasting. One reason is that geostationary satellite imagery is the only meteorological observing tool that can follow the evolution of clouds from the synoptic scale down to the cumulus scale. Therefore, it can depict atmospheric activity which is up to two orders of magnitude smaller than can be resolved by conventional meteorological observations. This unique ability of the satellite provides the meteorologist a mechanism to infer weather events down to the mesoscale.

A well-known phenomenon which occurs as a thunderstorm propagates past a station is the rise and oscillation of the surface pressure. Downdrafts descending from thunderstorm cells are the source of the air forming the cold dome over the ground, which leads to the rise in surface pressure (Byers and Braham, 1949; Fujita, 1959, 1963). If the downdrafts of cold air are strong enough and last for a sufficient time, an organized high pressure system develops at the surface. This high pressure system is called the "mesohigh."

Purdom (1973), using satellite imagery, showed that the leading edge of a mesohigh appeared as an arc-shaped line of convective clouds moving out in all directions from a dissipating thunderstorm area. The

---

The citations on the following pages follow the style of the Journal of the Atmospheric Sciences.

arc-shaped cloud line, normally composed of cumulus, cumulus congestus, or cumulonimbus clouds, has been named the "arc cloud" (Purdom, 1973, 1976, 1979). As the leading edge of the cold air spreads outward from the storm area, it undercuts and lifts the warmer, moister air ahead of it and the arc cloud is formed.

In many ways, the structure of the leading edge of the cold air associated with the arc cloud (also referred to as the mesoscale outflow boundary) resembles a true cold front. Byers and Braham (1948) remarked that the "air mass discontinuity acts as a miniature cold front and that the movement of this pseudofront has a marked influence on the initial formation of new cells." Normally, abrupt changes in wind direction and speed, called the gust front, rapid cooling and rising pressure, sometimes called the density surge line (Sinclair and Purdom, 1982, 1984), pressure surge line (Fujita, 1955), or pressure jump line (Tepper, 1950a), accompany the passage of the outflow boundary.

Large, long-lived convective weather systems are most commonly referred to as mesoscale convective systems (MCSs). Maddox (1980) has described a specific type of MCS which he has named the "mesoscale convective complex." The definition is presented in Table 1. The definition is based on the areal extent and duration of specific cloud top temperatures observed in enhanced Geostationary Operational Environmental Satellite (GOES) infrared (IR) imagery.

The MCC, an organized meso-α scale convective system (Orlanski, 1975), is nocturnal in nature and occurs most frequently during the warm season months, March through September (Maddox, 1980; Maddox et al., 1982; Rodgers et al., 1983; Rodgers et al., 1985). Maddox surmises that

Table 1. Mesoscale convective complex (MCC) definition. The definition is based upon analysis of enhanced IR satellite imagery (after Maddox, 1980).

	Physical Characteristics
Size:	A. Cloud shield with IR temperature less than or equal to -32°C must have an area greater than or equal to 100,000 km^2.
	B. Interior cold cloud region with temperature less than or equal to -52°C must have an area greater than or equal to 50,000 km^2.
Initiate:	Size definitions A and B first satisfied.
Duration:	Size definitions A and B must be met for a period greater than or equal to 6 h.
Maximum extent:	Contiguous cold cloud shield (IR temperature less than or equal to -32°C) reaches maximum size.
Shape:	Eccentricity (minor axis/major axis) greater than or equal to 0.7 at time of maximum extent.
Terminate:	Size definitions A and B no longer satisfied.

during the genesis stage MCCs entrain mid-level, potentially cool environmental air, which produces strong, evaporationally-driven downdrafts, surface mesohighs and outflow boundaries. Similar results were obtained by Zipser (1969) in his study of a tropical convective system which developed during the Line Islands Experiment. Zipser concluded that the evaporationally-driven downdrafts had mid-tropospheric origins, somewhere between 60 kPa and 40 kPa, where environmental air of equivalent potential temperature similar to that at the surface was located.

In the development stage of an MCC, a merging of the mesohighs of individual thunderstorms produces a single large mesohigh. Vertical motions along the forward edge of the spreading, cooler air generate the arc cloud. However, the arc cloud is on a larger time and space scale than the gust front for an individual thunderstorm. The large mesohigh and surrounding arc cloud have been collectively termed an arc cloud complex (ACC) by Brundidge (1983).

The dissipation stage of the MCC is characterized by a rapid demise of the intense convection. One reason Maddox (1980) gives for the dissipation is that "the cold air dome beneath the system may become so intense that the surface convergence zone moves away from the region of mean mesoscale ascent into a region of mid- and upper-level sibsidence."

ACCs can last for many hours. Even after the demise of the MCC (or more generally the MCS), the cool air and outflow boundary may still be evident. As Maddox (1980) states, "Although the MCC rapidly loses its meso-α scale organization, the cool air and outflow boundary at the surface may persist for many hours." Sinclair and Purdom (1982) believe that the regeneration of weak precipitation along portions of the arc,

coupled with sub-cloud evaporation is one explanation for an arc cloud line being able to maintain its identity as a single feature for several hours.

Because of the long life-span of some ACCs, a chain of storm events often occurs, leading to the formation of other MCSs. Miller (1984), in a case study of an ACC, found convection along the arc cloud at different times during its life, which eventually resulted in the formation of an MCS much larger than the ACC. Bartels (1983), in a study of a dual MCC, showed that an outflow boundary associated with the western MCC was related to an MCC type system that developed over Oklahoma during the following afternoon.

Fritsch et al. (1981) showed that MCCs produce widespread regions of measureable rainfall and that they account for a significant portion of growing-season rainfall over much of the United States' corn and wheat belts. Maddox (1980) stated that many MCCs produce locally intense rainfalls and flash flooding. In Bartels' (1983) study, rains from the western MCC resulted in flash flooding. Evacuations were required in Springfield, MO and Joplin, MO, as some homes had water 3 ft deep. Since ACCs can develop into new MCCs, the ACC can be related to the occurrence of flash floods.

ACCs are often the forerunners of severe weather. Tepper (1950b) reported a case of tornado formation at the intersection of two pressure jump lines. Fujita (1963) and Miller (1972) stress the importance of intersecting boundaries, stating that these areas are favored locations for severe weather development. Using satellite imagery, Purdom (1974) showed that the intersection of an arc cloud with other existing

boundaries locates an area for new convection to develop. If atmospheric conditions are favorable, severe weather often forms at the point of intersection.

As well as the increased threat of severe weather, the ACC is a dangerous source of potential aircraft accidents (Greene, 1977). In an observational study of outflow boundaries, Goff (1976) found a wide variation between one gust front case and another. However, the updrafts along the gust front were generally concentrated in a region a few kilometers wide, with vertical motions as high as 6 to 7 m s^{-1}. Sinclair and Purdom (1984) found similar vertical motions during aircraft penetrations of the density surge line (DSL). They found upward vertical motion, with peaks as high as 10 m s^{-1}, at the DSL interface region. Between 2 and 7 km behind the DSL, a distinct transition was found from upward to downward vertical motions. Vertical motions in the sinking air ranged from -3 to -3 m s^{-1}. Therefore, if an aircraft were on final approach and encountered an outflow boundary, the extreme change in vertical motions over such a short distance across the DSL might lead to an aircraft accident (Sinclair and Purdom, 1984).

In summary, the importance of ACCs is that they can develop into new MCSs, they can be associated with the initiation of severe weather and their associated wind shear can lead to potential aircraft mishaps. The study of ACCs must include detailed studies of the entity which produces them, namely, MCSs, if our ability to forecast their occurrence is to improve. It is well-known that some MCSs produce well-defined, extremely-potent ACCs, whils others do not. What characteristics are different in MCSs that produce ACCs compared to the MCSs that yield no

ACC?

Byers and Braham (1948) showed that rain at the surface was in the downdraft area of thunderstorm cells. They also showed that the maximum intensity of rain at the surface and the maximum intensity of associated surface divergence have a very high correlation (see Fig. 1). That is, an area of heavy rain at the surface coincides with an area of strong divergence in the surface winds. The divergence is caused by the downdrafts spreading out across the ground.

In a case study of three ACCs, Brundidge (1984) hypothesized that the appearance of the arc cloud is a direct result of heavy rainfall on the south side of an MCS. This agrees with the findings of Byers and Braham (1948). From their findings, it logically follows that heavy precipitation can create strong downdrafts and subsequently a strong gust front and mesohigh. The presence of the gust front and mesohigh, in turn, is revealed in the magnitude of the surface divergence and the pattern of the surface divergence field. Therefore, heavy precipitation on the south side of an MCS can create strong downdrafts, which lead to a strong gust front and mesohigh, and eventually an arc cloud forms along the leading edge of the gust front.

Woodley et al. (1972), in their study of rainfall estimation from satellite cloud photographs, discovered several important facts about rain clouds. Two facts pertinent to this study are:

1. Clouds with cold tops in the IR imagery produce more rainfall than those with warmer tops.

2. The highest and coldest clouds form where the thunderstorms are most vigorous and the rain heaviest.

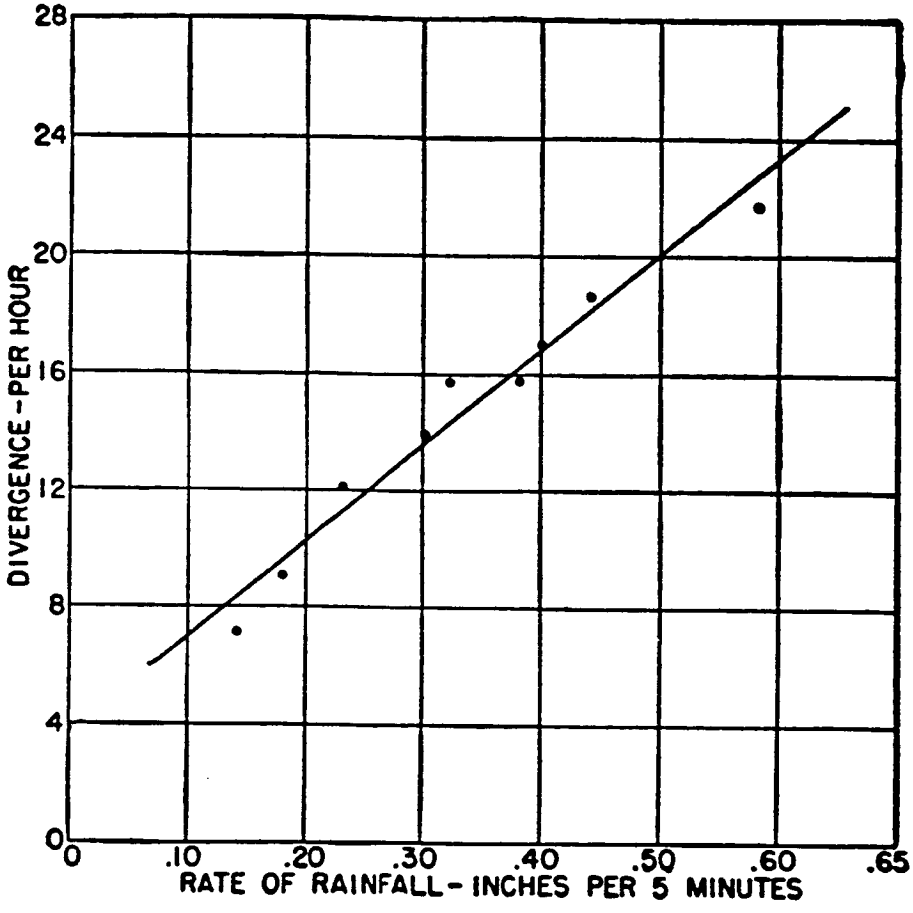

Fig. 1. Relationship between maximum intensity of rain and the maximum intensity of associated surface divergence. The line through the scatter of points is the linear regression line for the distribution. The correlation coefficient is 0.98 (after Byers and Braham, 1949).

Gagin et al. (1985) attempted to provide a comprehensive formulation of the dependence between the depth of the convective cells and their gross precipitation features. In their study, they concluded that taller cells produce larger total rain volumes by virtue of their greater rainfall intensities, their longer duration as precipitating entities and their larger precipitating areas.

Based on the studies cited above, it appears that precipitation patterns and rates, cloud top temperatures, thunderstorm heights and surface divergence patterns are interrelated and seem to play an important role for the conversion of an MCS to an ACC. It has been the purpose of this study to compare these features between MCSs that become ACCs and ones that do not. Research of this type will enable us to understand better the occurrence of ACCs and may provide the signatures manifested in satellite and radar observations which would permit forecasting the development of significant arc clouds.

CHAPTER II

RESEARCH PROCEDURES

Products Used in the Study

Several products and sources of information were used to aid in this investigation of arc cloud complexes. These were as follows:

1. The records of hourly precipitation from the climatological networks of raingauges obtained from the National Climatic Data Center (NCDC) located in Asheville, North Carolina. Figs. 2-10 show the locations by states of the various raingauges used in this study. The data received from the NCDC were plotted and analyzed on the state maps to determine patterns and rates of rainfall.

2. Sectional surface maps corresponding to the time and location of the MCSs were plotted and analyzed. Patterns in the temperature, pressure and wind fields helped ascertain the existence and strength of gust fronts.

3. Hourly radar summary charts from the National Weather Service (NWS) were used to provide comparisons of the precipitation pattern at the surface among the various MCSs. They also were used to obtain the maximum thunderstorm height, within the MCS, which occurred at the radar observation time (normally 35 min past each hour).

4. GOES imagery was used for:

    a. An aid in determining the existence of an arc cloud.

    b. Determining the duration of the arc cloud, if one existed. This aided in the classification of the MCS. The classifications of the MCSs will be discussed later.

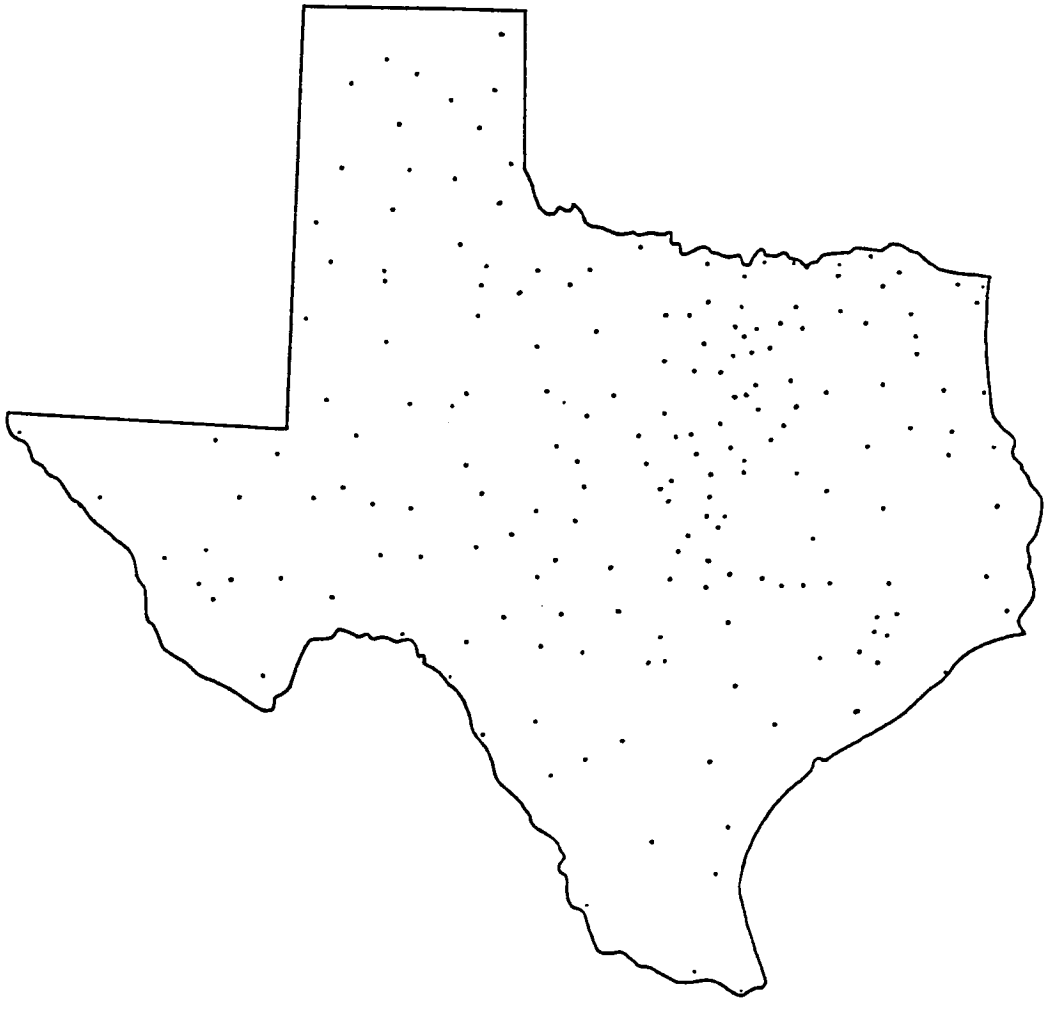

Fig. 2. Location of the climatological raingauge network in Texas.

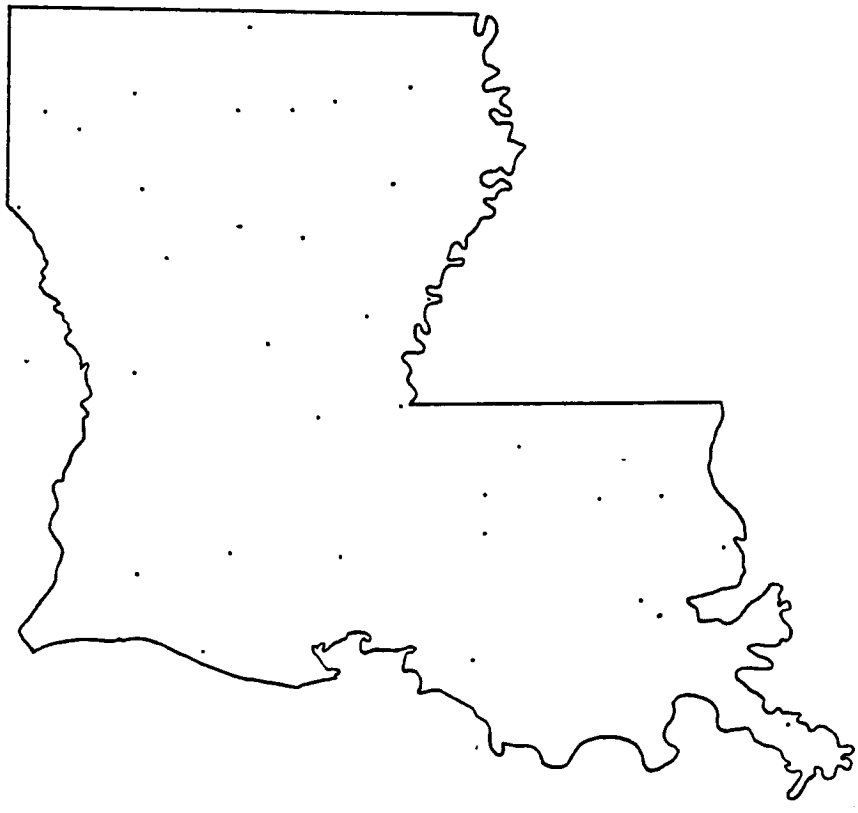

Fig. 3. Location of the climatological raingauge network in Louisiana.

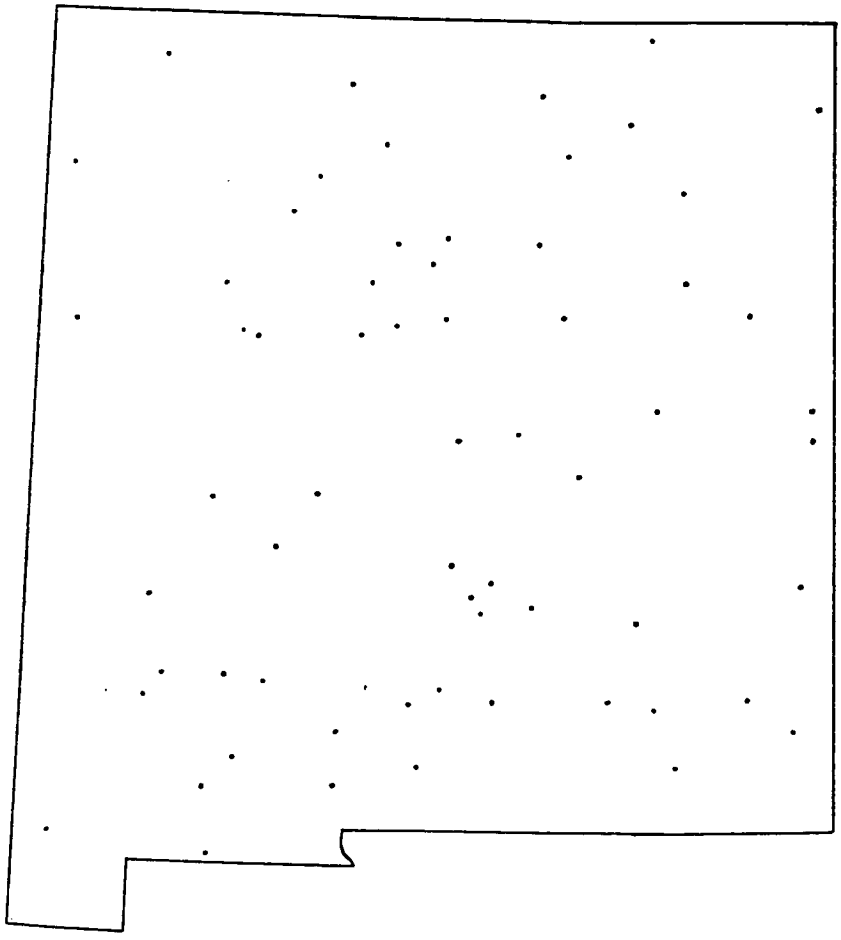

Fig. 4. Location of the climatological raingauge network in New Mexico.

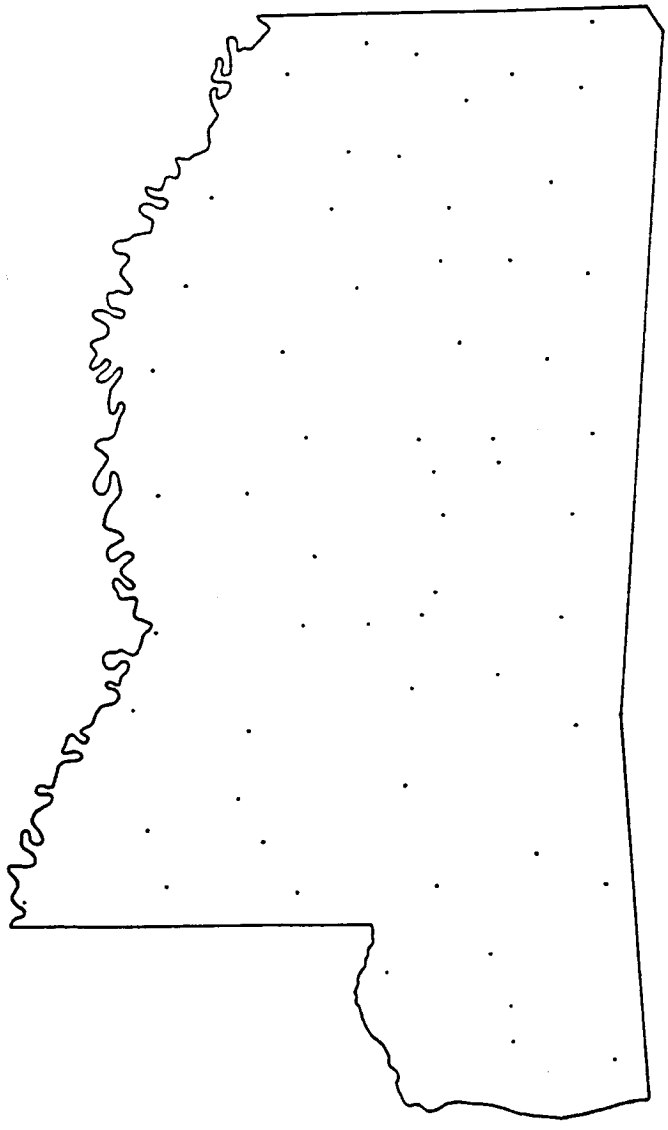

Fig. 5. Location of the climatological raingauge network in Mississippi.

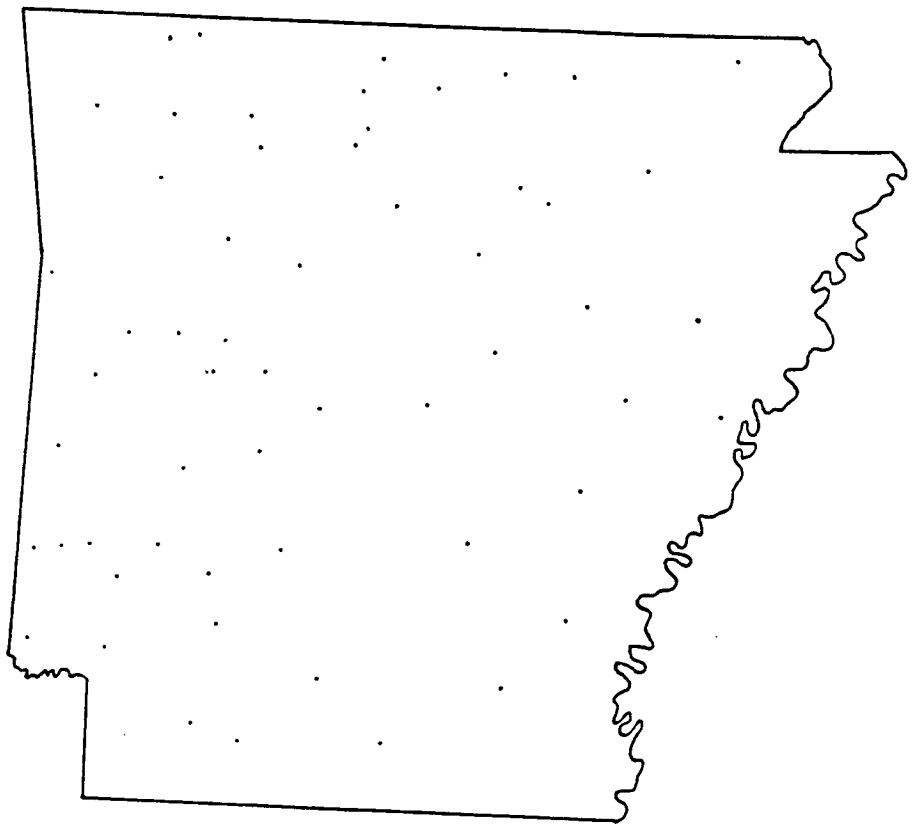

Fig. 6. Location of the climatological raingauge network in Arkansas.

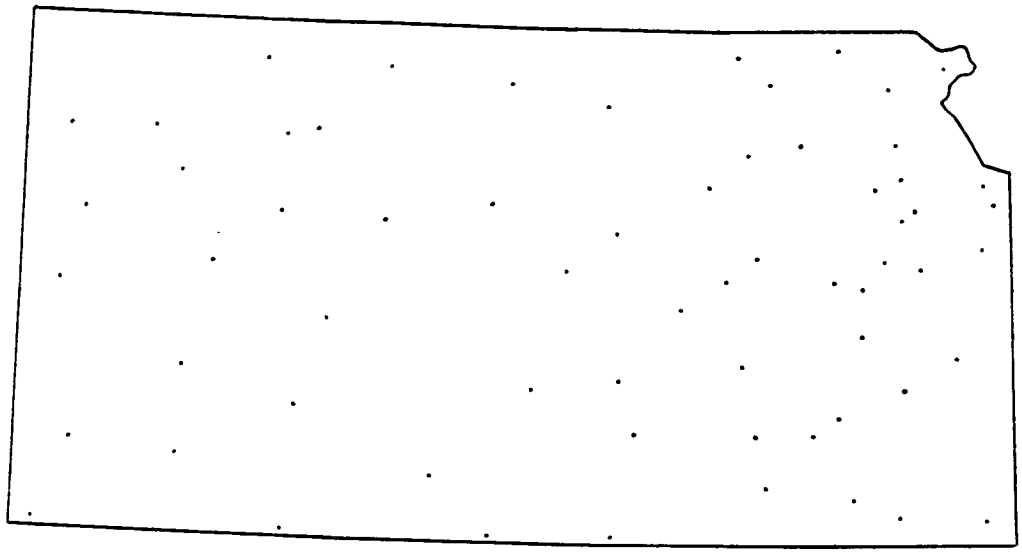

Fig. 7. Location of the climatological raingauge network in Kansas.

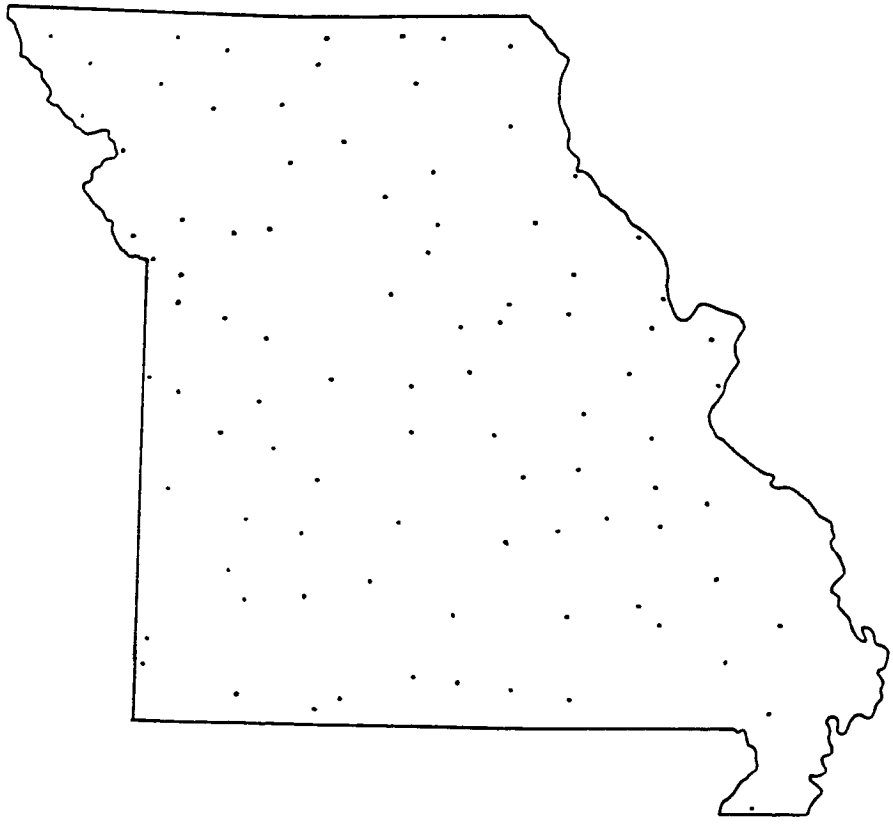

Fig. 8. Location of the climatological raingauge network in Missouri.

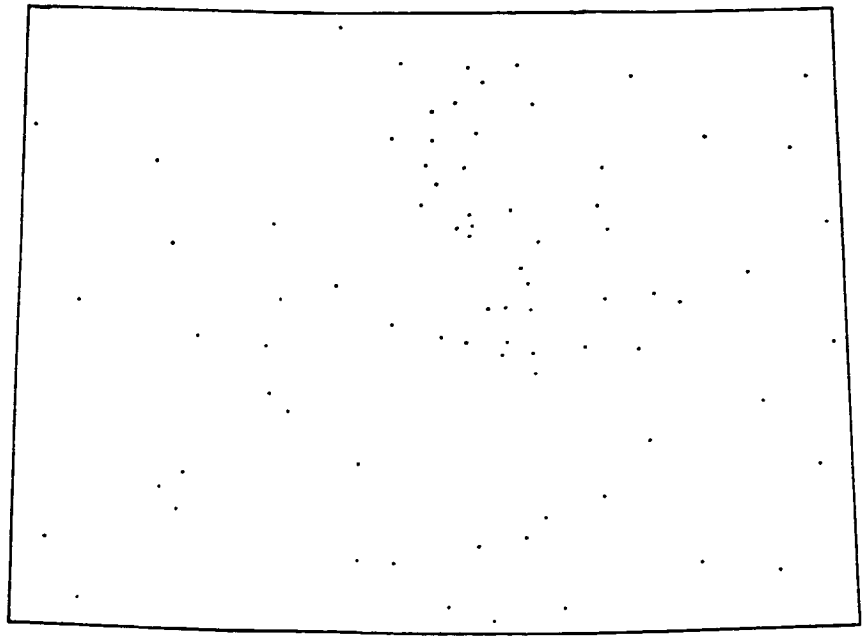

Fig. 9. Location of the climatological raingauge network in Colorado.

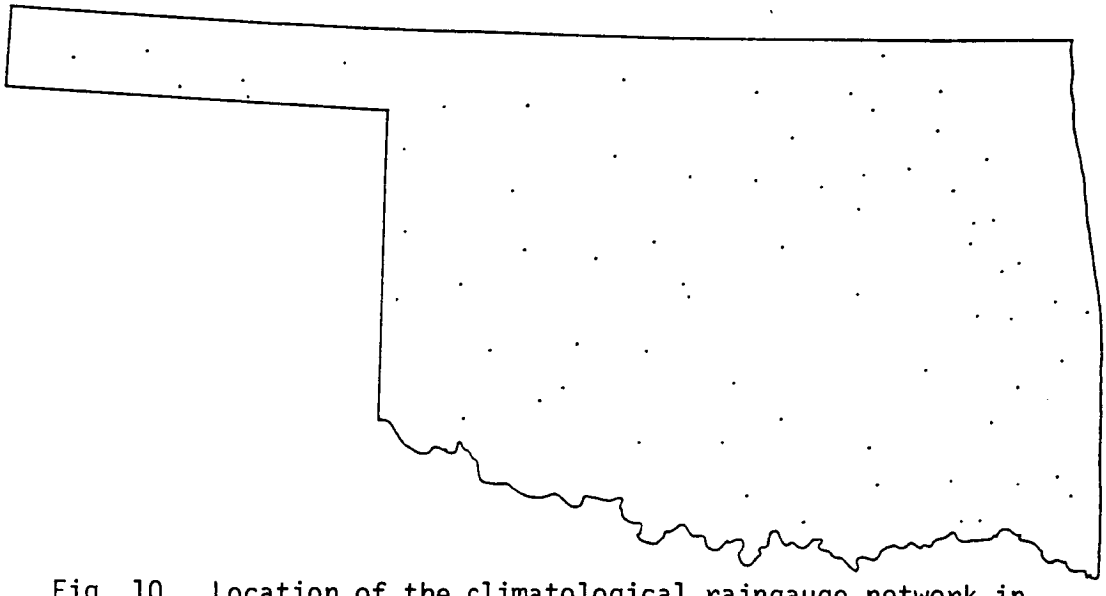

Fig. 10. Location of the climatological raingauge network in Oklahoma.

5. The Man-Computer Interactive Data Access System (McIDAS) of the Atmospheric Sciences Division of the Systems Dynamic Laboratory, Marshall Space Flight Center, provided the following products:

a. Hourly surface divergence patterns.[1]

b. Hourly contoured analysis of the cloud top temperatures as determined from the GOES IR imagery.[1]

c. Hourly surface equivalent potential temperature analysis.[1]

d. Additional satellite images.

e. A computer printout, on an hourly basis, of the size of the MCS as it appears in the satellite IR imagery. The size is referenced to the number of pixels that are contained within four specific temperature ranges: -32°C to -98°C; -52°C to -98°C; -58°C to -98°C; -62°C to -98°C.

Overview

A total of 12 cases was chosen for this study. Three publications were primarily used in selecting the various cases (Maddox et al., 1982; Rodgers et al., 1983, 1985). These articles were annual summaries of the times and locations of MCCs that occurred during 1981, 1982 and 1983. The MCSs that were chosen were studied by Brundidge (1983, 1984) and Miller (1984) and were known to produce ACCs. The cases that were finally included in this study are listed in Table 2. Also, dates and details of the life cycles of each event are listed. Of the cases selected, most of the MCSs originate or terminate in Texas. This

[1]The analysis and contours by the McIDAS are computer products obtained objectively by use of the Barnes (1973) interpolation scheme.

Table 2. Mesoscale convective systems (MCSs) included in study. Initiate and terminate times are after Maddox et al., 1982; Rodgers et al., 1983, 1985.

Case number	Date	Time (GMT)		
		Initiate	Maximum extent**	Terminate
1	10/11 Apr 81	2315/10	0300/11	0531/11
2	9 May 81	0115/09	0500/09	1015/09
3	27 May 81	0515/27	1000/27	1400/27
4	17 May 82	0030/17	0400/17	0730/17
5	19 May 82	*	0900/19	*
6	10/11 Jun 82	2245/10	0700/11	1530/11
7	26 Jun 82	*	1100/26	*
8	27 Jun 82	0800/27	0900/27	1400/27
9	28/29 Jun 82	2230/28	0200/29	0430/29
10	20 May 83	0130/20	0800/20	1300/20
11	11 Jun 83	0530/11	0900/11	1200/11
12	14 Jun 83	0130/14	0600/14	1600/14

*These cases were not MCCs; therefore, initiate and terminate times were not available.

**The times listed are the maximum extent of the area, as depicted on IR satellite imagery, with temperatures $\leq$ -62°C. This information was determined by the use of McIDAS.

stipulation was employed because of the denser climatological rainguage network in Texas, compared to the other states (see Figs. 2-10).

Each case was carefully analyzed to determine if a gust front existed. Hourly surface maps, hourly surface divergence patterns provided by the McIDAS and satellite pictures, both visual and IR, were used to determine the existence and duration of a gust front.

The various MCSs were then categorized as follows:

1. MCS produces gust front and the gust front persists more than 6 h. This is referred to as a category 1 MCS.

2. MCS produces gust front and the gust front persists for 6 h or less. This is referred to as a category 2 MCS.

After the cases were categorized, each case was further analyzed for the following characteristics associated with the MCS:

1. Maximum hourly surface divergence.

2. Coldest hourly cloud top temperature.

3. Maximum hourly point precipitation rates.

4. Sum of the three largest hourly precipitation rates. An explanation of this analysis procedure is as follows. Assume an MCS produced the following rainfall rates, for a particular hour, at six climatological rainguage sites: 0.8, 2.2, 1.5, 0.3, 1.7 and 2.0 in h^{-1}. The sum of the three largest precipitation rates, for this hour, would be 2.2 + 2.0 + 1.7 = 5.9 in h^{-1}. By using this analysis technique, an areal coverage of the heavy precipitation is inferred, rather than just at a single point.

5. Maximum hourly thunderstorm height.

Finally, composite analyses of the five characteristics were

accomplished for each category. The composites were used to determine significant differences between the categories. The differences suggested some possible causative factors that aid in the formation of ACCs.

CHAPTER III

DIVISION OF MCSs INTO CATEGORIES

Category 1 MCSs

Category 1 MCSs are defined as follows: The MCS produces a gust front and the gust front persists more than 6 h. Seven MCSs are classified in this category. The seven MCSs are from Cases 2, 3, 4, 7, 8, 10 and 11. A brief discussion of the synoptic situation and storm characteristics associated with each category 1 MCS follows.

Case 2: 9 May 1981

During the late afternoon of 8 May 1981, a cluster of thunderstorms developed over north central Texas. By 0115 GMT 9 May 1981, the cluster of storms had conglomerated and an MCC was initiated. Fig. 11 shows the 50 kPa analysis for 1200 GMT 9 May 1981. A short-wave trough extended through the central United States. This flow pattern had contributed to the production of the MCC. The precipitation pattern at 0235 GMT is depicted in the NWS radar summary chart (Fig. 12). The large precipitation area in north central Texas, associated with the MCC, developed on the north side of a warm front. The warm front was evident in the 0300 GMT surface θ_e analysis, which was obtained by use of the McIDAS. The tight gradient of the θ_e isolines in northern Texas, indicating the presence of the warm front, is shown in Fig. 13.

By 0500 GMT, a mesohigh and strong gust front first appeared in the surface pressure analysis (not shown). The gust front was located in northeastern Texas and was moving southeast. As it passed Shreveport,

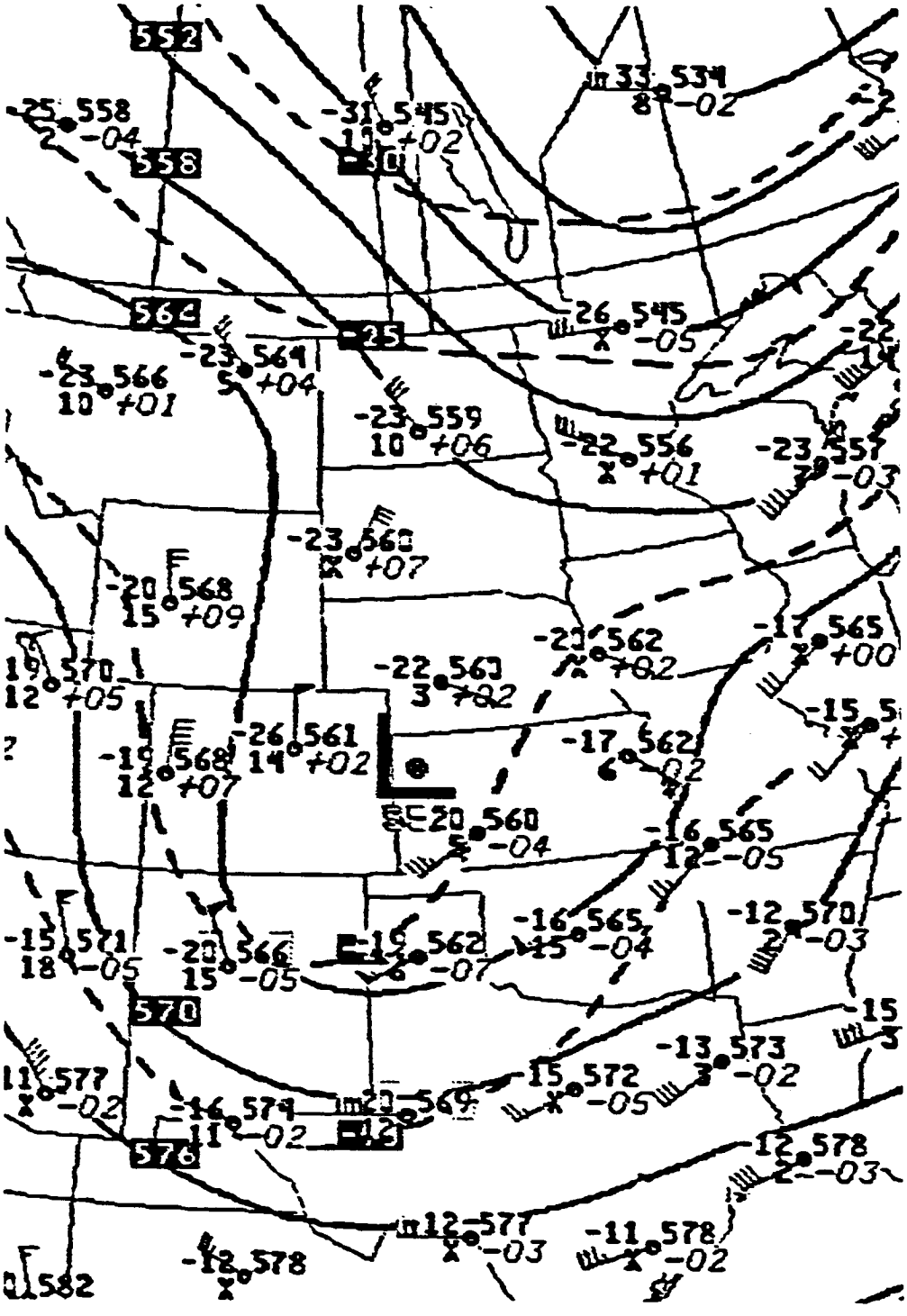

Fig. 11. 50 kPa height (dm) and temperature (°C) fields for 1200 GMT 9 May 1981. Height contours (solid lines) are every 60 m; isotherms (dashed lines) are every 5°C.

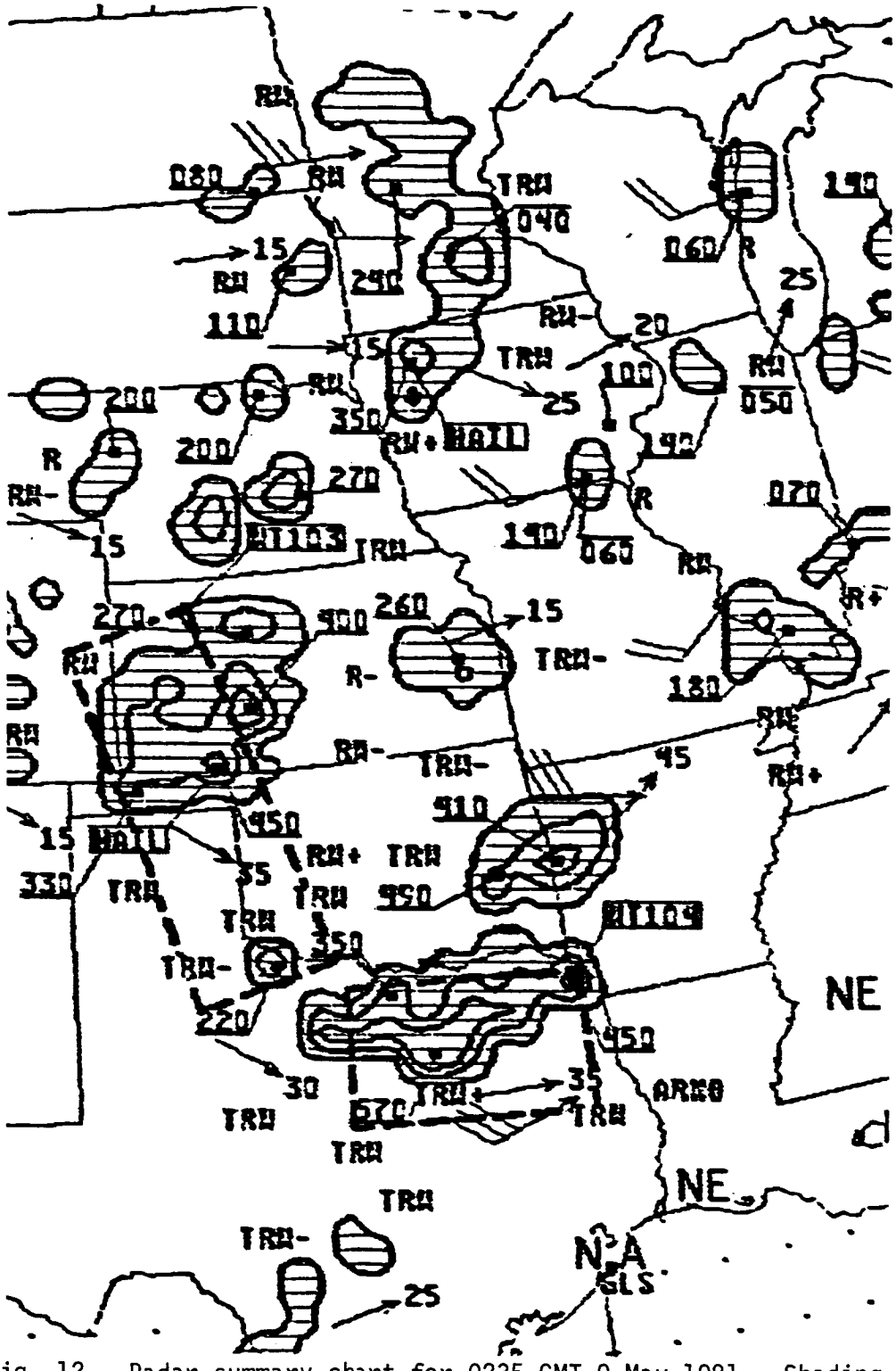

Fig. 12. Radar summary chart for 0235 GMT 9 May 1981. Shading indicates echo areas. Contours at echo intensities 1, 3, and 5; echo heights are in hundreds of feet; cell movement given at end of arrows in knots; area and line movement given by pennant with full barb = 10 kt.

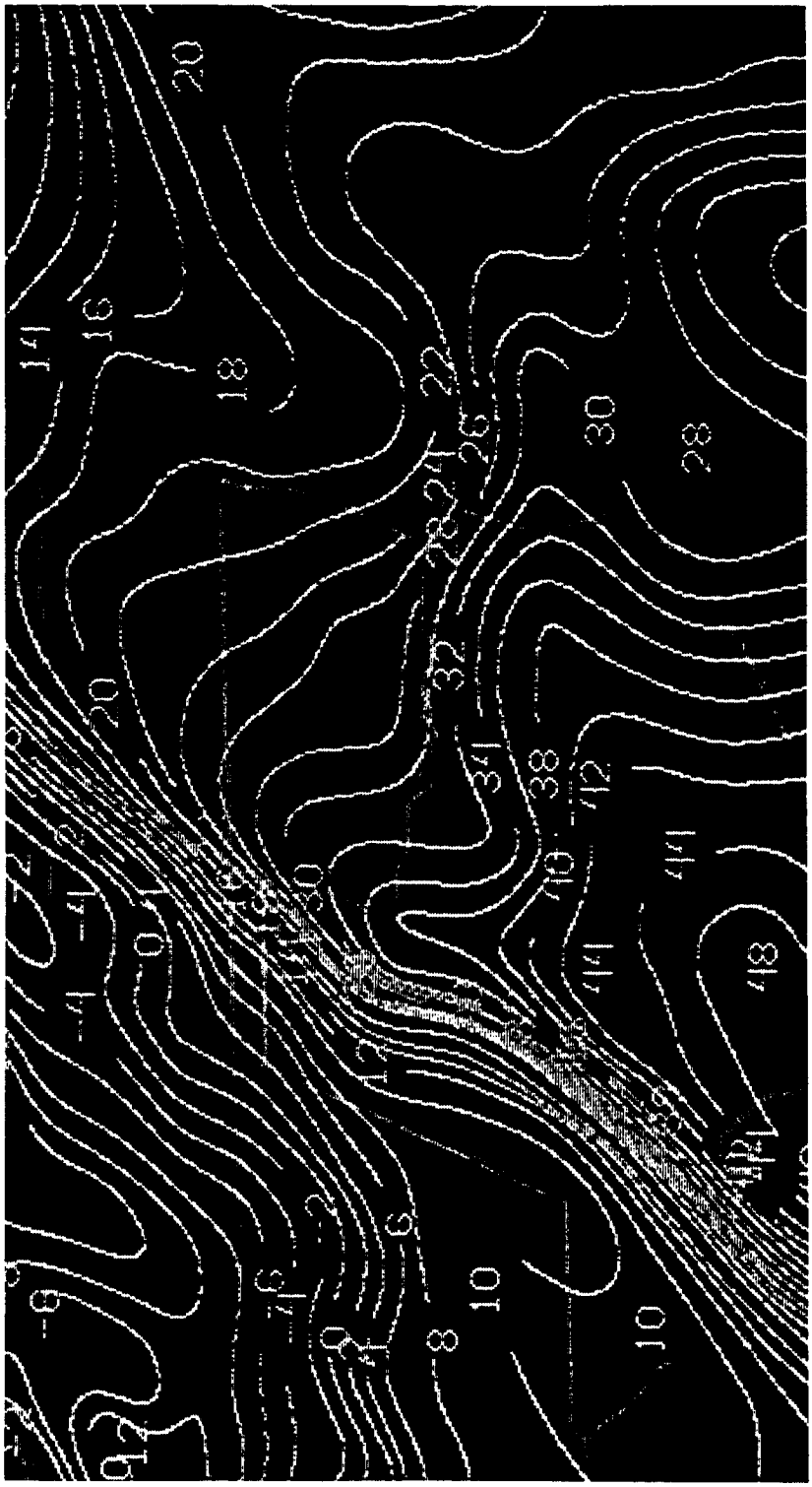

Fig. 13. Surface θ_e (°C) field for 0300 GMT 9 May 1981.

LA (SHV), a peak wind of 35 kt was recorded (0723 GMT). The strong, gusty wind was one of the indicators that the gust front was quite powerful. Even near termination of the MCC, at 1000 GMT, a strong meso-high and gust front were still evident in the surface pressure analysis (see Fig. 14). Since the pressures to the rear of the gust front were higher than the environmental pressures ahead of it, the gust front would be expected to remain quite active (Miller, 1972). In fact, the 1300 GMT visible satellite image, shown in Fig. 15, still showed evidence of the gust front and mesohigh. Convection had formed along the leading edge of the gust front in southern Louisiana, while subsidence associated with the mesohigh had created partial clearing in central Louisiana.

The characteristics associated with this MCC were very pronounced and are shown in Table 3. In the few hours after the initiation of the MCC (the initiation of the MCC was 0115 GMT), the maximum hourly thunderstorm heights were quite impressive. The heights from 0135 GMT to 0535 GMT, were 60,000, 57,000, 55,000, 55,000, and 53,000 ft, respectively. The hourly surface divergence remained large after the maximum extent of the MCC. In fact, the largest magnitude of the surface divergence was reached at 0800 GMT (3×10^{-5} s^{-1}), 3 h after the maximum extent of the MCC. The maximum sum of the three largest hourly point precipitation rates was 5.96 in h^{-1}. Similarily, the largest hourly maximum point precipitation rate was 2.2 in h^{-1}. Of particular interest, is the fact that the sum of the three largest hourly point precipitation rates, stayed above 1.5 in h^{-1} for eight consecutive hours. The coldest hourly cloud top temperatures, during the few hours after

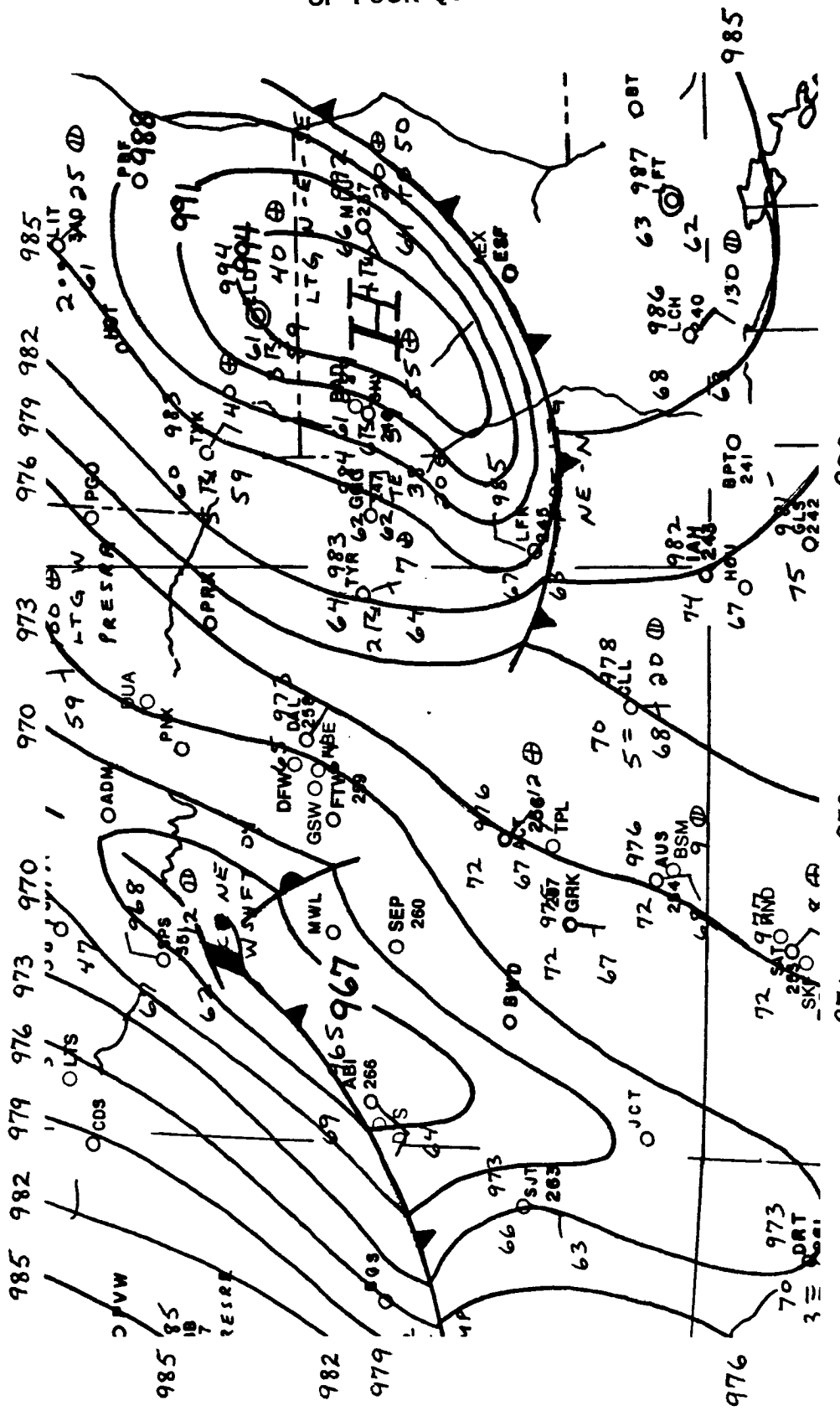

Fig. 14. Surface pressure field for 1000 GMT 9 May 1981. Altimeter setting contours are every 0.03 in Hg. The gust front, located in eastern Texas and central Louisiana, is denoted by a cold front symbol. Note: 982 corresponds to an altimeter setting of 29.82 in Hg.

Fig. 15. GOES visible image for 1300 GMT 9 May 1981.

Table 3. Characteristics associated with the MCC of Case 2 (8/9 May 1981). The maximum thunderstorm heights were determined at approximately 35 min past each hour. Dashes indicate that the parameter was not determined.

Time (GMT)	Maximum thunderstorm height (x 100 ft)	Maximum surface divergence (x 10^{-5} s^{-1})	Sum of the three largest precipitation rates (in h^{-1})	Maximum point precipitation rate (in h^{-1})	Coldest cloud top temperature (°C)
2300		-	-	-	-
	540				
0000		-	0.66	0.40	-
	550				
0100		-	2.50	1.30	-
	600				
0200		1	5.00	1.50	-63
	570				
0300		1	3.05	1.25	-63
	550				
0400		1	5.96	2.20	-63
	550				
0500		1	2.10	1.10	-68
	530				
0600		2	2.40	0.90	-68
	520				
0700		3	2.40	1.40	-63
	470				
0800		3	2.45	1.45	-63
	480				
0900		2	1.30	0.70	-58
	420				
1000		2	0.73	0.58	-
	400				
1100		-	0.30	0.40	-
	-				
1200		-	0.10	0.10	-
	-				
1300		-	0.00	0.00	-
	-				

MCC initiation, were quite cold, as was expected in view of the great heights of the thunderstorms.

Case 3: 27 May 1981

By 0515 GMT 27 May 1981, an MCS over southeastern Oklahoma had reached the critical size criteria of the MCC definition. The 50 kPa pattern associated with this MCC is reproduced in Fig. 16. Notice the trough-ridge-trough configuration; with ridging located over the area of the MCC. This pattern was quite different from the previous case. However, at the surface, conditions were very similar to that of Case 2. Although the NWS's surface analysis (not shown) did not depict a frontal boundary near the MCC, the surface θ_e analysis for 0900 GMT (Fig. 17) indicated a distinct contrast of air masses. This contrast of air masses was also evident prior to the MCC formation, indicating that it was not an MCC-produced phenomenon. The ambient surface air temperature and surface dew point temperature for two stations, Enid, OK (END) and Waco, TX (ACT), are used to illustrate the contrast of air masses. Enid's ambient surface air temperature and surface dew point temperature for 0900 GMT were 10°C and 13°C, respectively, while at the same time, Waco's were 24°C and 22°C. A definite contrast of air masses existed across the MCC.

About 2 h after the initiation of the MCC, a mesohigh and gust front formed near the Oklahoma/Texas borders and subsequently moved rapidly southeast. Once again, the strength of the gust front was revealed by the strong and gusty winds which it produced. At 0935 GMT, as the gust front passed Dallas, TX (DAL), a peak wind of 45 kt was

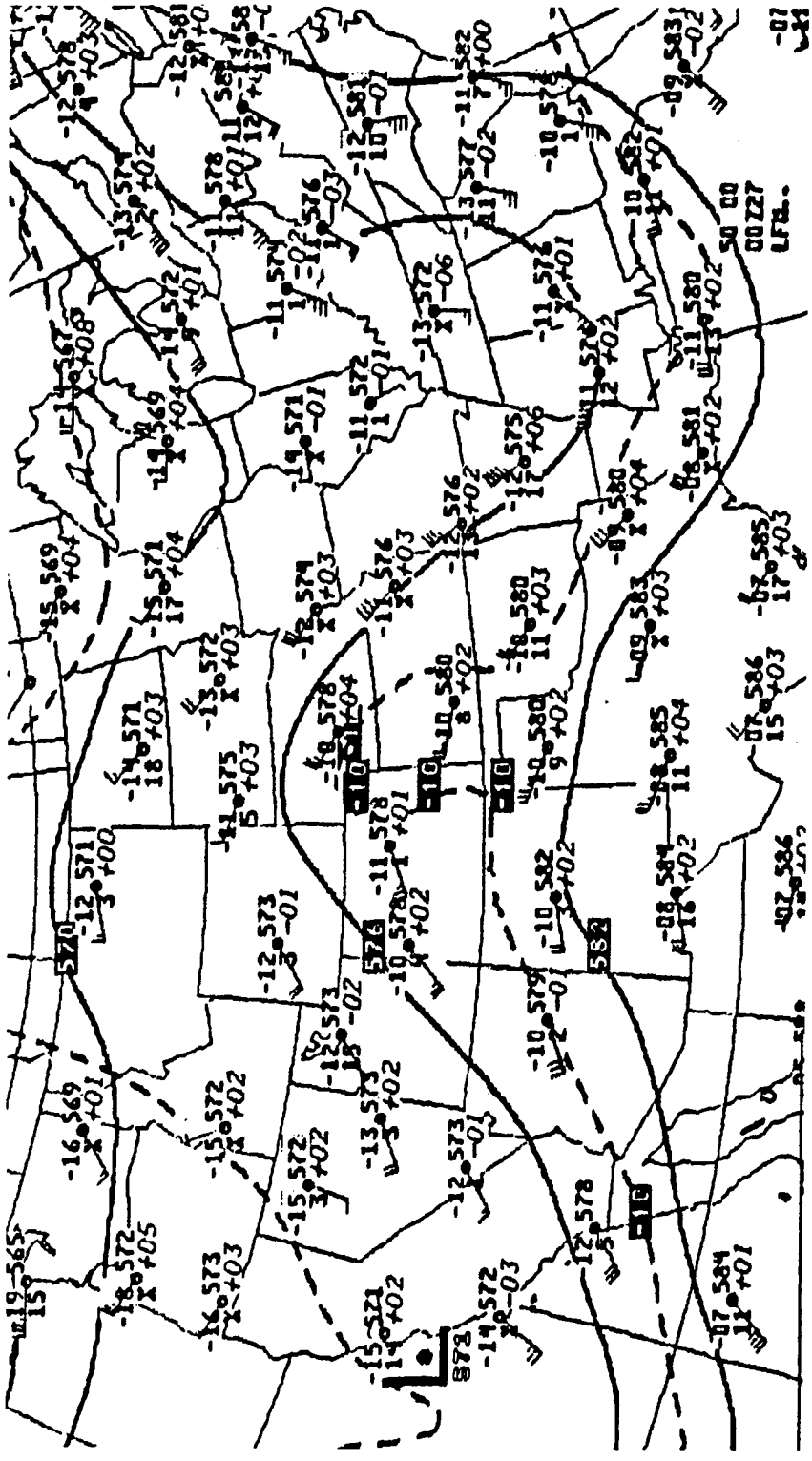

Fig. 16. 50 kPa height (dm) and temperature (°C) fields for 0000 GMT 27 May 1981. Height contours (solid lines) are every 60 m; isotherms (dashed lines) are every 5°C.

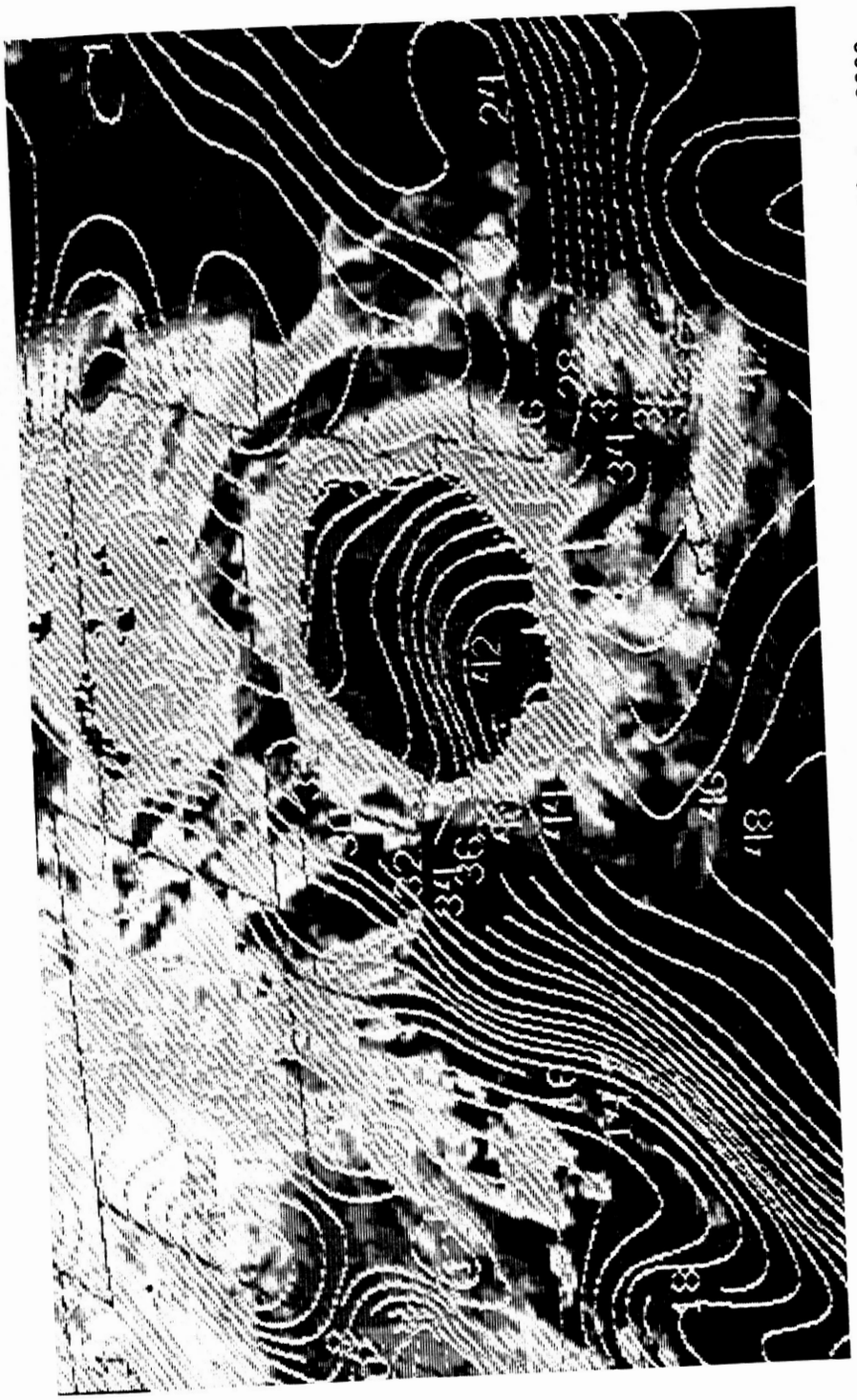

Fig. 17. Surface θ_e (°C) field overlaid upon GOES image (MB enhancement) for 0900 GMT 27 May 1981.

recorded.

Upon close inspection of the first visible satellite pictures for the day (1200 to 1300 GMT), an arc cloud, separated from the parent storm, was perceived. Fig. 18 shows the visible satellite picture for 1500 GMT. By this time, the arc cloud had nearly reached the Gulf coast of eastern Texas. After this time, the arc cloud weakened and was no longer discernable in the satellite images after 1800 GMT.

Characteristics associated with the MCC are given in Table 4. Most of the characteristics were not as pronounced as those of the MCC in Case 2. However, they were significantly stronger than the characteristics of the MCSs classified in category 2, as will be shown later. Two characteristics of the MCC for this case are worth emphasizing. Even after the termination of the MCC (1400 GMT), the maximum surface divergence increased to 3×10^{-5} s^{-1} (at 1400 and 1500 GMT), compared to 2×10^{-5} s^{-1} of the previous 6 h. Also, notice that the sum of the three largest precipitation rates stayed at or above 1.5 in h^{-1} for 6 h. It may be recalled that for Case 2, this condition existed for 8 h.

Case 4: 17 May 1982

A storm area formed in Kansas and western Oklahoma on 16 May 1982. This storm area developed on the east side of a stationary front as analyzed by the NWS (not shown). The front extended from South Dakota to the Texas panhandle and beyond to the southeast corner of New Mexico. Fig. 19 shows the 50 kPa analysis for 1200 GMT 16 May 1982. The trough located over Arizona and New Mexico moved eastward and initiated the formation of the storm area. By 0030 GMT 17 May 1982 the storm area was

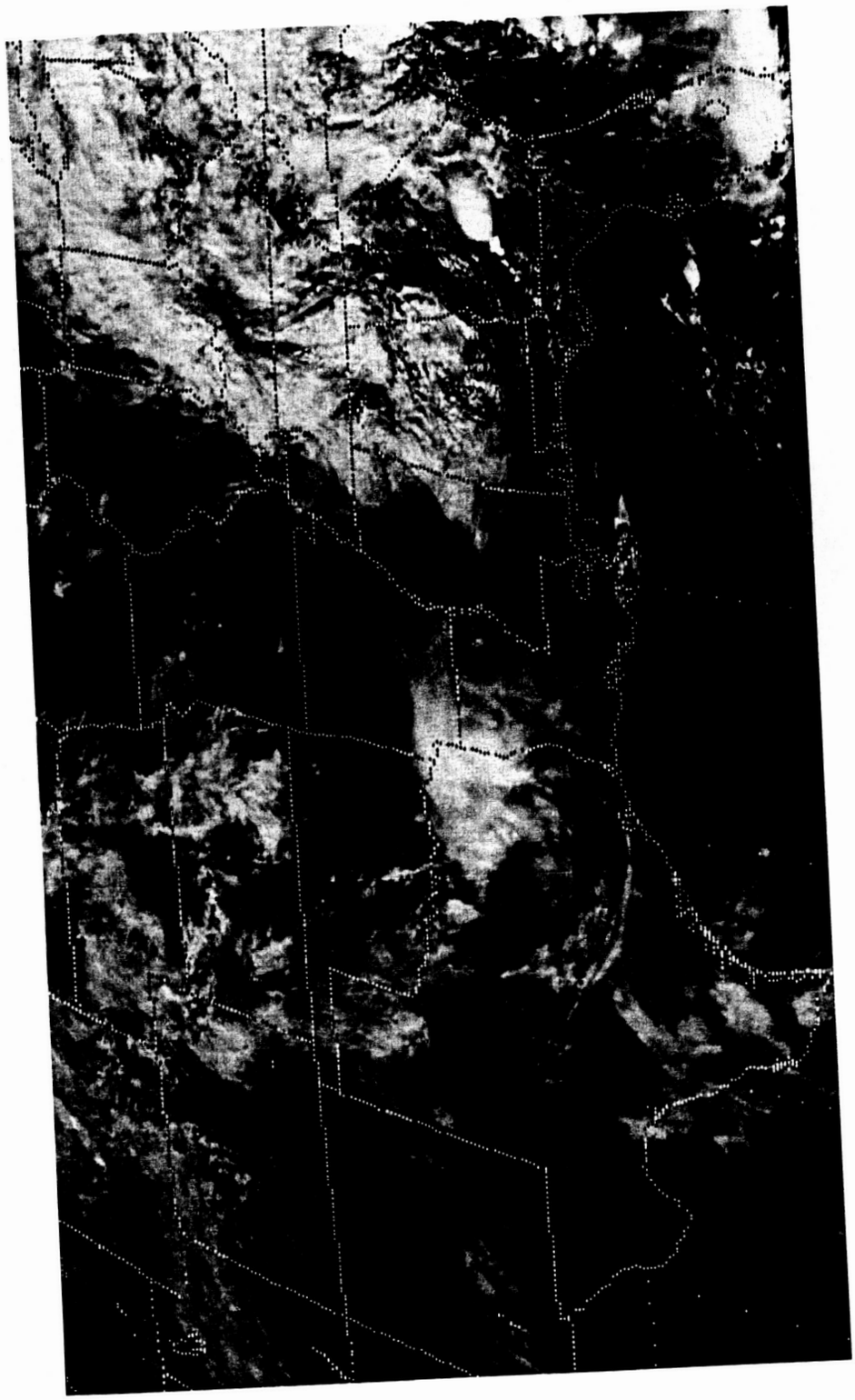

Fig. 18. GOES visible image for 1500 GMT 27 May 1981.

Table 4. Characteristics associated with the MCC of Case 3 (27 May 1981). The maximum thunderstorm heights were determined at approximately 35 min past each hour. Dashes indicate that the parameter was not determined.

Time (GMT)	Maximum thunderstorm thunderstorm (x 100 ft)	Maximum surface divergence (x $10^{-5}s^{-1}$)	Sum of the three largest precipitation rates (in h^{-1})	Maximum point precipitation rate (in h^{-1})	Coldest cloud top temperature (°C)
0400		-	0.60	0.50	-
	520				
0500		-	1.00	0.50	-
	550				
0600		3	1.00	0.70	-
	580				
0700		3	0.73	0.43	-73
	560				
0800		2	1.59	1.30	-68
	520				
0900		2	1.50	0.60	-73
	550				
1000		2	2.70	0.99	-68
	480				
1100		2	2.93	1.13	-68
	470				
1200		2	2.50	0.90	-68
	320				
1300		2	1.61	1.01	-
	250				
1400		3	0.60	0.20	-
	160				
1500		3	0.60	0.20	-
	-				
1600		-	0.10	0.10	-
	-				

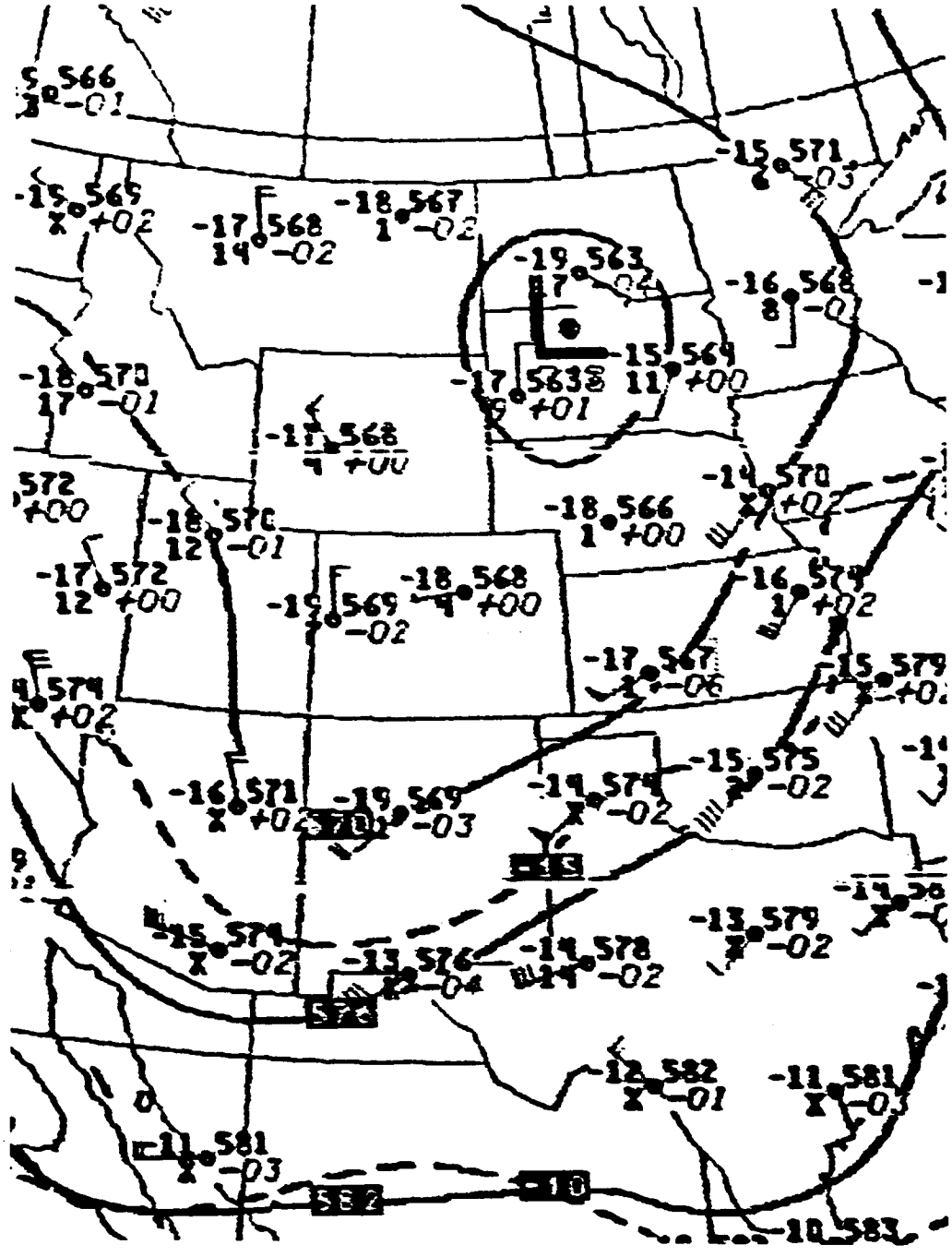

Fig. 19. 50 kPa height (dm) and temperature (°C) fields for 1200 GMT 16 May 1982. Height contours (solid lines) are every 60 m; isotherms (dashed lines) are every 5°C.

large enough to be classified as an MCC. Fig. 20 shows the MCC at 0415 GMT, near the time of maximum extent. About 2 h earlier, at 0200 GMT, a mesohigh and gust front formed. The gust front extended from Chanute, KS (CNU) to Oklahoma City, OK (OKC) to Lubbock, TX (LBB).

The gust front associated with this MCC was very strong, producing gusty winds and severe weather. At 0300 GMT, along the leading edge of the gust front, Fort Sill, OK (FSI) reported a tornado to the west. The following stations reported wind gusts greater than 34 kt as the gust front passed: Oklahoma City, OK (0233 GMT, 35 kt); Tulsa, OK (0436 GMT, 35 kt); Wichita Falls, TX (0506 GMT, 37 kt); McAlester, OK (0640 GMT, 36 kt); Dallas, TX (0830 GMT, 35 kt).

Fig. 21 shows the GOES IR image, with the MB enhancement curve, for 1000 GMT. The thunderstorms had weakened considerably and the MCC had already terminated. At this time, however, the gust front and large mesohigh were still very pronounced, as depicted in the surface analysis shown in Fig. 22. The mesohigh encompassed southeast Oklahoma and most of northern Texas. It was about this time that an arc cloud in the IR imagery first became discernible.

Eventually, a massive ACC formed. Fig. 23 shows the arc cloud, located in Texas, at 1832 GMT. The arrows point to its leading edge. The arc cloud finally lost its identity in the satellite images around 2200 GMT.

Table 5 shows the characteristics associated with this MCC. The maximum thunderstorm height of 65,000 ft occurred at 0135 GMT. This correlated quite well with the maximum point rainfall rate, which occurred during the hour ending at 0200 GMT. The behavior of the values

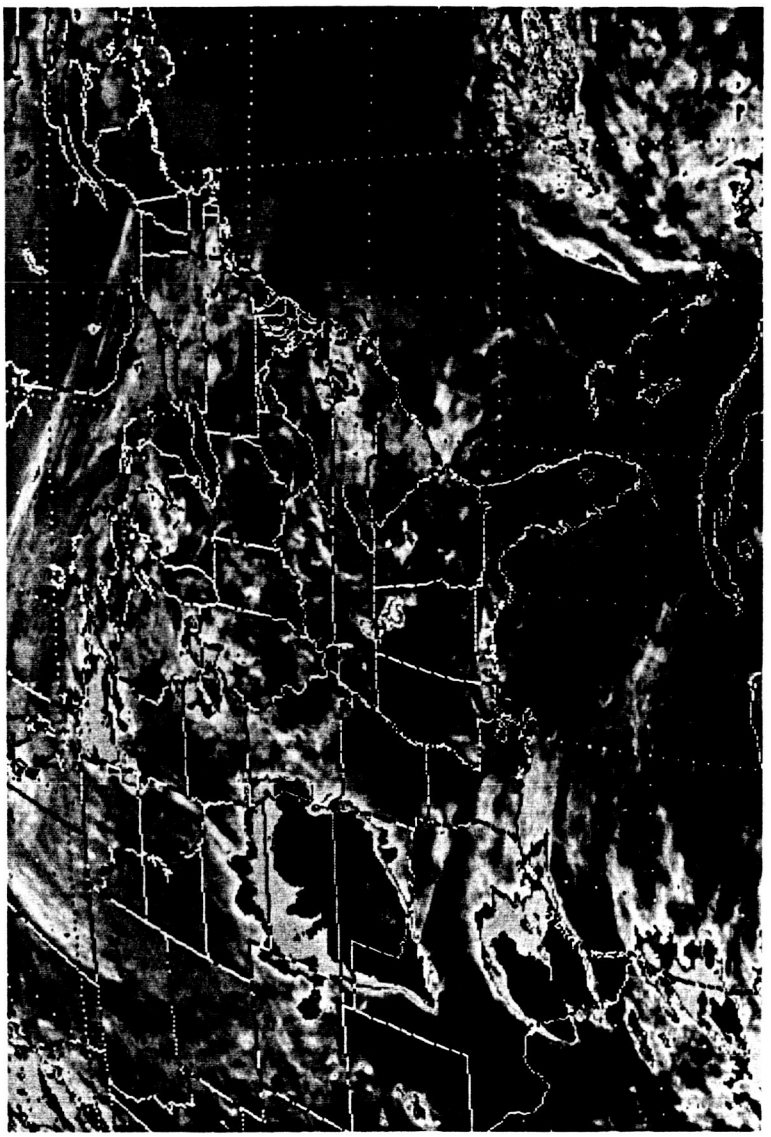

Fig. 20. GOES IR image with MB enhancement for 0415 GMT 17 May 1982.

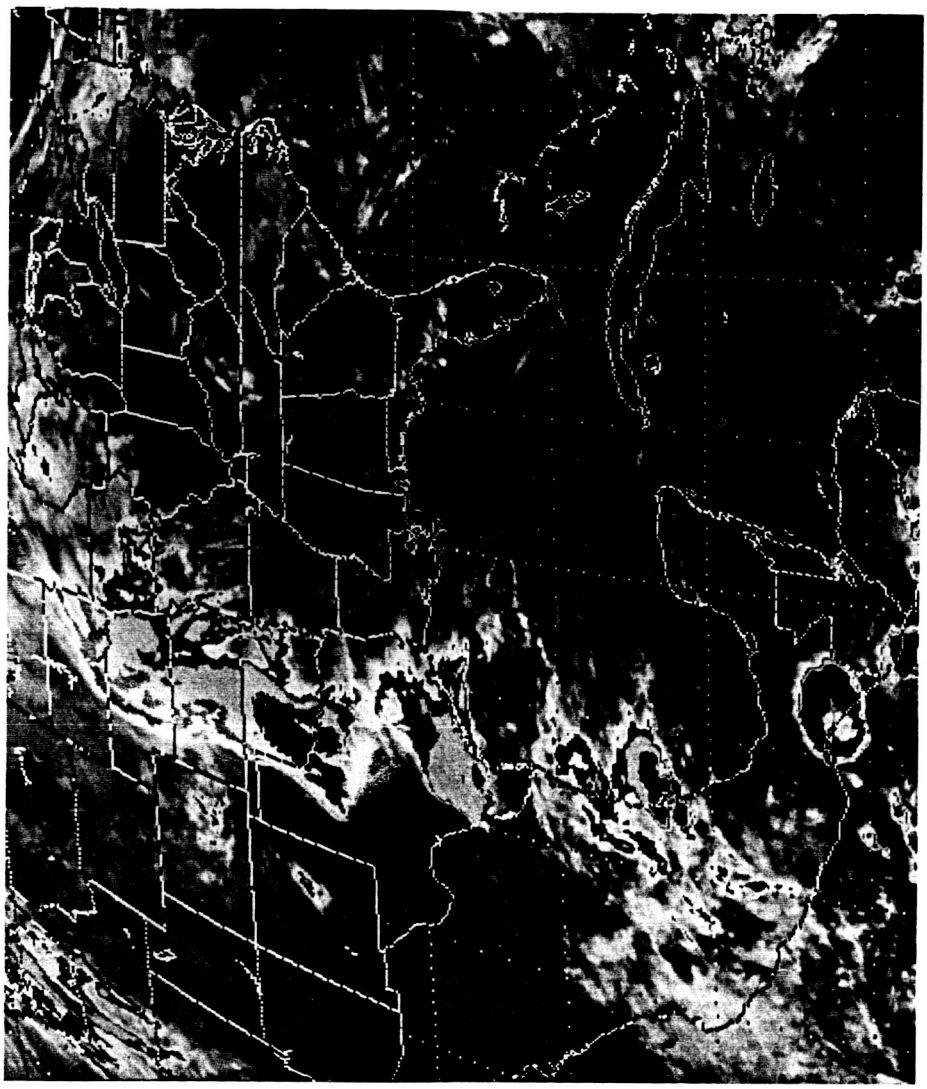

Fig. 21. GOES IR image with MB enhancement for 1000 GMT 17 May 1982.

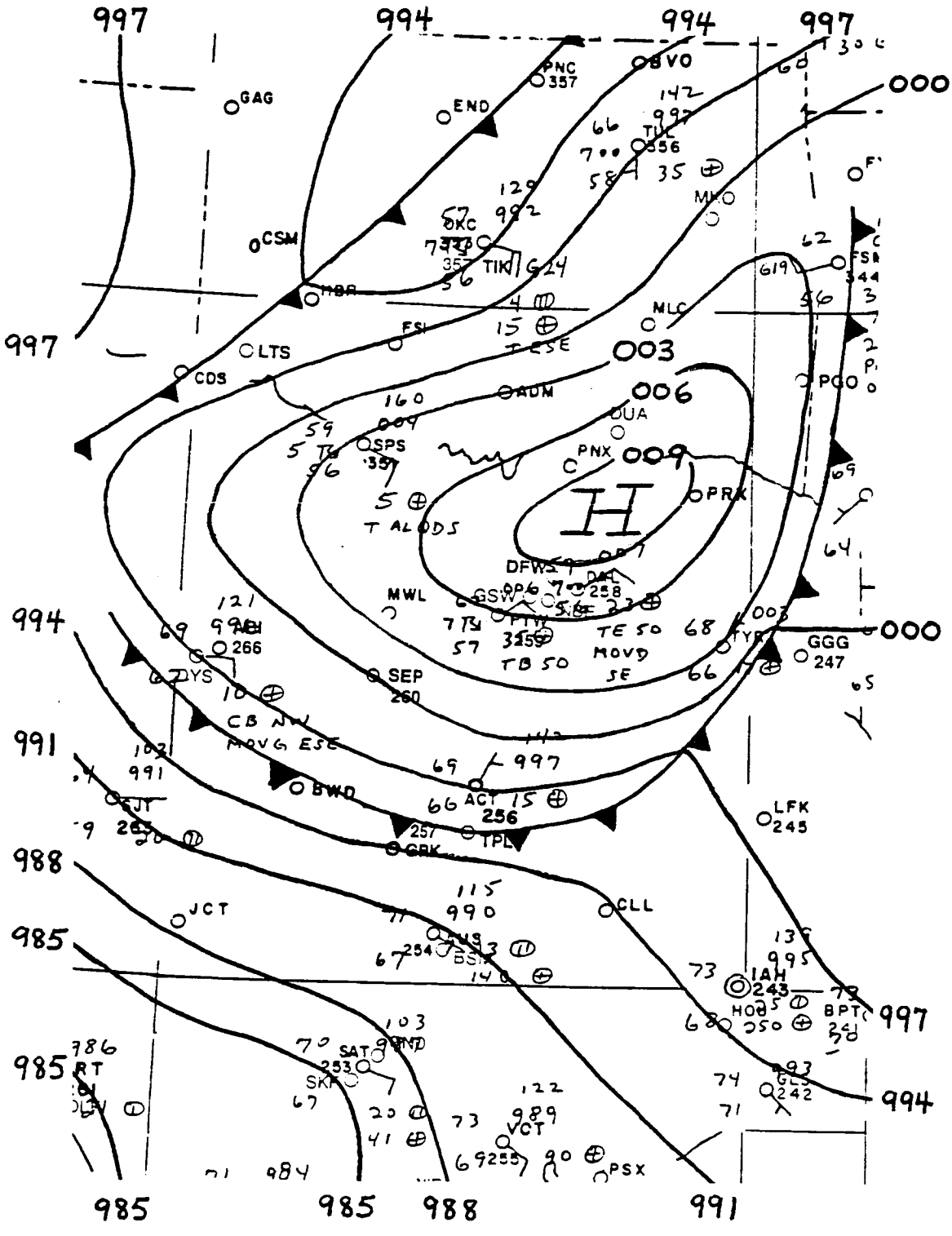

Fig. 22. Surface pressure field for 1000 GMT 17 May 1982. Altimeter setting contours are every 0.03 in Hg. The gust front, located in northeastern Texas and western Arkansas, is denoted by a cold front symbol.

Fig. 23. GOES visible image for 1832 GMT 17 May 1982.

Table 5. Characteristics associated with the MCC of Case 4 (16/17 May 1982). The maximum thunderstorm heights were determined at approximately 35 min past each hour. Dashes indicate that the parameter was not determined.

Time (GMT)	Maximum thunderstorm height (x 100 ft)	Maximum surface divergence (x 10^{-5} s^{-1})	Sum of the three largest precipitation rates (in h^{-1})	Maximum point precipitation rate (in h^{-1})	Coldest cloud top temperature (°C)
2300		-	2.20	1.70	-
	590				
0000		-	3.83	1.80	-
	620				
0100		1	3.29	1.76	-73
	650				
0200		2	2.80	2.30	-73
	530				
0300		4	2.90	1.40	-68
	510				
0400		2	3.20	1.10	-68
	520				
0500		2	2.74	0.94	-68
	550				
0600		2	3.58	1.50	-63
	580				
0700		3	2.50	1.10	-63
	630				
0800		4	3.00	1.10	-
	420				
0900		4	1.52	0.60	-
	410				
1000		4	1.40	0.70	-
	400				
1100		3	1.78	0.90	-
	390				
1200		4	2.73	1.63	-
	-				
1300		5	1.52	0.60	-
	-				
1400		4	1.39	0.75	-
	-				

of the sums of the three largest hourly rainfall rates was similar to the previous cases. The sum of the rainfall rates stayed above 1.5 in h^{-1} for 11 straight hours, compared to 8 and 6 h for Cases 2 and 3, respectively. Very cold cloud top temperatures were associated with the early stages of the MCC, with temperatures as low as -73°C. As expected, the large mesohigh, created by the downdrafts of the thunderstorms, was associated with strong surface divergence. The maximum of 5×10^{-5} s^{-1} occurred at 1300 GMT.

Of the 12 cases included in this study, the MCC of this case produced the largest ACC.

Case 7: 26 June 1982

During the afternoon of 25 June 1982, convection developed to the lee of the Rockies and moved eastward. During the evening hours an MCS developed over the western plains stretching from the Texas panhandle to southwestern South Dakota. Wetzel et al. (1983) described a similar sequence of events. They found that afternoon orogenic thunderstorms, such as those that develop along the foothills of the Rockies, often move eastward and provide the beginnings of significant Plains mesosystems.

The synoptic setting leading to the formation of the MCS was described by Miller (1984). At 50 and 30 kPa, the MCS developed near the inflection point downstream of a short-wave trough and in an area of cold advection. The flow at both 30 and 20 kPa was diffluent over the MCS, indicating the liklihood of convergence below. At both 70 and 85 kPa there was slight warm advection near the MCS. Thus, the troposphere

was undergoing destabilization due to differential advection.

Two gust fronts were produced by the MCS. The first gust front formed around 0600 GMT 26 June 1982 and dissipated by 1500 GMT. The second gust front was first detected in the surface analysis at 1100 GMT and dissipated around 2200 GMT. Fig. 24 is the surface analysis for 1200 GMT and shows both gust fronts. The gust fronts are denoted by cold front symbols.

Both gust fronts moved to the southeast and eventually produced arc clouds. Evidence of the first arc cloud could first be detected in the IR satellite imagery at 0830 GMT. The second arc cloud was first visible in the satellite images at 1430 GMT and eventually grew into a large ACC. Fig. 25 shows the second arc cloud, extending from central Oklahoma to north central Texas and then southwestward to the southeast portions of New Mexico, at 1832 GMT.

Table 6 shows the characteristics associated with this MCS. The maximum hourly thunderstorm heights oscillated, corresponding to the formation of the two arc clouds. The heights fell drastically, from 54,000 ft to 41,000 ft, between 0735 GMT and 0935 GMT, bracketing the time the first arc cloud appeared. Similarily, between 1335 GMT and 1535 GMT, the heights fell from 48,000 ft to 34,000 ft, again around the time of arc cloud formation. The coldest cloud top temperatures oscillated in a similar fashion. The sum of the three largest precipitation rates stayed above 1.5 in h^{-1} from 0300 to 0800 GMT, a total of 6 h. The only exception to this was the hour ending at 0600 GMT, where it appeared likely that the heavy precipitation fell between the climatological raingauge sites. After this period of heavy precipitation, the

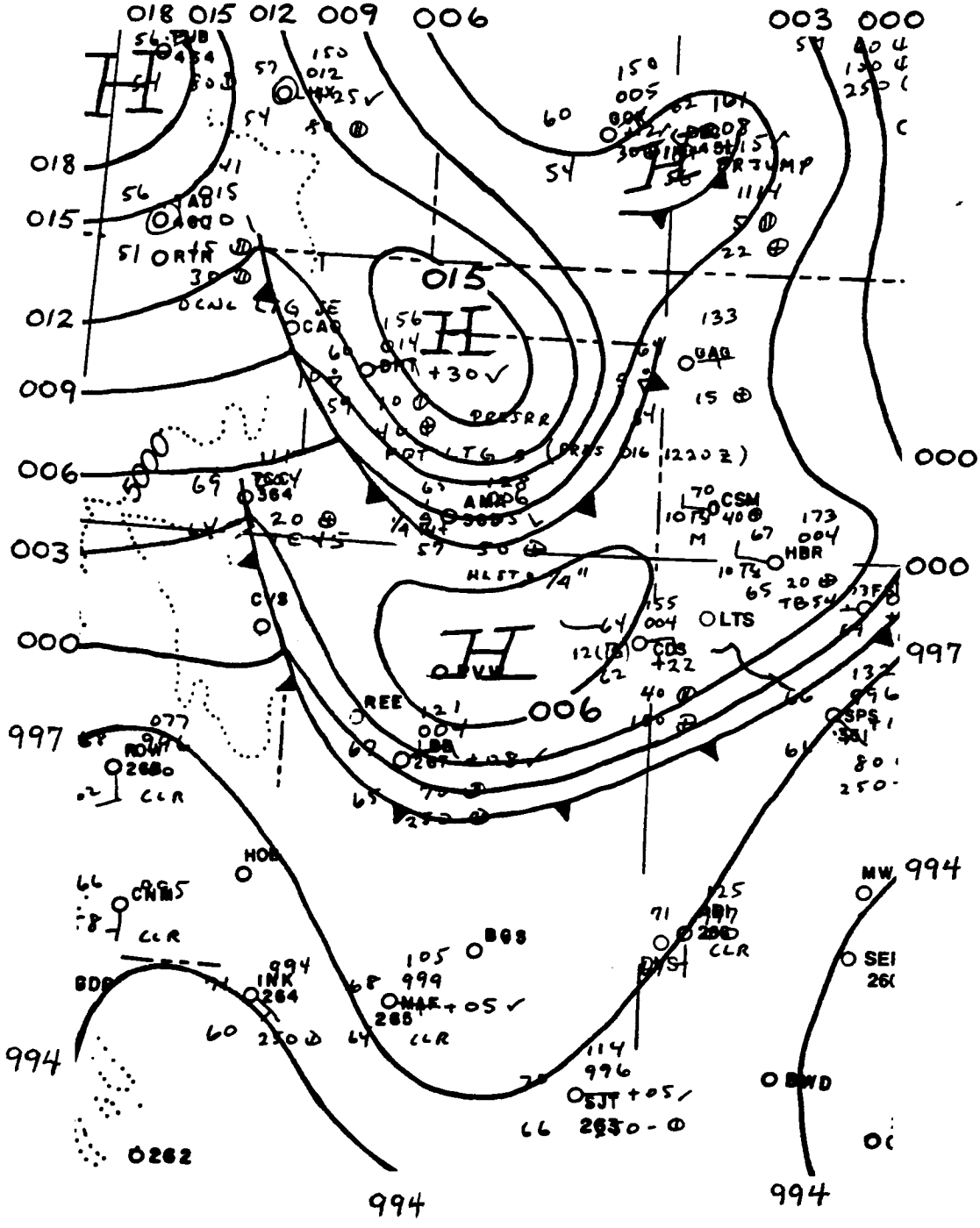

Fig. 24. Surface pressure field for 1200 GMT 26 June 1982. Altimeter setting contours are every 0.03 in Hg. The gust fronts are denoted by cold front symbols.

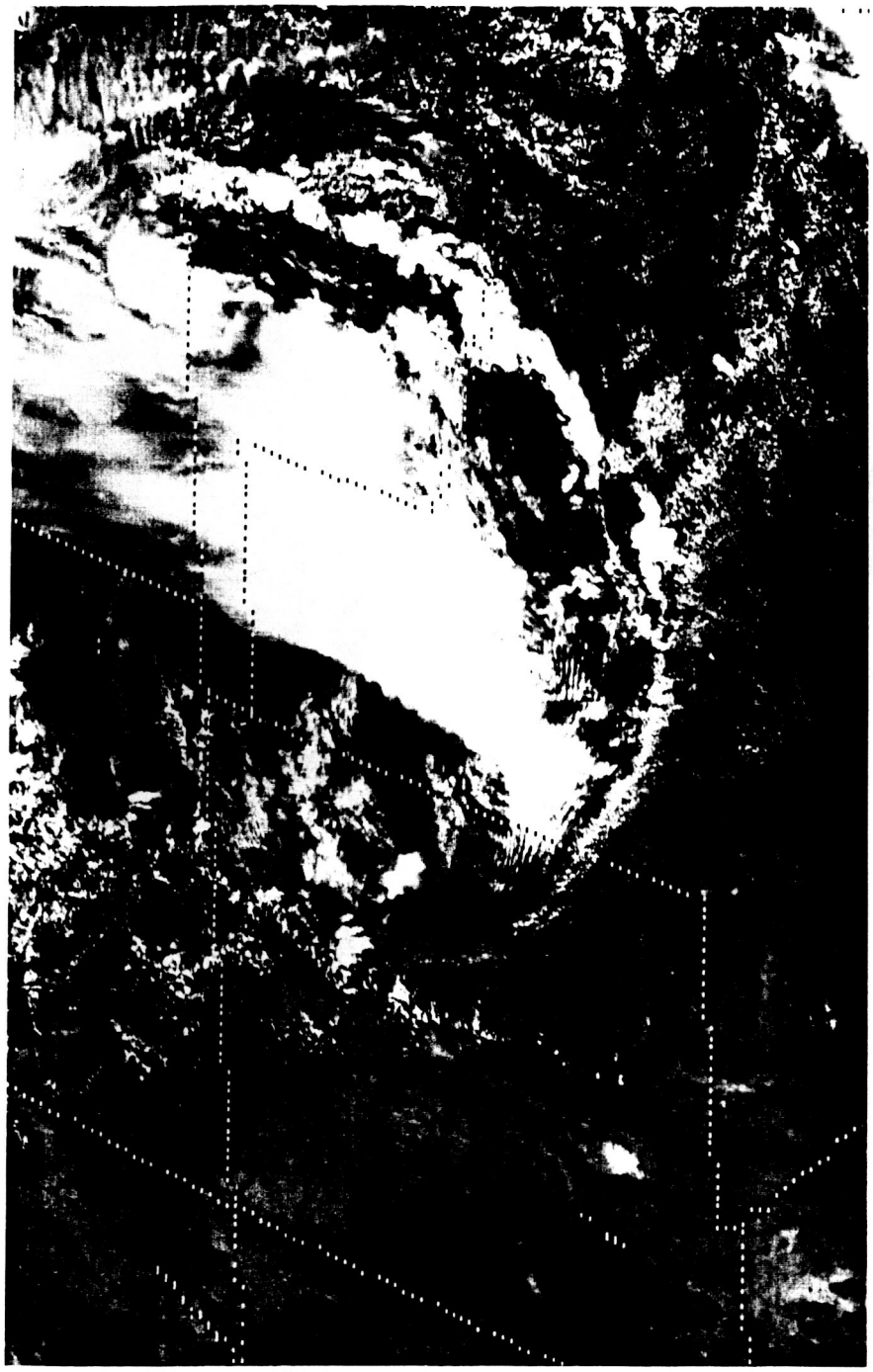

Fig. 25. GOES visible image for 1832 GMT 26 June 1982.

Table 6. Characteristics associated with the MCS of Case 7 (26 June 1982). The maximum thunderstorm heights were determined at approximately 35 min past each hour. Dashes indicate that the parameter was not determined.

Time (GMT)	Maximum thunderstorm height (x 100 ft)	Maximum surface divergence (x 10^{-5} s^{-1})	Sum of the three largest precipitation rates (in h^{-1})	Maximum point precipitation rate (in h^{-1})	Coldest cloud top temperature (°C)
0000	-	-	1.40	0.90	-
0100	-	-	0.50	0.20	-
0200	-	-	0.50	0.20	-
0300	-	-	1.88	0.80	-
0400	-	-	1.54	0.61	-
0500	550	-	1.50	0.50	-
0600	600	-	0.70	0.44	-
0700	540	-	2.00	1.10	-
0800	540	-5	1.51	0.90	-68
0900	480	2	1.26	0.60	-63
1000	410	1	1.36	0.60	-63
1100	400	1	1.25	0.60	-68
1200	400	1	1.94	1.25	-68
1300	480	3	0.81	0.50	-68
1400	480	3	0.80	0.60	-68
1500	450	4	1.63	0.90	-63
1600	340	-	0.50	0.20	-
1700	-	-	0.30	0.10	-
	-				

first arc cloud formed. Another peak in the sum of the three largest precipitation rates occurred the hour ending at 1500 GMT (1.63 in h^{-1}). This seemed to correspond with the formation of the second arc cloud.

Case 8: 27 June 1982

During the afternoon of 26 June 1982, the large arc cloud discussed in the previous case intersected with an east-west oriented line of cumulus and formed an MCS over western Texas. The MCS moved southeast, reached its most intense stage around 0330 GMT 27 June 1982 and slowly dissipated thereafter. Only a weak gust front and mesohigh were produced by the MCS.

Another MCS developed during the afternoon of 26 June 1982. This MCS developed to the lee of the Rockies in northeast New Mexico and essentially followed the same movement as the first MCS. Fig. 26 shows both MCSs at 0700 GMT 27 June 1982. The eastern MCS was dissipating, while the western MCS was still intensifying. By 0800 GMT, the western MCS was large enough to be classified as an MCC.

The western MCC produced a much stronger gust front and mesohigh compared to the eastern MCS. This was clearly evident in the surface pressure field for 1200 GMT, presented in Fig. 27. The remains of the mesohigh produced by the eastern MCS were still apparent and were located southeast of Austin, TX (AUS). The central pressure of this mesohigh was approximately 29.97 in of mercury. The mesohigh produced by the western MCC had a central pressure of about 30.13 in of mercury. The strength of the western mesohigh and gust front was reflected in San Angelo's (SJT) winds, which gusted to 45 kt during the passage of the

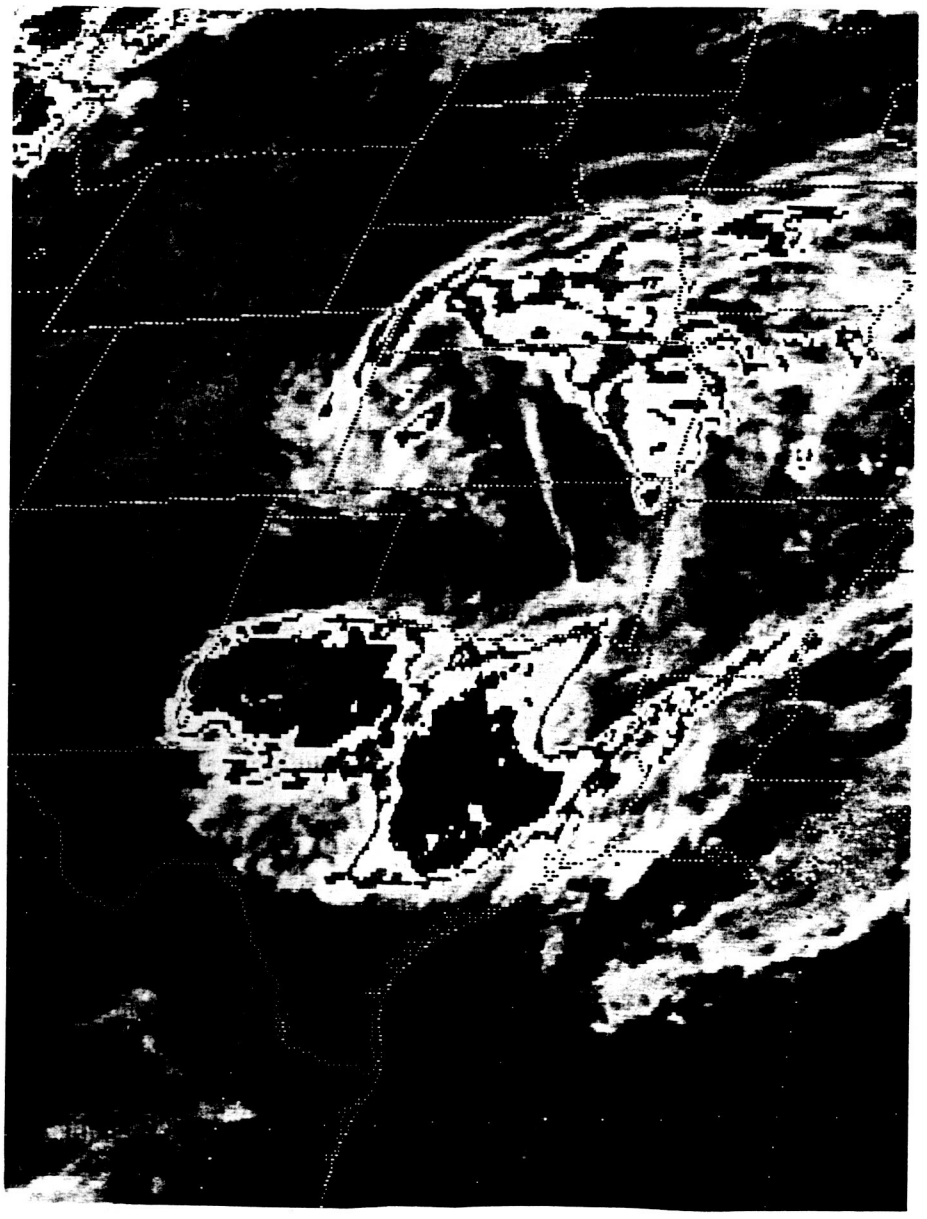

Fig. 26. GOES IR image with MB enhancement for 0700 GMT 27 June 1982.

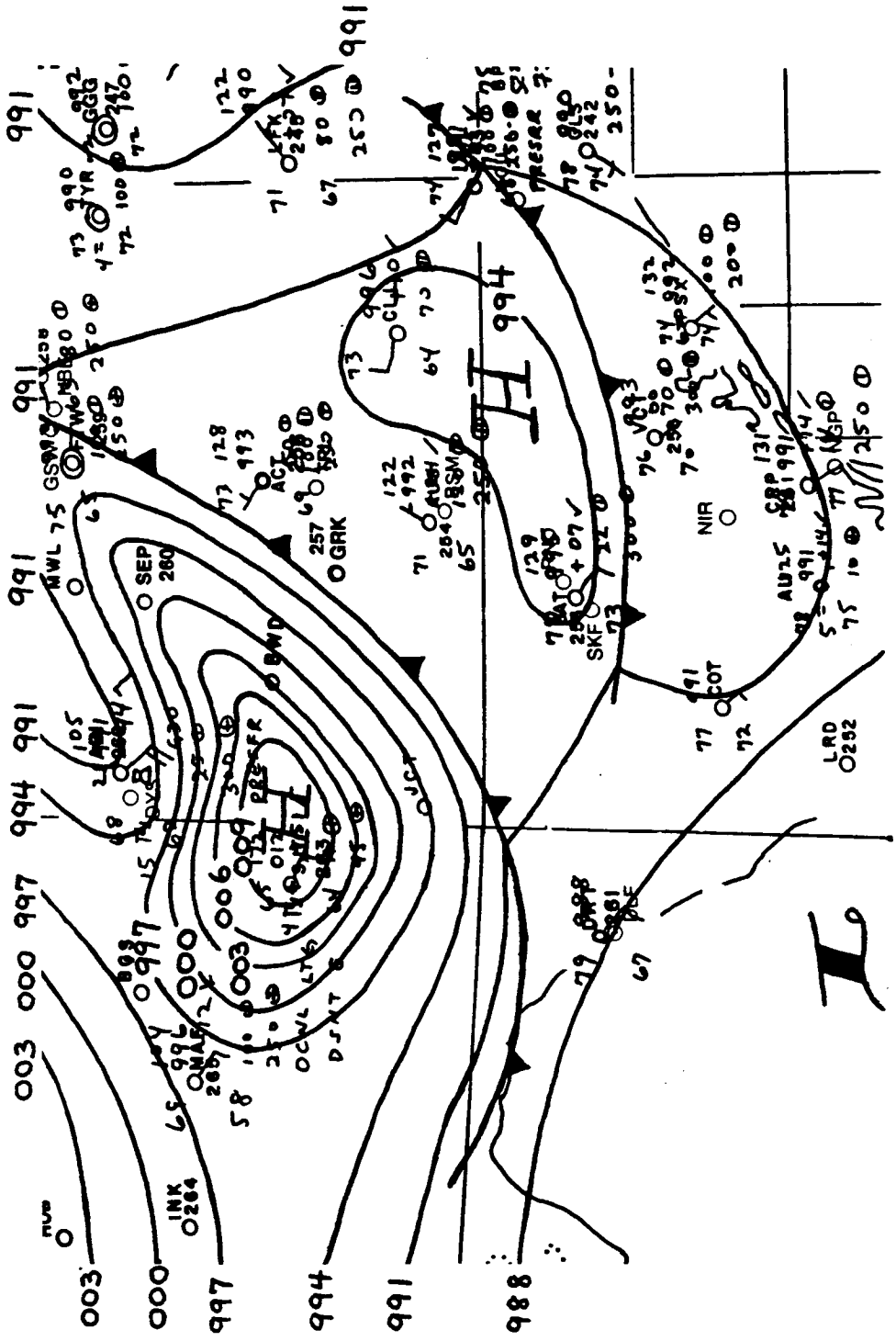

Fig. 27. Surface pressure field for 1200 GMT 27 June 1982. Altimeter setting contours are every 0.03 in Hg. The gust fronts are denoted by cold front symbols.

gust front (0958). An arc cloud, associated with the gust front and separated from the main MCS cloud shield, first became evident in the satellite images at 1200 GMT.

The characteristics of the western MCC are similar to the previous category 1 MCSs and are displayed in Table 7. Dramatic characteristic changes occurred around the time of arc cloud formation. The maximum hourly thunderstorm heights dropped from 48,000 ft at 1135 GMT to 30,000 ft at 1335 GMT, the sum of the three largest precipitation rates fell from 3.72 in h^{-1} at 1100 GMT to 0.9 in h^{-1} at 1300 GMT, the maximum point precipitation rate reduced from 1.5 to 0.5 in h^{-1} and the coldest cloud top temperatures warmed from -73 to -58°C. Two other interesting features are seen in the characteristics associated with the MCC. The magnitude of the maximum surface divergence remained large after the maximum extent of the MCC (0900 GMT). Also, the sum of the three largest precipitation rates stayed above 1.5 in h^{-1} for 7 h, excluding the hour ending at 0800 GMT, when it appeared the heavy precipitation fell between reporting climatological raingauge sites. Therefore, heavy precipitation fell over a significant area for a long time, preceding the formation of the arc cloud.

Case 10: 20 May 1983

On the afternoon and evening of 19 May 1983, an enormous convective storm system evolved from the merger of several smaller MCSs. The initial thunderstorms developed around 2000 GMT 19 May 1983, just to the east of a north-south dry line, which was located in western Texas. Another almost equally vigorous system developed 2 h later in northeast

Table 7. Characteristics associated with the MCC of Case 8 (27 June 1982). The maximum thunderstorm heights were determined at approximately 35 min past each hour. Dashes indicate that the parameter was not determined.

Time (GMT)	Maximum thunderstorm height (x 100 ft)	Maximum surface divergence (x 10^{-5} s^{-1})	Sum of the three largest precipitation rates (in h^{-1})	Maximum point precipitation rate (in h^{-1})	Coldest cloud top temperature (°C)
0000	-	-	0.80	0.80	-
0100	500	-	0.90	0.50	-
0200	500	-	0.10	0.10	-
0300	470	-	0.20	0.10	-
0400	490	-	0.20	0.10	-
0500	540	-	0.01	0.01	-
0600	520	3	2.30	1.60	-73
0700	520	4	2.00	1.00	-68
0800	500	5	0.85	0.50	-73
0900	500	3	1.85	0.90	-73
1000	500	2	2.49	1.30	-73
1100	480	3	3.72	1.50	-73
1200	330	2	1.69	0.90	-68
1300	300	3	0.90	0.50	-58
1400	260	4	0.60	0.20	-
1500	450	4	0.30	0.10	-
1600	490	-	0.32	0.20	-
1700	530	-	-	-	-

Texas in the vicinity of a weak warm front. By 0130 GMT 20 May 1983, the two MCSs merged into an MCC. The 50 kPa analysis for 0000 GMT 20 May 1983 is shown in Fig. 28. This flow configuration, termed the "New Orleans Type" (Belville and Stewart, 1983), consisted of a deep trough and closed circulation over the southwest United States. This pattern is often responsible for early spring heavy rainfall events in the southeast (Belville and Stewart, 1983).

By 0400 GMT, a mesohigh and gust front, located in southeast Texas, were evident in the surface analysis (not shown). The gust front was an important factor influencing the National Severe Storms Forecast Center to issue Tornado Watch Number 179 at 0458 GMT. The watch bulletin stated that an outflow boundary, located from Lufkin, TX, west-southwest to south of San Antonio, TX, would be the focus for continued development of very strong thunderstorms. As the gust front interacted with the very unstable airmass, numerous reports of severe weather were reported. Two examples were wind gusts of 53 kt at San Antonio at 0453 GMT and a confirmed tornado at Houston's Intercontinental Airport at 0720 GMT. After 0900 GMT, the southern portion of the gust front moved into the northwest Gulf of Mexico. However, the northern portion was still discernable in the surface analysis as it passed stations in Louisiana. For instance, Lake Charles reported a wind gust of 40 kt at 0928 GMT and Lafayette's winds changed from calm at 1100 GMT to a westerly component of 10 kt at 1200 GMT.

At 1200 GMT an arc cloud was discernable in the visible satellite image. Fig. 29 shows the arc cloud, at 1300 GMT, extending from southeastern Louisiana into the northwest Gulf of Mexico. At this time, the

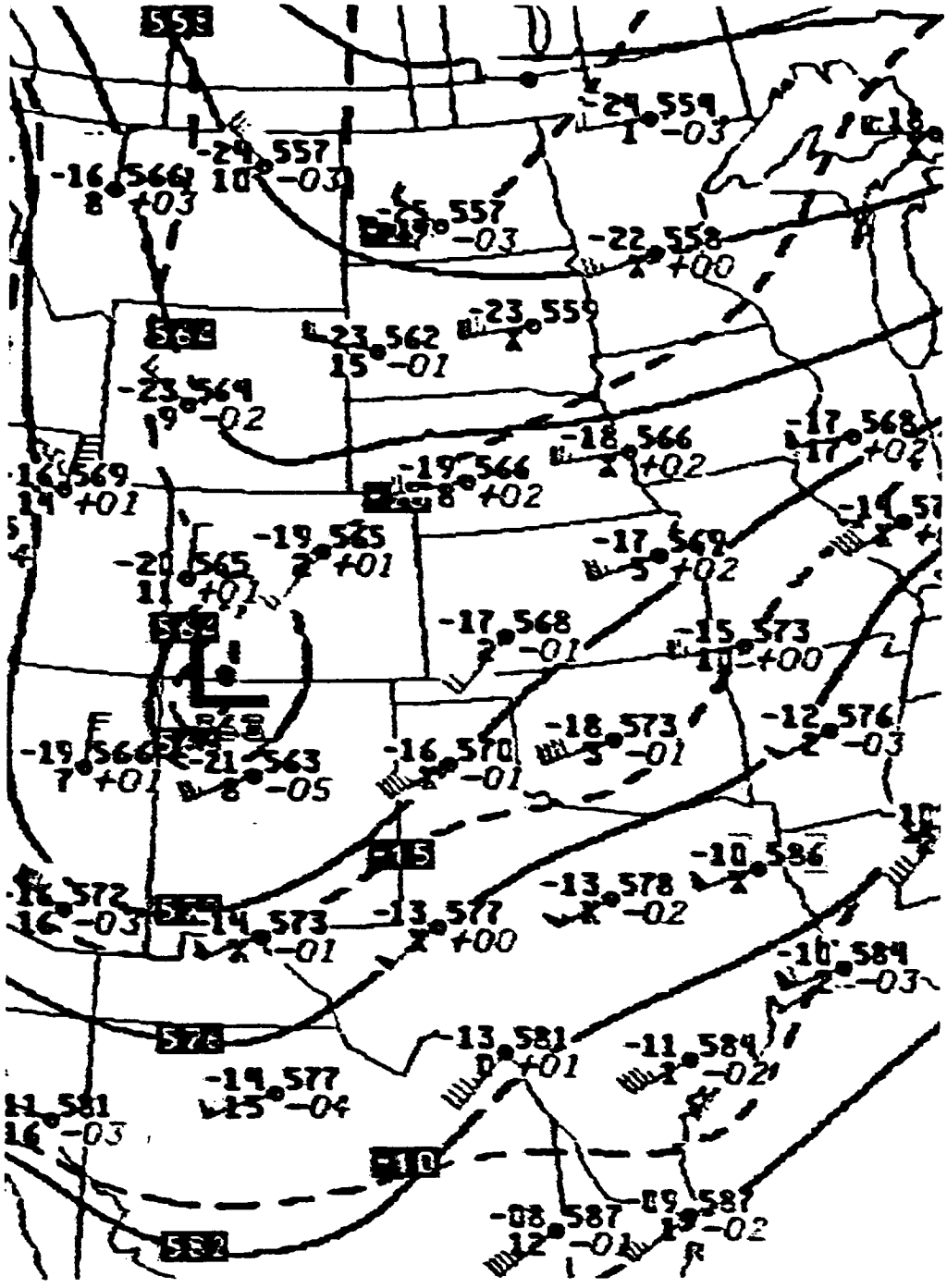

Fig. 28. 50 kPa height (dm) and temperatures (°C) fields for 0000 GMT 20 May 1983. Height contours (solid lines) are every 60 m; isotherms (dashed lines) are every 5°C.

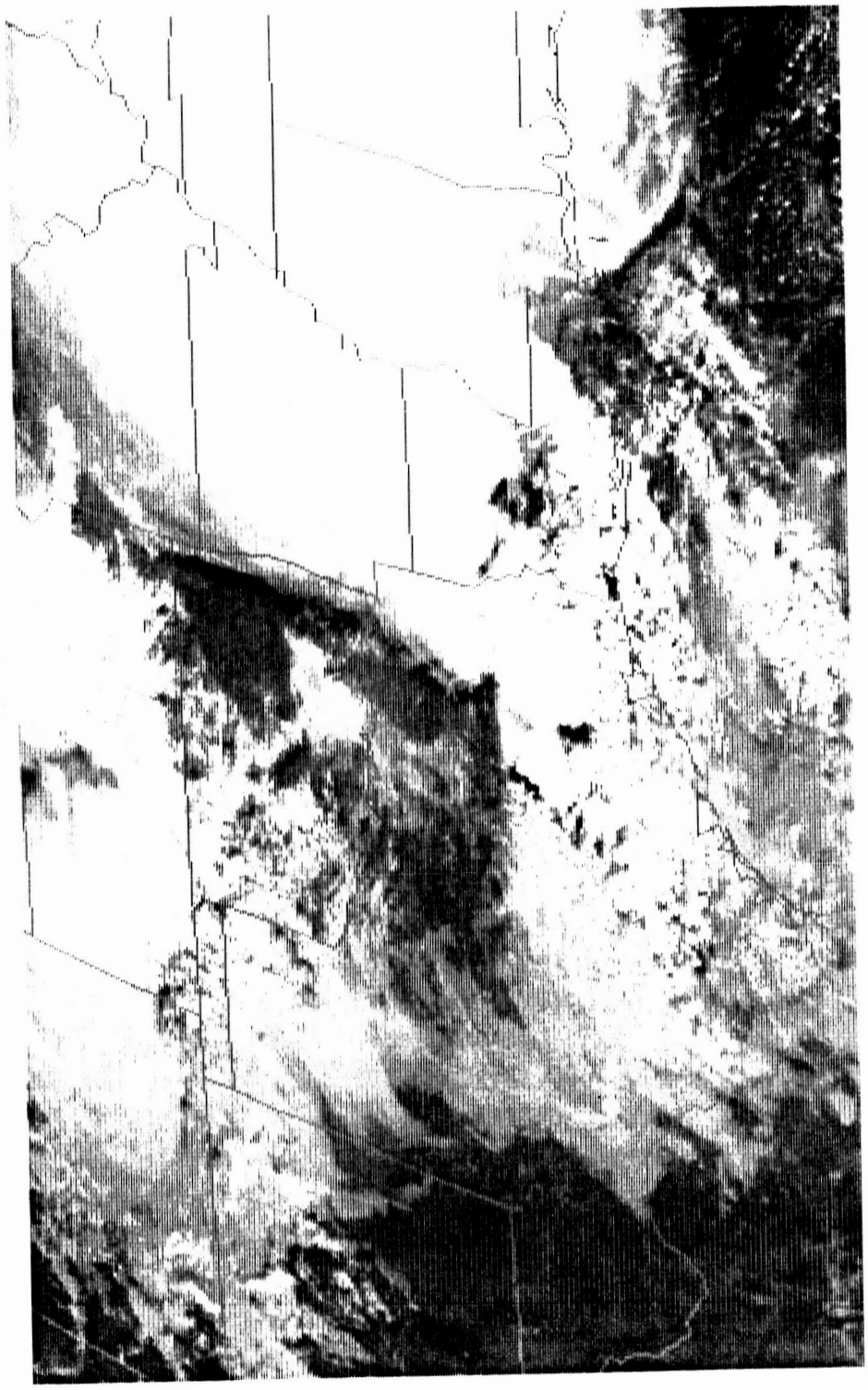

Fig. 29. GOES visible image for 1300 GMT 20 May 1983.

NWS's surface analysis depicted a cold front extending from the Tennessee Valley southwestward to southeast Texas (not shown). Normally, pronounced clearing occurs behind arc clouds. The lack of clearing in southeast Texas (see Fig. 29) can be partially explained by the presence of the existing cold front.

The characteristics associated with the MCC are displayed in Table 8. The extreme intensity of the MCC is obvious. The highest reported thunderstorm height of 66,000 ft was reached at 0635 GMT. The largest point precipitation rate and the maximum sum of the three largest hourly precipitation rates, of 2.1 in h^{-1} and 4.10 in h^{-1}, respectively, occurred at 0700 GMT, just before the time of maximum extent of the storm. Also, the sum of the three largest hourly precipitation rates stayed above 1.5 in h^{-1} for 5 straight hours. The only exception to this occurred the hour ending at 0600 GMT, when it again appeared that the heavy precipitation fell between the climatological raingauge sites. This was determined by following the movement of the coldest cloud tops on satellite images and by keeping continuity of the most intense precipitation. The coldest cloud top temperatures of -78°C occurred at both 0700 and 0800 GMT. It should be noted that the decrease of the maximum hourly surface divergence after 1000 GMT, was probably due to the lack of wind reports behind the gust front as it moved into the Gulf of Mexico.

Case 11: 11 June 1983

On the evening of 10 June 1983, thunderstorms formed over eastern New Mexico and western Texas ahead of a short-wave trough in the

Table 8. Characteristics associated with the MCC of Case 10 (20 May 1983). The maximum thunderstorm heights were determined at approximately 35 min past each hour. Dashes indicate that the parameter was not determined.

Time (GMT)	Maximum thunderstorm height (x 100 ft)	Maximum surface divergence (x 10^{-5} s^{-1})	Sum of the three largest precipitation rates (in h^{-1})	Maximum point precipitation rate (in h^{-1})	Coldest cloud top temperature (°C)
0000		2	-	-	-
	-				
0100		4	-	-	-63
	-				
0200		2	-	-	-63
	-				
0300		2	0.40	0.40	-63
	610				
0400		2	0.70	0.40	-68
	630				
0500		2	2.65	1.00	-73
	640				
0600		1	1.20	0.80	-73
	660				
0700		0	4.10	2.10	-78
	550				
0800		1	2.74	1.20	-78
	520				
0900		1	2.16	0.92	-73
	540				
1000		2	0.99	0.43	-73
	420				
1100		0	0.87	0.40	-68
	330				
1200		0	0.15	0.10	-63
	350				
1300		0	0.21	0.10	-58
	350				
1400		-	0.40	0.20	-
	320				
1500		-	0.71	0.40	-
	-				
1600		-	0.06	0.06	-
	-				

mid-troposphere. At 0000 GMT 11 June 1983, the short-wave trough was evident in the 50 kPa analysis and extended from western Kansas to southwestern New Mexico (Fig. 30). At the surface, the storms developed to the east of a dry line and in an area of strong convergence, with magnitudes as large as -3×10^{-5} s^{-1}, as determined by the McIDAS. The thunderstorms expanded and at 0530 GMT an MCC was initiated.

At 0800 GMT, a gust front and mesohigh developed. As the gust front passed Wichita Falls, TX, a wind gust of 44 kt was reported.

By 1300 GMT, an arc cloud was evident in the visible satellite image (Fig. 31). The arc cloud extended from southeastern Oklahoma to central Texas. At 1600 GMT, the gust front and mesohigh were still discernible in the surface analysis and the arc cloud was clearly evident in the satellite images (not shown).

Table 9 shows the characteristics associated with the MCC. Although the characteristics were not as pronounced as some of the previous category 1 MCSs, heavy precipitation fell for a significant time. The sum of the three largest hourly precipitation rates stayed above 1.5 in h^{-1} for five consecutive hours.

Category 2 MCSs

Category 2 MCSs are defined as follows: The MCS produces a gust front and the gust front persists for 6 h or less. Four MCSs are classified in this category. The four MCSs are from Cases 1, 5, 6 and 9. A brief discussion of the synoptic situation and storm characteristics associated with each category 2 MCS follows.

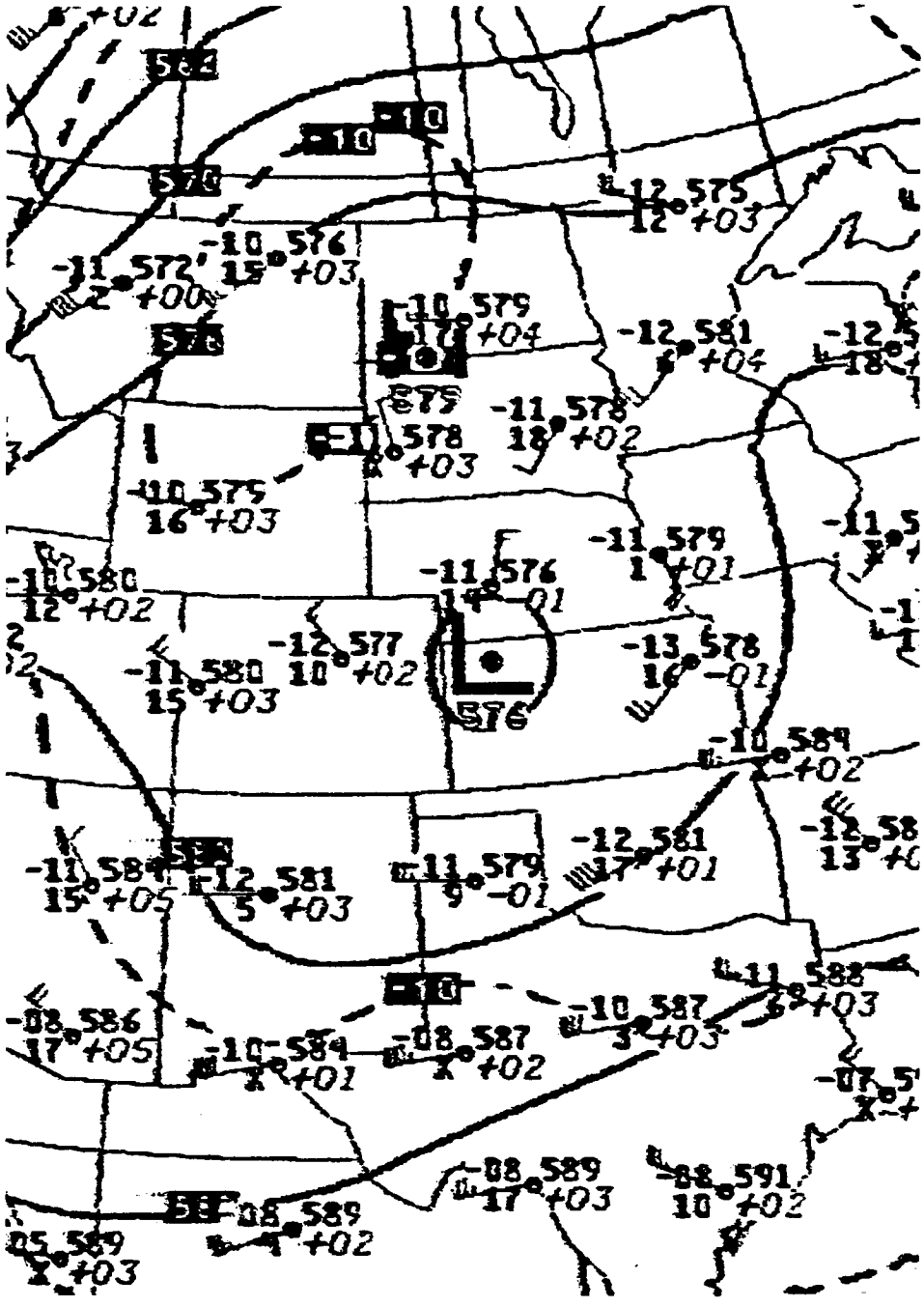

Fig. 30. 50 kPa height (dm) and temperature (°C) fields for 0000 GMT 11 June 1983. Height contours (solid lines) are every 60 m; isotherms (dashed lines) are every 5°C.

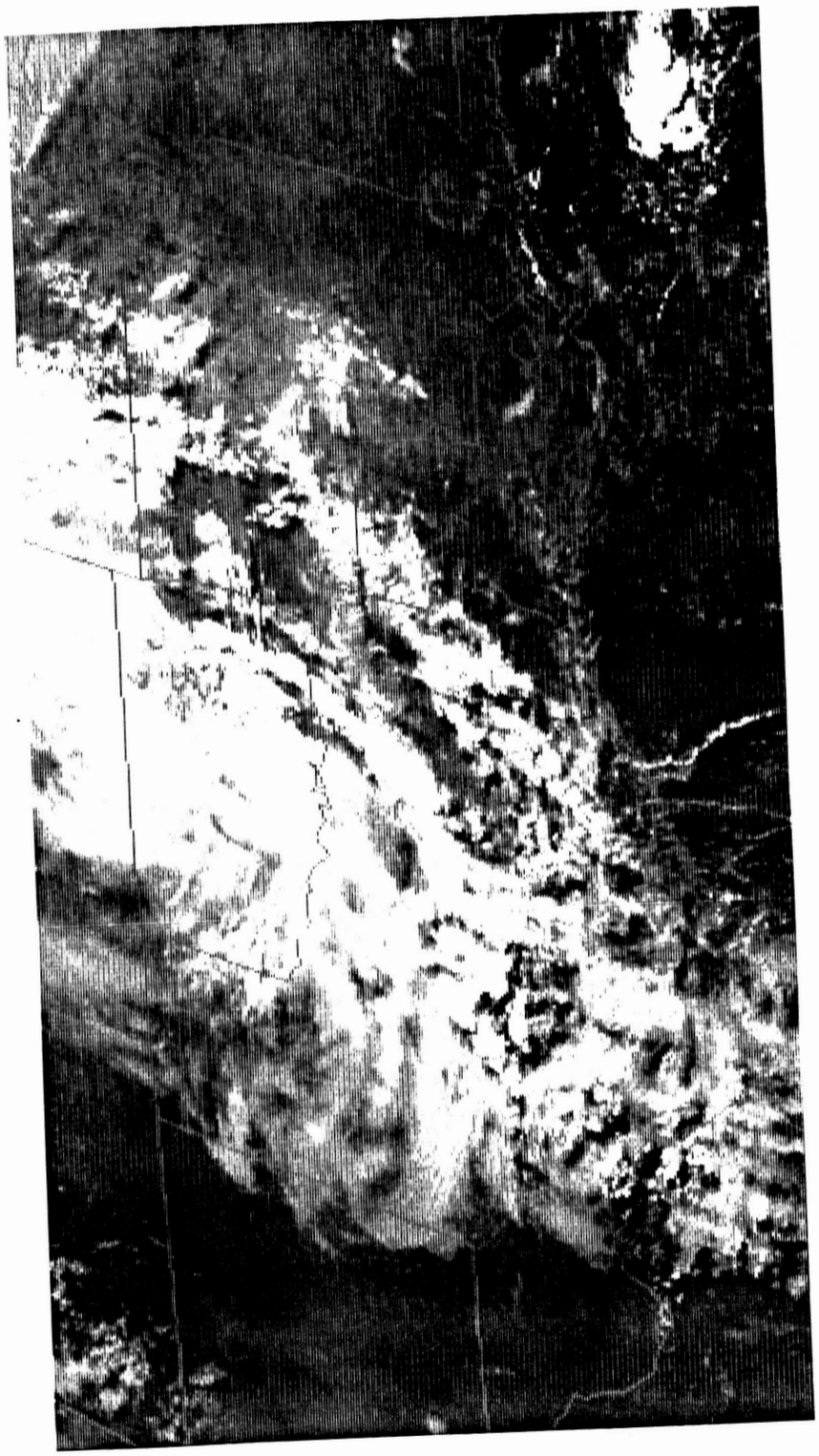

Fig. 31. GOES visible image for 1300 GMT 11 June 1983.

Table 9. Characteristics associated with the MCC of Case 11 (11 June 1983). The maximum thunderstorm heights were determined at approximately 35 min past each hour. Dashes indicate that the parameter was not determined.

Time (GMT)	Maximum thunderstorm height (x 100 ft)	Maximum surface divergence (x 10^{-5} s^{-1})	Sum of the three largest precipitation rates (in h^{-1})	Maximum point precipitation rate (in h^{-1})	Coldest cloud top temperature (°C)
0200	-	-	0.16	0.10	-
0300	-	-	1.12	0.50	-
0400	500	-3	0.67	0.40	-58
0500	510	-3	1.10	0.60	-58
0600	520	-1	2.30	0.90	-63
0700	510	-3	1.80	0.70	-63
0800	450	-2	1.60	0.60	-63
0900	440	3	2.00	0.90	-68
1000	390	1	1.55	0.60	-63
1100	320	2	1.08	0.50	-58
1200	310	2	0.88	0.44	-58
1300	300	-	0.01	0.01	-
1400	300	-	0.30	0.10	-

Case 1: 10/11 April 1981

On 10 April 1981 an MCC developed over the Texas panhandle during the late afternoon. It developed along a stationary front, which extended from southeastern Minnesota to north central Kansas and then southward to the Texas panhandle. Convection occurred all along this front (see Fig. 32). The MCC developed in response to a short wave in the mid-troposphere. Of course, a number of other conditions must have co-existed to support MCC development, such as lower tropospheric warm advection, ample moisture and convective instability (Maddox, 1981). Fig. 33 shows the 70 kPa analysis for 0000 GMT 11 Apr 1981. The short wave trough line is clearly evident, located over the western portion of the Texas panhandle.

By 0200 GMT 11 Apr 1981, an organized surface high pressure system and gust front, produced by the downdrafts of the thunderstorms associated with the MCC, first appeared. Fig. 34 shows the surface analysis for 0300 GMT. The gust front, denoted by the cold front symbols, was located from just west of Oklahoma City, OK (OKC), to Fort Sill, OK (FSI) and southwestward to just south of Childress, TX (CDS). Note the west wind at Hobart, OK (HBR) and the southeastern winds at Amarillo, TX (AMA) and Dalhart, TX (DHT). These diverging winds are a typical pattern associated with the presence of the mesohigh and gust front. Fig. 32 shows the surface divergence field overlaid upon the GOES IR imagery, both for 0300 GMT. A well-organized divergence pattern, with magnitudes up to 4×10^{-5} s^{-1}, was centered over the northeastern Texas panhandle.

The MCC terminated at 0531 GMT (see Table 2, page 19). The gust front quickly lost its identity and by 0700 GMT was no longer evident in

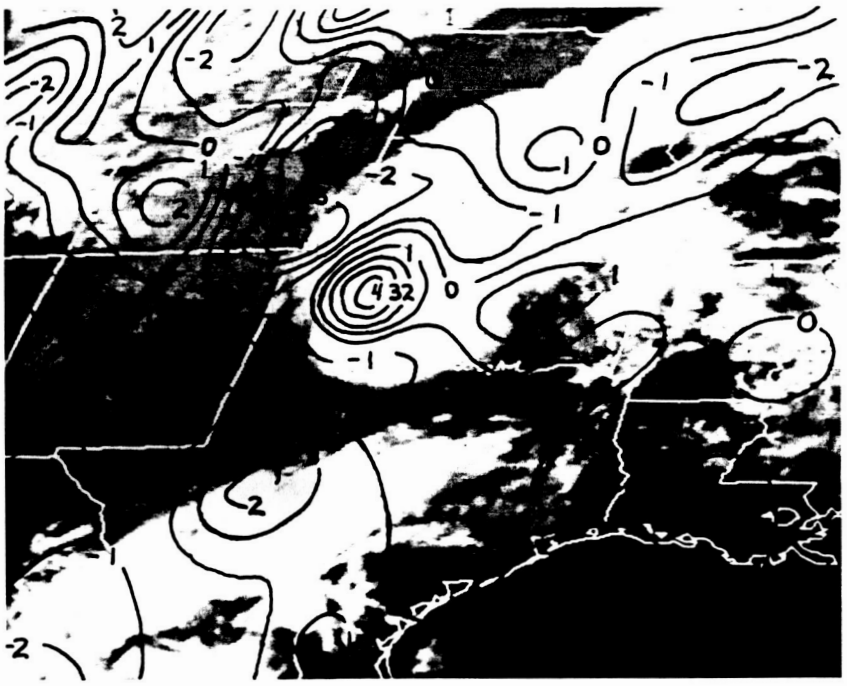

Fig. 32. Surface divergence field overlaid upon GOES IR image for 0300 GMT 11 April 1981. Values are times 10^{-5} s^{-1} and isolines are drawn at an increment of 1 x 10^{-5} s^{-1}.

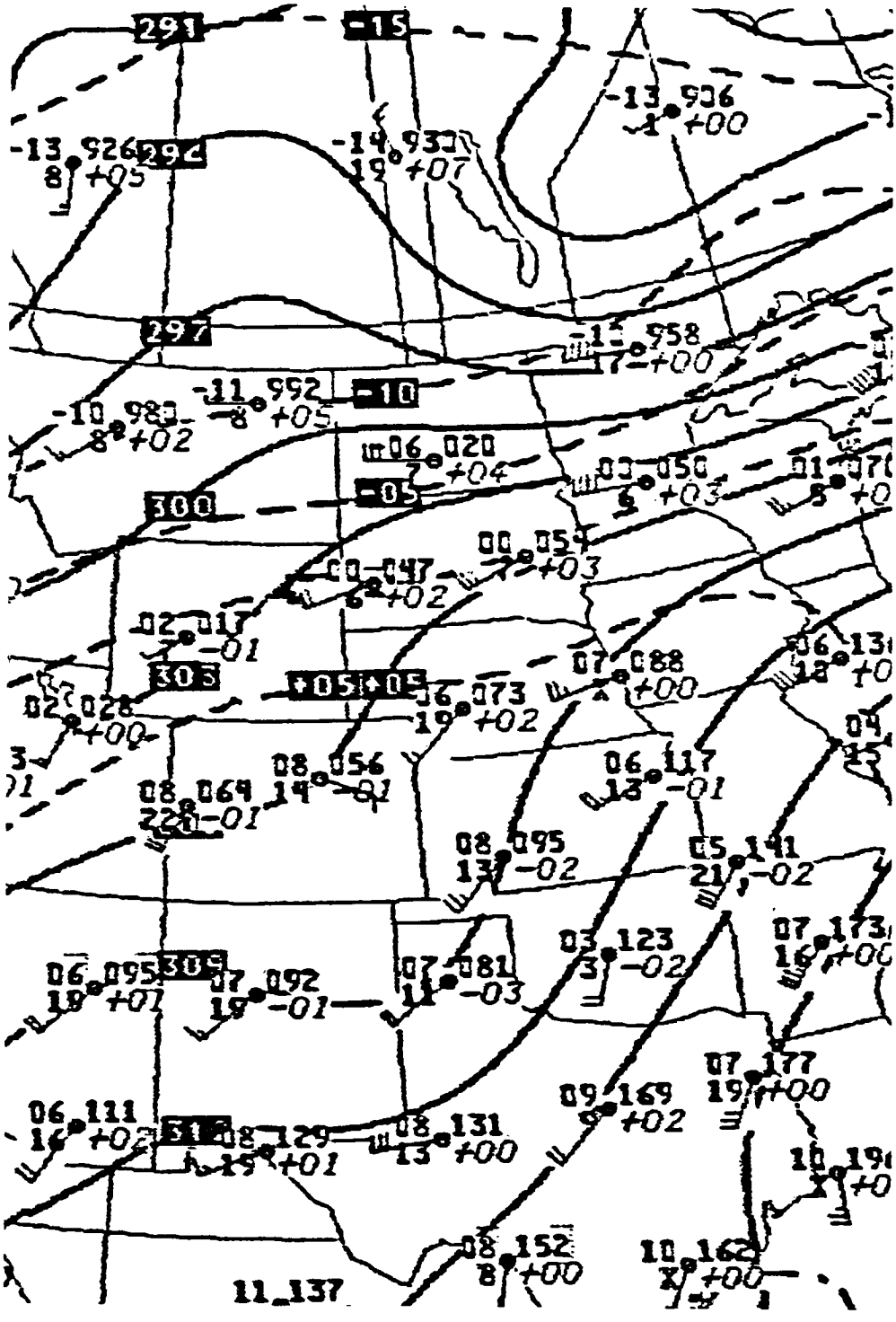

Fig. 33. 70 kPa height (dm) and temperature (°C) fields for 0000 GMT 11 April 1981. Height contours (solid lines) are every 30 m; isotherms (dashed lines) are every 5°C.

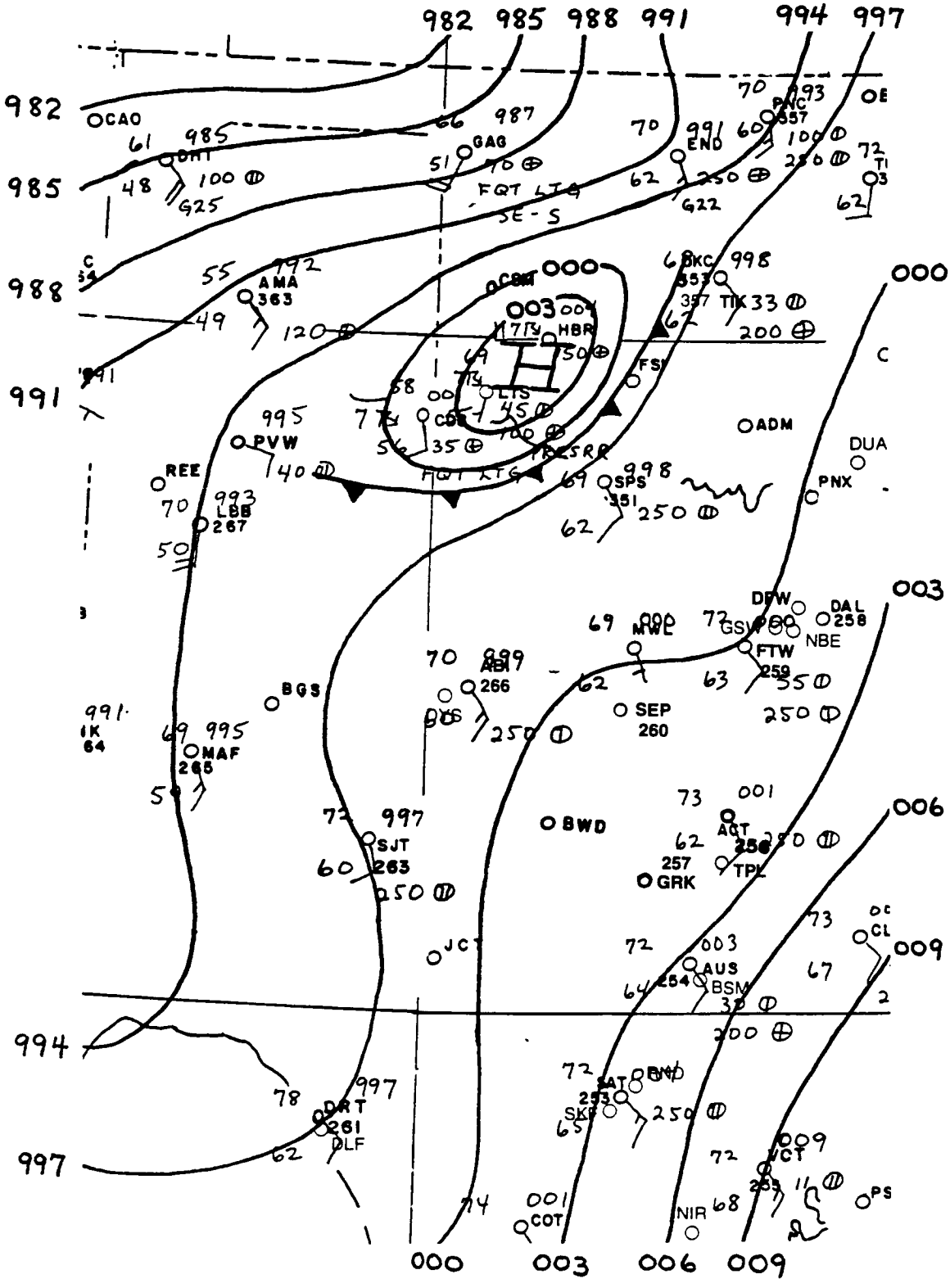

Fig. 34. Surface pressure field for 0300 GMT 11 April 1981. Altimeter setting contours are every 0.03 in Hg. The gust front is denoted by a cold front symbol.

the surface analysis (not shown). Therefore, the gust front lasted for 5 h, from 0200 to 0700 GMT. No arc cloud was ever apparent in the satellite images.

Table 10 shows specific characteristics associated with this MCC. The maximum thunderstorm height of 56,000 ft occurred at 0435 GMT. After the termination of the MCC, as expected, the heights quickly lowered. The hourly surface divergence reached its maximum at 0200 and 0300 GMT, near the time of maximum extent (see Table 2) of the system, as measured by the number of pixels in the IR satellite imagery contained by the -62°C isotherm. The surface divergence slowly weakened thereafter, which indicated the gust front was also weakening. The maximum sum of the three largest hourly precipitation rates and the largest point precipitation rate were 1.5 in h^{-1} and 1.0 in h^{-1}, respectively. These rainfall rates are rather light compared to the MCSs classified in category 1. The coldest hourly cloud top temperatures followed a similar pattern as the maximum hourly thunderstorm tops; a rapid warming of the temperatures, which corresponds to a lowering of the thunderstorm heights, occurred shortly after termination of the MCC.

Case 5: 19 May 1982

During the nighttime hours of 19 May 1982, two MCSs developed over western Kansas and western Oklahoma. The first MCS began forming around 0030 GMT and subsequently dissipated around 0800 GMT. The second MCS, the one of most importance for this study, formed around 0800 GMT, in western Oklahoma and dissipated by 1300 GMT. Fig. 35 shows the GOES IR image at 0800 GMT. The first MCS, now dissipated, was located in

Table 10. Characteristics associated with the MCC of Case 1 (10/11 April 1981). The maximum thunderstorm heights were determined at approximately 35 min past each hour. Dashes indicate that the parameter was not determined.

Time (GMT)	Maximum thunderstorm height (x 100 ft)	Maximum surface divergence (x 10^{-5} s^{-1})	Sum of the three largest precipitation rates (in h^{-1})	Maximum point precipitation rate (in h^{-1})	Coldest cloud top temperature (°C)
2300	510	-	0.59	0.40	-
0000	500	-	0.50	0.20	-63
0100	460	2	0.00	0.00	-63
0200	510	4	0.30	0.20	-63
0300	490	4	1.40	0.80	-63
0400	560	3	1.50	1.00	-63
0500	530	2	1.17	0.50	-63
0600	500	2	0.62	0.40	-58
0700	430	2	0.30	0.10	-
0800	300	2	0.50	0.30	-
0900	-	1	0.13	0.10	-
1000	-	1	0.10	0.10	-

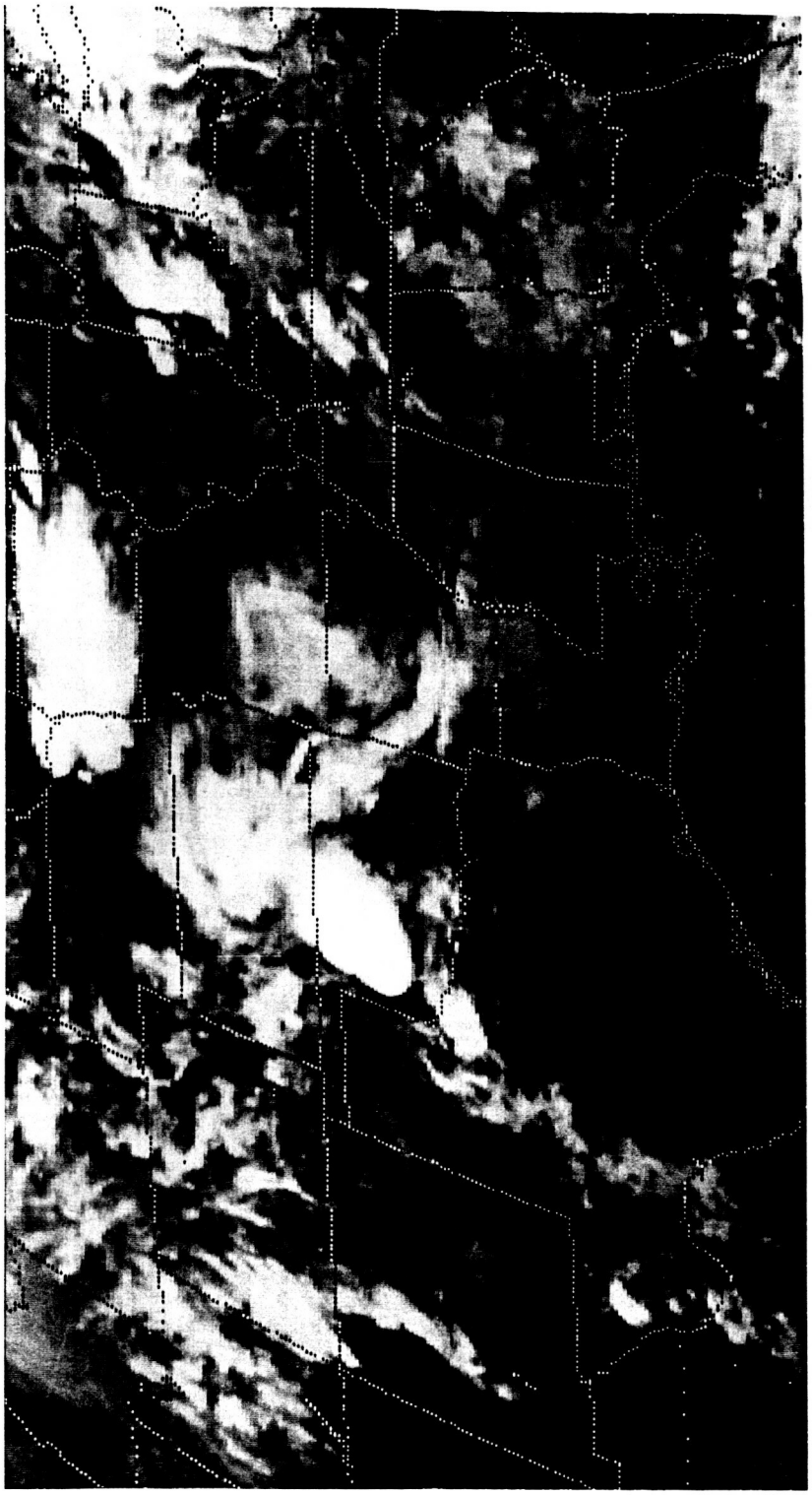

Fig. 35. GOES IR image for 0800 GMT 19 May 1982.

central Kansas. The second MCS, in the development stage, was located in western Oklahoma.

The mid-tropospheric flow pattern, associated with the development of the MCSs, is depicted in the 50 kPa analysis, Fig. 36. A deepening, negatively tilted trough, encompassed the western United States. However, the axis of a weak ridge was located just to the west of the development region. There was no indication in the flow, over the development region, of a weak embedded trough, which normally accompanies the formation of MCSs. This might have been one factor which led to the short duration of the MCSs.

A weak mesohigh and gust front, associated with the second MCS, appeared over western Oklahoma at 1000 GMT. By 1100 GMT, evidence of a small arc cloud could be seen in the GOES IR image. However, the gust front, mesohigh and arc cloud were undetectable in the surface analysis and satellite images after 1600 GMT.

Brundidge (1983) also studied this case. He gave three reasons for the short life and relative unimportance of this arc cloud:

1. The cold-air layer at the ground was very shallow, amounting to only about 200 m in depth.

2. The wind in the shallow layer had no northerly component; therefore, the outflow was not undercutting and lifting the warm, moister, surface air in northern Texas to maintain convection.

3. It appeared that the storm was simultaneously raining itself out and drawing drier air into the system, thus reducing the energy supply.

Table 11 shows the characteristics associated with primarily the

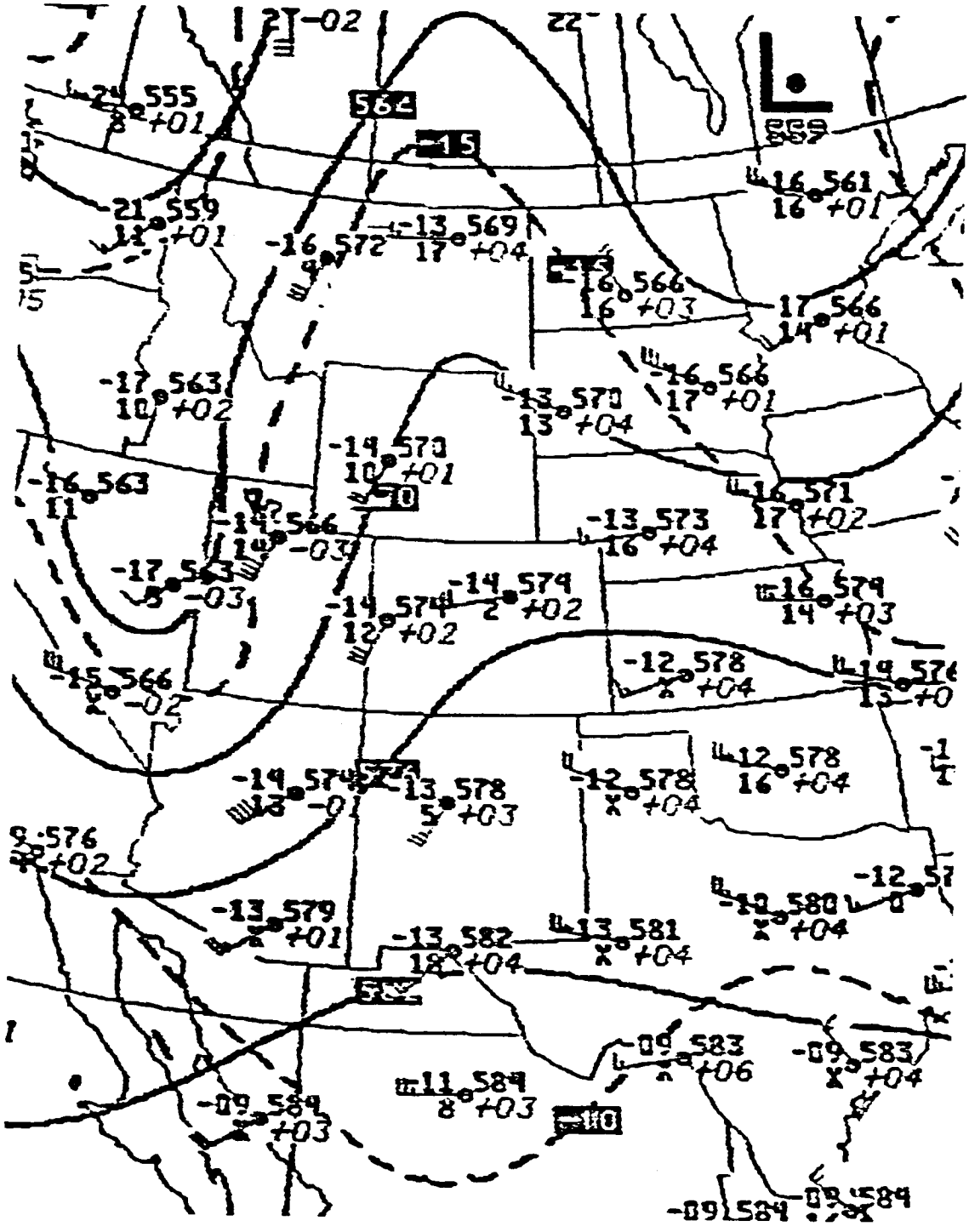

Fig. 36. 50 kPa height (dm) and temperature (°C) fields for 0000 GMT 19 May 1982. Height contours (solid lines) are every 60 m; isotherms (dashed lines) are every 5°C.

Table 11. Characteristics associated with the MCS of Case 5 (19 May 1982). The maximum thunderstorm heights were determined at approximately 35 min past each hour. Dashes indicate that the parameter was not determined.

Time (GMT)	Maximum thunderstorm height (x 100 ft)	Maximum surface divergence (x 10^{-5} s^{-1})	Sum of the three largest precipitation rates (in h^{-1})	Maximum point precipitation rate (in h^{-1})	Coldest cloud top temperature (°C)
0300		-	0.08	0.05	-
	490				
0400		3	0.08	0.08	-63
	460				
0500		3	0.12	0.09	-63
	420				
0600		1	0.32	0.17	-63
	490				
0700		1	0.52	0.32	-63
	490				
0800		1	0.23	0.20	-63
	450				
0900		-1	1.19	1.10	-63
	420				
1000		0	1.05	0.60	-63
	380				
1100		0	1.50	1.00	-63
	400				
1200		1	0.30	0.10	-58
	350				
1300		-	0.70	0.50	-
	310				
1400		-	0.10	0.10	-
	290				

second MCS. However, any characteristics given before 0800 GMT were associated with the first MCS. Similar to Case 1, the characteristics were very weak. For the second MCS, the maximum thunderstorm height was only 45,000 ft and the maximum surface divergence was only 1 x 10^{-5} s^{-1}. The maximum sum of the three largest hourly rainfall rates was 1.5 in h^{-1}, the same as Case 1. Also, the largest hourly point precipitation rate was only 1.1 in h^{-1}, compared to 1.0 in h^{-1} for Case 1. Lastly, the coldest cloud top temperature was only -63°C.

Case 6: 10/11 June 1982

A very large MCC formed over western Texas on 10 June 1982. At 50 kPa, near zonal flow existed over the development area at 0000 GMT 11 June 1982 (Fig. 37). At the same time, very strong warm advection was present at both 85 and 70 kPa (not shown). Maddox (1983), in view of the quasi-geostrophic equations (in particular the tendency and omega equations), noted that the MCC develops in a region of upward vertical motion and that the upward motion "is primarily a reflection of strong low-level warm advection rather than of strong differential PVA."

The lifetime of the MCC, initiation to termination, was 2245 GMT 10 June 1982 to 1530 GMT 11 June 1982. Analysis of the cloud top temperatures, provided by the McIDAS and the plotted precipitation rates, revealed that the MCC actually consisted of two separate MCSs. The first MCS developed in the Texas panhandle and moved into southwest Oklahoma. The most intense phase of the MCS lasted from approximately 0300 to 0800 GMT. Fig. 38 shows the surface divergence overlaid upon the GOES IR imagery with MB enhancement, both for 0700 GMT. According

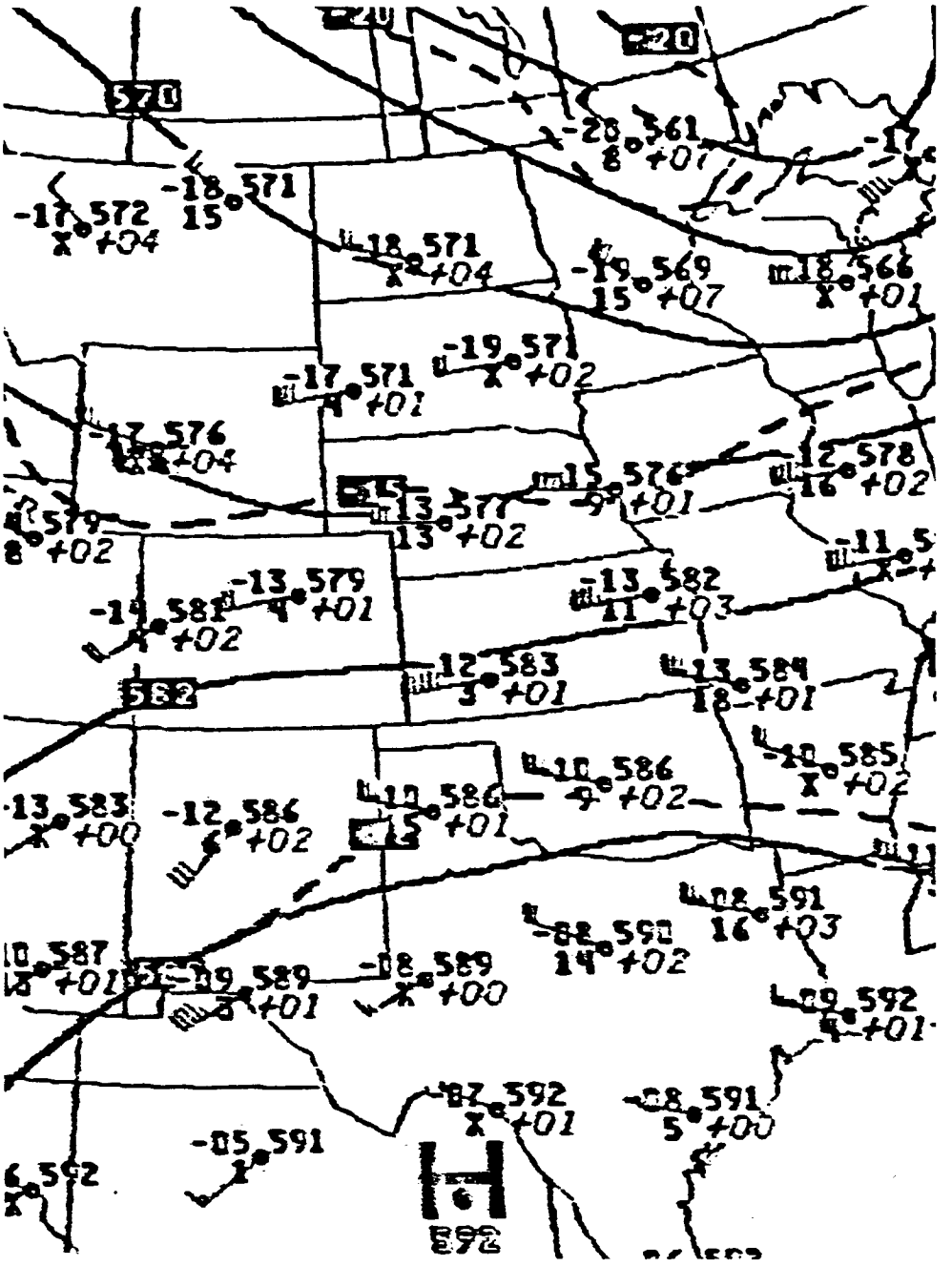

Fig. 37. 50 kPa height (dm) and temperature (°C) fields for 0000 GMT 11 June 1982. Height contours (solid lines) are every 60 m; isotherms (dashed lines) are every 5°C.

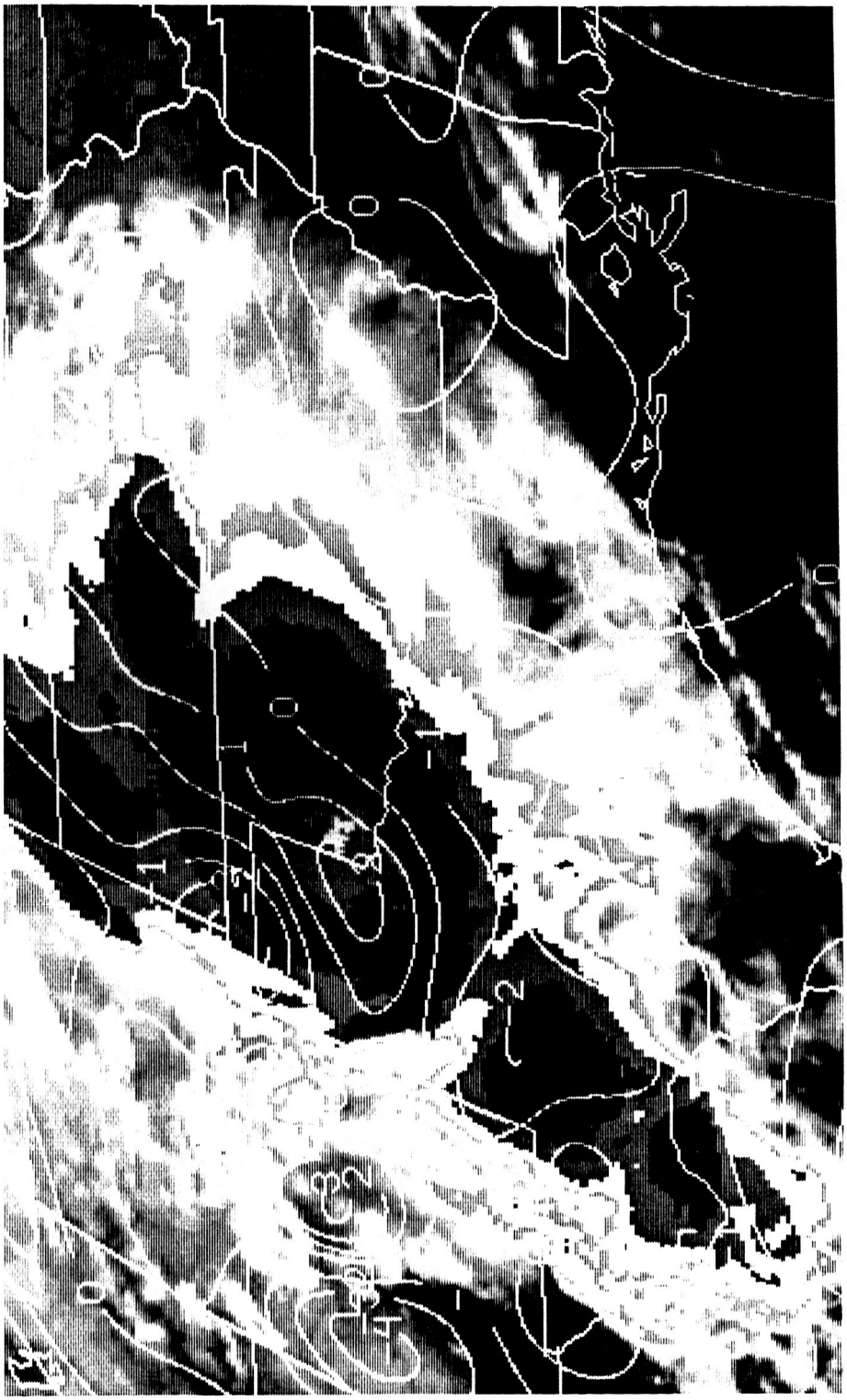

Fig. 38. Surface divergence field overlaid upon GOES IR image for 0700 GMT 11 June 1982. Values are times 10^{-5} s^{-1} and isolines are drawn at an increment of 1 x 10^{-5} s^{-1}.

to the MB enhancement curve, the large black area in the Texas panhandle and in western Oklahoma, corresponds to cloud top temperatures between -58°C and -62°C. The repeat gray area and the whitish area, enclosed by the black area, represent the coldest cloud top temperatures. Therefore, the maximum thunderstorm tops associated with the first MCS were located in the eastern portions of the Texas panhandle and in southwestern Oklahoma. An organized mesohigh and gust front, produced by this MCS, appeared in the surface analysis at 0500 GMT (Fig. 39). After the demise of the MCS, the mesohigh and gust front weakened. By 1000 GMT, the mesohigh and gust front were ill-defined in the surface analysis. The second MCS developed in northeastern Oklahoma, around the time the first MCS was terminating. The mesohigh and gust front associated with the second MCS were much weaker than those produced by the first MCS. No arc cloud was produced by either MCS.

The characteristics of the first MCS are displayed in Table 12. The sum of the three largest hourly precipitation rates stayed above 1.5 in h^{-1} for only 3 h. Of the two precious MCSs classified in category 2, this sum stayed at or above 1.5 in h^{-1} for only 1 h. Another interesting feature is exhibited in the trend of the maximum hourly surface divergence. The magnitudes of the divergence were strong, as high as 4×10^{-5} s^{-1}, before the demise of the mesohigh and gust front. However, after 1000 GMT, the divergence weakened, which corresponded to the weakening of the mesohigh and gust front.

Case 9: 28/29 June 1982

A short-lived MCC developed over northeastern Texas during the

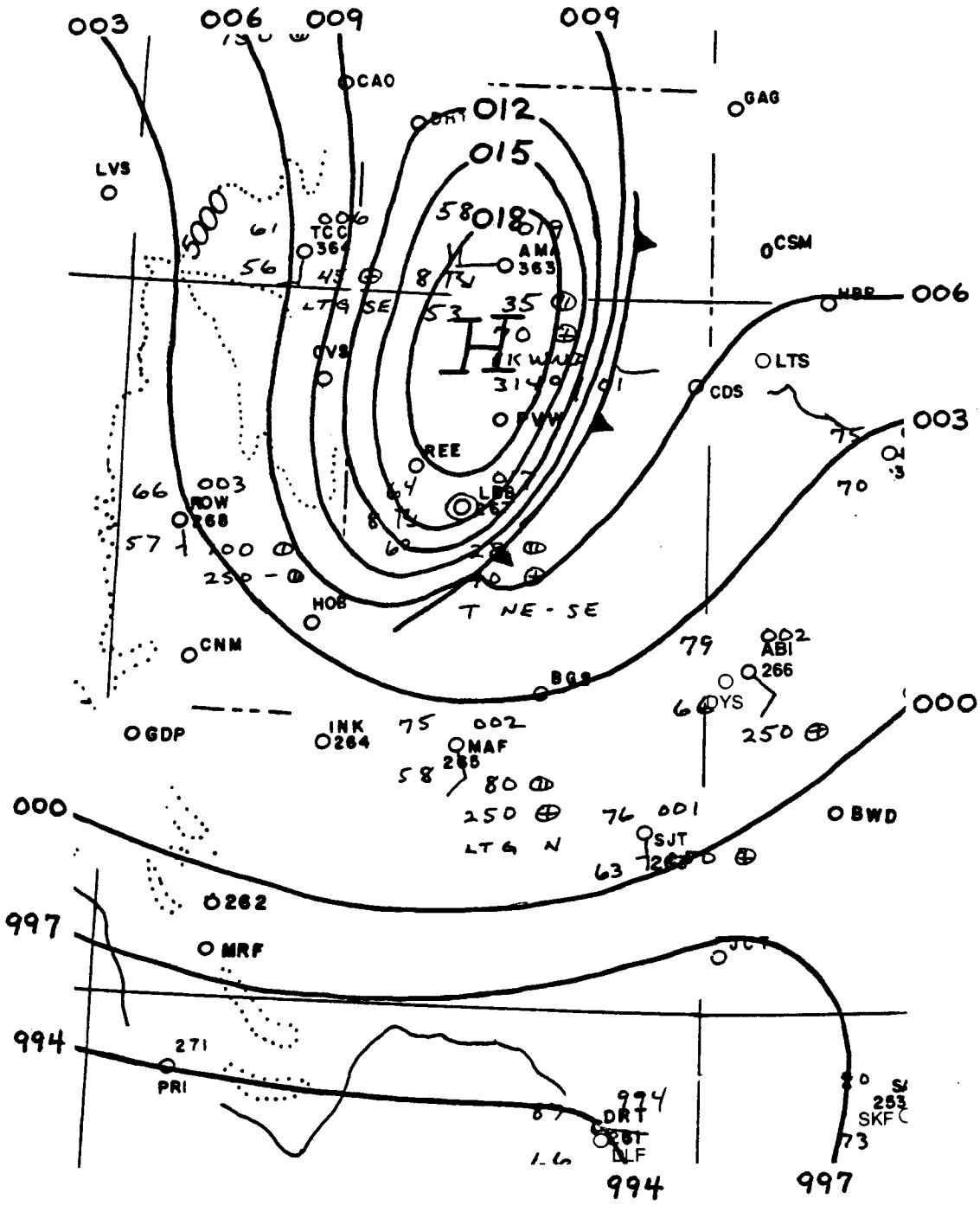

Fig. 39. Surface pressure field for 0500 GMT 11 June 1982. Altimeter setting contours are every 0.03 in Hg. The gust front is denoted by a cold front symbol.

Table 12. Characteristics associated with the MCC of Case 6 (11 June 1982). The maximum thunderstorm heights were determined at approximately 35 min past each hour. Dashes indicate that the parameter was not determined.

Time (GMT)	Maximum thunderstorm height (x 100 ft)	Maximum surface divergence (x 10^{-5} s^{-1})	Sum of the three largest precipitation rates (in h^{-1})	Maximum point precipitation rate (in h^{-1})	Coldest cloud top temperature (°C)
0100	-	-	1.40	1.00	-
0200	520	-	0.40	0.20	-
0300	530	-	1.20	1.00	-
0400	550	2	1.32	0.70	-73
0500	540	4	1.99	0.90	-73
0600	550	3	2.59	1.30	-73
0700	500	2	1.83	0.70	-73
0800	460	3	0.91	0.31	-73
0900	480	4	1.40	0.70	-68
1000	410	3	1.40	0.70	-68
1100	340	1	0.57	0.20	-
1200	380	2	0.22	0.10	-
1300	400	1	0.29	0.10	-

afternoon of 28 June 1982. Fig. 40 depicts the 50 kPa analysis for 0000 GMT 29 June 1982. This was near the initiation time of the MCC. An upper level trough was associated with the MCC and a very pronounced ridge was situated to the west. At 85 kPa, warm air advection (i.e., quasi-geostrophically forced upward motion) was evident over eastern Texas (not shown). Absolute moisture contents within the air mass feeding the MCC were high. For instance, at 85 kPa, the moisture content for Victoria, TX (VCT) was 11 g kg^{-1} at 0000 GMT 29 June 1982. Maddox (1982), in a composite study of 10 MCCs, described a similar synoptic setting for the development of MCCs.

At 0000 GMT 29 June 1982, a gust front and mesohigh appeared in the surface analysis (Fig. 41). The MCC terminated at 0430 GMT (see Fig. 42). By 0500 GMT the gust front and mesohigh had virtually disappeared in the surface analysis (Fig. 43). The weakness of the gust front, during its lifetime, was verified by the lack of strong winds as it passed reporting weather stations. The strongest wind gust was only 15 kt, which occurred at both Lufkin, TX (LFK) and College Station, TX (CLL). No arc cloud was produced by this MCC.

The characteristics associated with the MCC are depicted in Table 13. The maximum hourly thunderstorm heights were impressive, reaching 58,000 ft at 0135 GMT. However, the heights quickly lowered after 0235 GMT. The maximum surface divergence reached magnitudes of 3×10^{-5} s^{-1} at 0400 and 0500 GMT and then rapidly weakened. The sum of the three largest hourly precipitation rates and the maximum hourly point precipitation rates were quite large before 0100 GMT, but dramatically dropped thereafter. As the precipitation rates decreased, the coldest cloud top

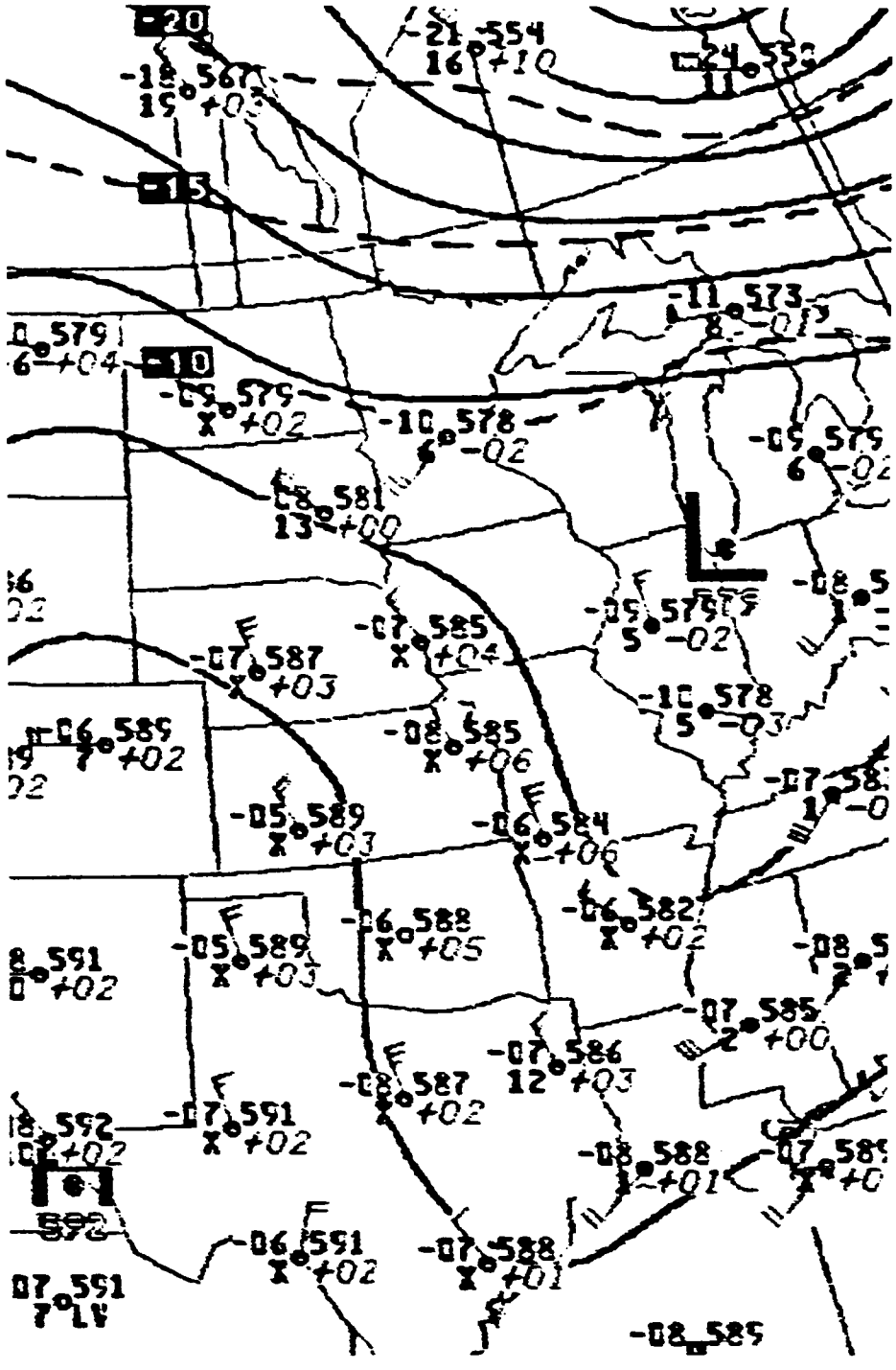

Fig. 40. 50 kPa height (dm) and temperature (°C) fields for 0000 GMT 29 June 1982. Height contours (solid lines) are every 60 m; isotherms (dashed lines) are every 5°C.

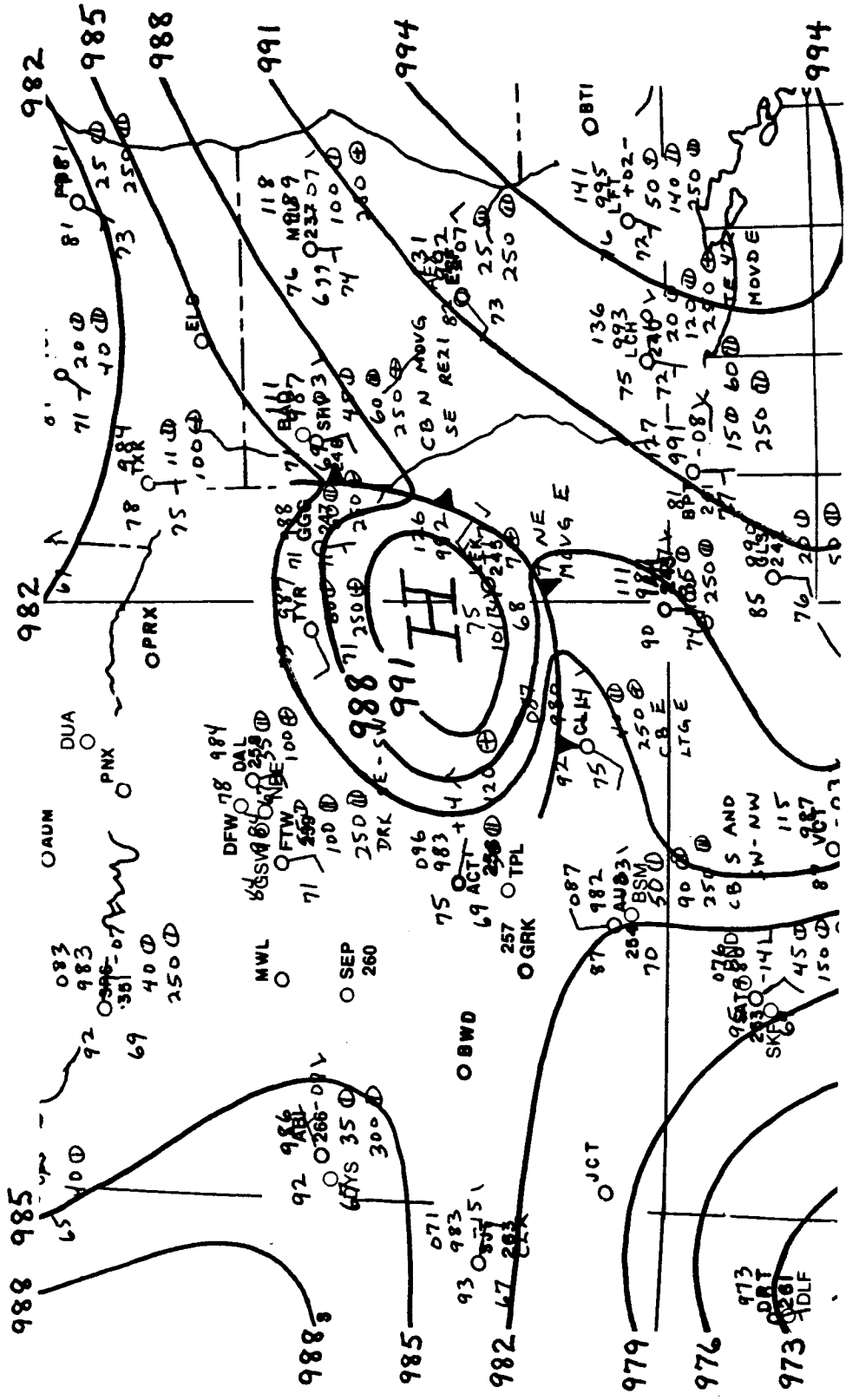

Fig. 41. Surface pressure field for 0000 GMT 29 June 1982. Altimeter setting contours are every 0.03 in Hg. The gust front is denoted by a cold front symbol.

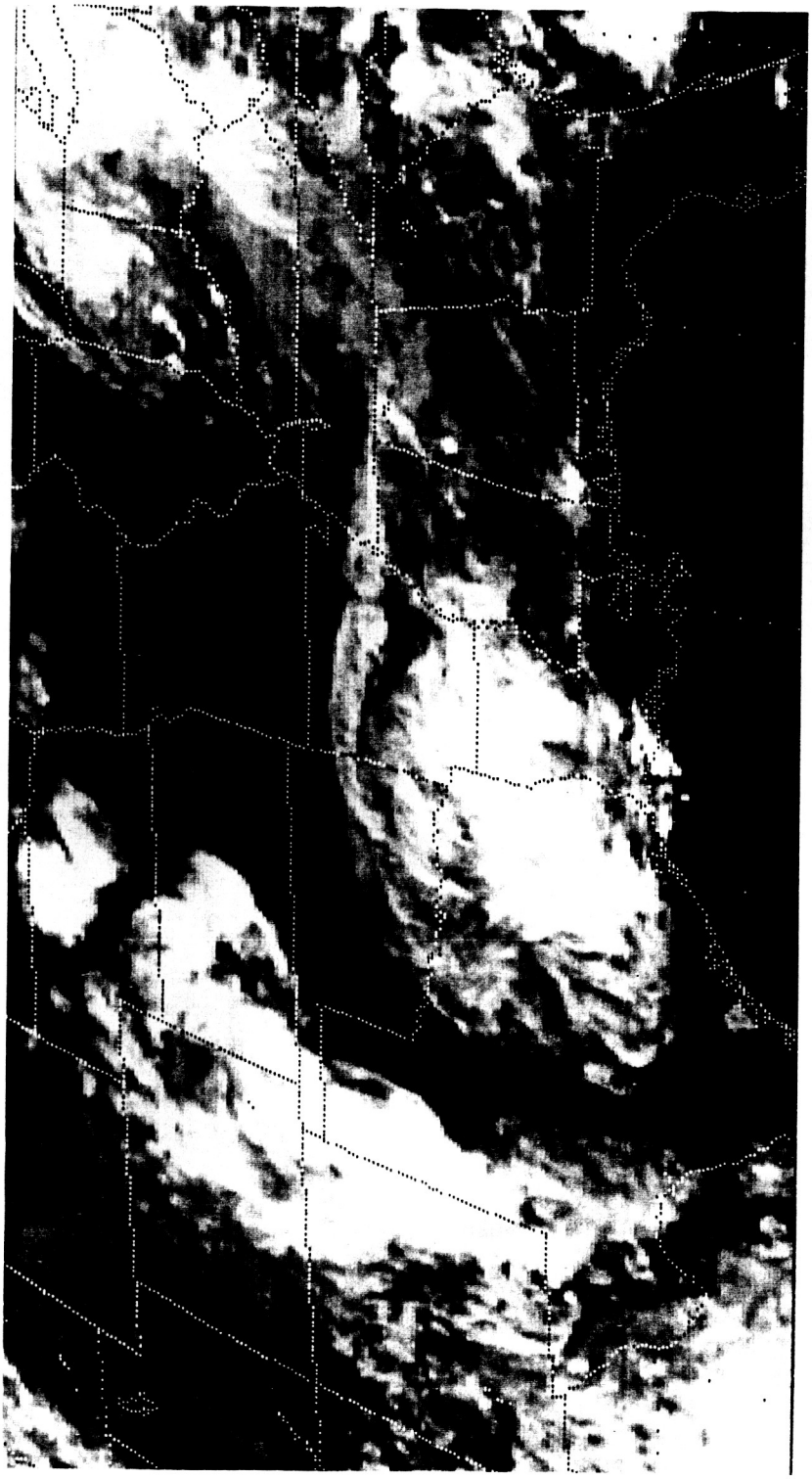

Fig. 42. GOES IR image for 0430 GMT 29 June 1982.

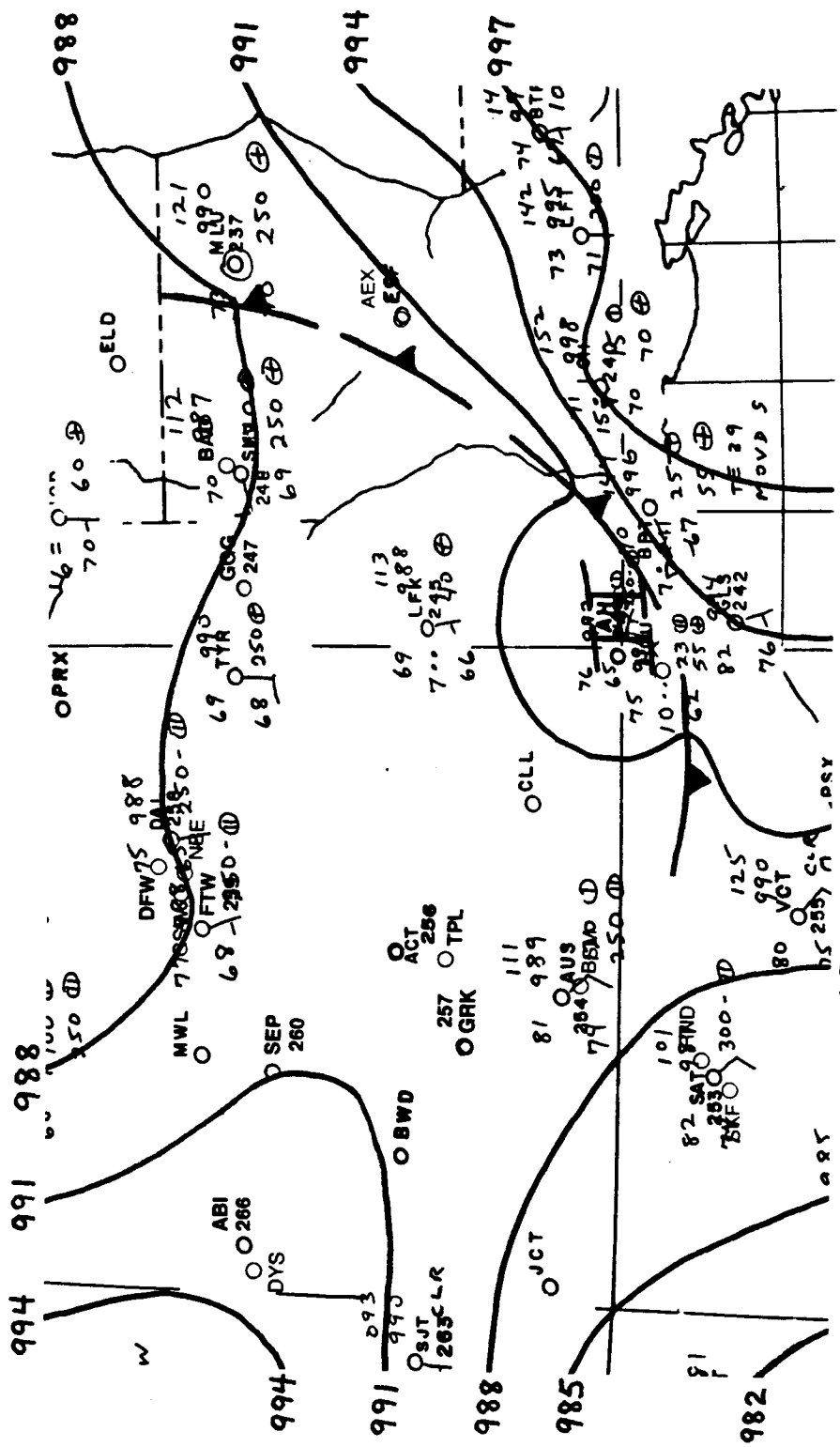

Fig. 43. Surface pressure field for 0500 GMT 29 June 1982. Altimeter setting contours are every 0.03 in Hg. The gust front is denoted by a cold front symbol.

Table 13. Characteristics associated with the MCC of Case 9 (28/29 June 1982). The maximum thunderstorm heights were determined at approximately 35 min past each hour. Dashes indicate that the parameter was not determined.

Time (GMT)	Maximum thunderstorm height (x 100 ft)	Maximum surface divergence (x 10^{-5} s^{-1})	Sum of the three largest precipitation rates (in h^{-1})	Maximum point precipitation rate (in h^{-1})	Coldest cloud top temperature (°C)
2100	510	-	2.72	1.62	-
2200	500	-2	2.46	0.90	-73
2300	570	0	1.80	1.00	-73
0000	550	1	0.99	0.40	-68
0100	580	0	1.60	1.30	-73
0200	550	1	0.60	0.40	-68
0300	450	2	0.50	0.30	-63
0400	420	3	0.88	0.48	-58
0500	340	3	0.23	0.17	-53
0600	360	1	0.40	0.20	-
0700	-	-1	0.20	0.10	-
0800	-	-	0.10	0.10	-
0900	-	-	0.10	0.10	-

temperatures warmed, which agrees with the findings of Gagin et al. (1985).

Case 12: 14 June 1983

During the afternoon of 13 June 1983, convection formed along a strong cold front, which was located through the central United States. An MCC developed near the southern portions of the cold front. By 0600 GMT 14 June 1983 it had reached its maximum extent. At this time, the MCC engulfed north central Texas and most of Oklahoma.

The precipitation pattern produced by the MCC was not typical of most MCCs. Heavy precipitation associated with the MCC fell exclusively along the cold front. Close inspection of the plotted hourly precipitation revealed that no precipitation fell along the southern edge of the MCC cloud shield. This was rather unusual, as many instances of an arc-shaped band of heavy precipitation along the southern portions of MCCs have been reported (Maddox, 1980, 1981; Leary and Rappaport, 1982; Howard and Maddox, 1983; and Bartels, 1983). Bartels (1983) stated, "Throughout the MCC life-cycle the most intense rainfall occurred near its southern periphery." Maddox (1980) argues that the most intense convective elements occur along the convergence zone produced by the interaction of the outflow boundary and the low-level inflow. This convergence zone occurs along the southern portion of the MCC. An example of this arc-shaped precipitation band, produced by the MCC from Case 2, is shown in Fig. 44. The arc-shaped band of heavy precipitation was located from eastern Texas to central Louisiana. Also, notice the circular shape in the overall precipitation pattern that was produced by

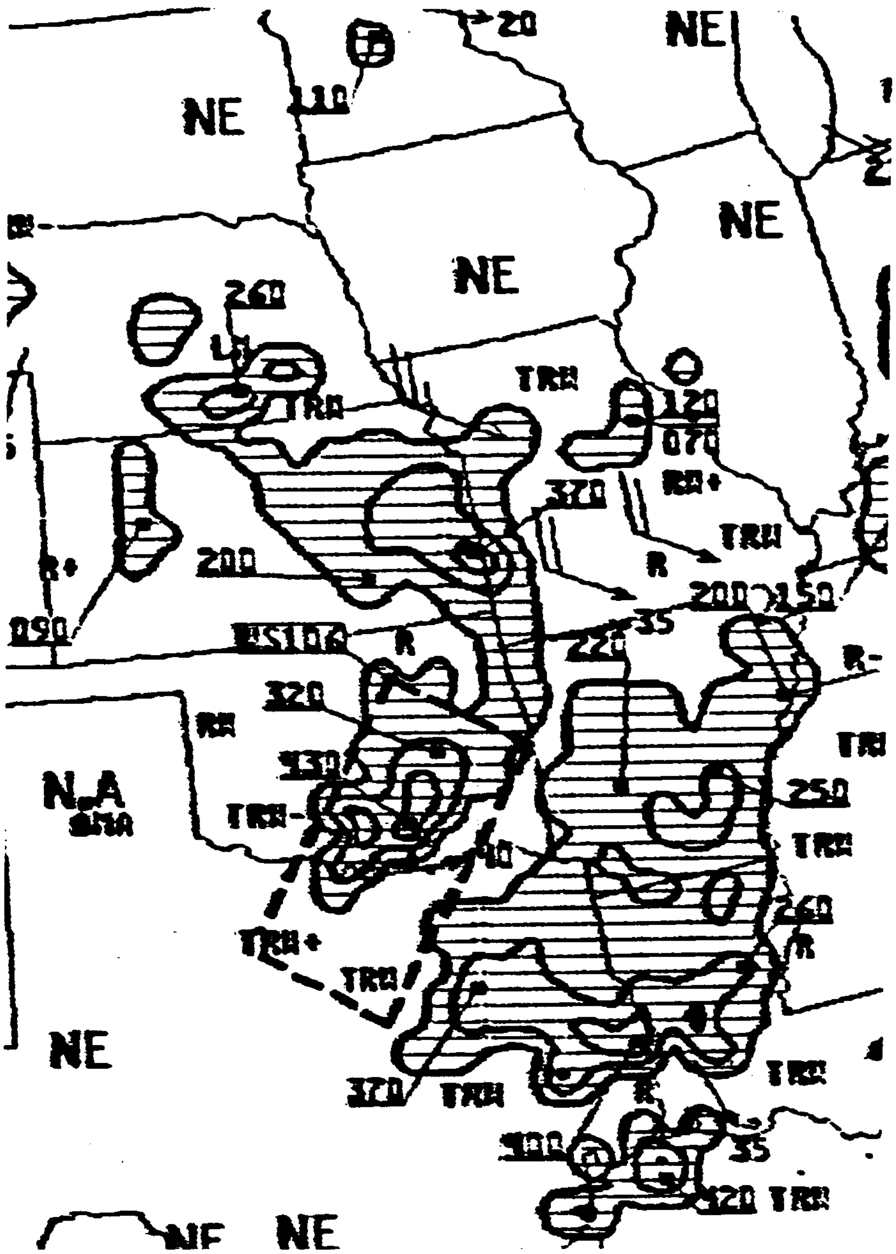

Fig. 44. Radar summary chart for 1035 GMT 9 May 1981. Shading indicated echo areas. Contours at echo intensities 1, 3, and 5; echo heights are in hundreds of feet; cell movement given at end of arrows in knots; area and line movement given by pennant with full barb = 10 kt.

the MCC of Case 2. This is typical of MCCs because of their circular shape, imposed by the MCC definition (refer to Table 1, page 3). In contrast, the precipitation pattern produced by the MCC of this case was markedly different. Fig. 45 displays this pattern and also shows the approximate location of the MCC cloud shield (scalloped area). There was no arc-shaped line of heavy precipitation on the southern periphery of the MCC. In fact, there was no precipitation falling there at all. Also, the overall precipitation pattern was much more elongated, like that produced by squall lines.

In summary, the precipitation pattern produced by the MCC of this case resembled that of a squall line, rather than an MCC. Therefore, this MCC was not classified in category 1 or 2 and was not used in the composite analyses (see next section).

Significant Events Associated with Category 1 and 2 MCSs

Table 14 summarizes the times that the following events occurred for both category 1 and 2 MCSs:

1. Maximum extent of the MCS.

2. First appearance of the gust front and mesohigh in the surface analysis.

3. First appearance, if any, of an arc cloud in the satellite images. In most cases, the first appearance of an arc cloud could only be determined by visible satellite images. It is extremely difficult to detect their existence in the IR images because arc clouds are normally composed of low, warm clouds. Therefore, the actual time of arc cloud formation could have been earlier than the time indicated in Table 14.

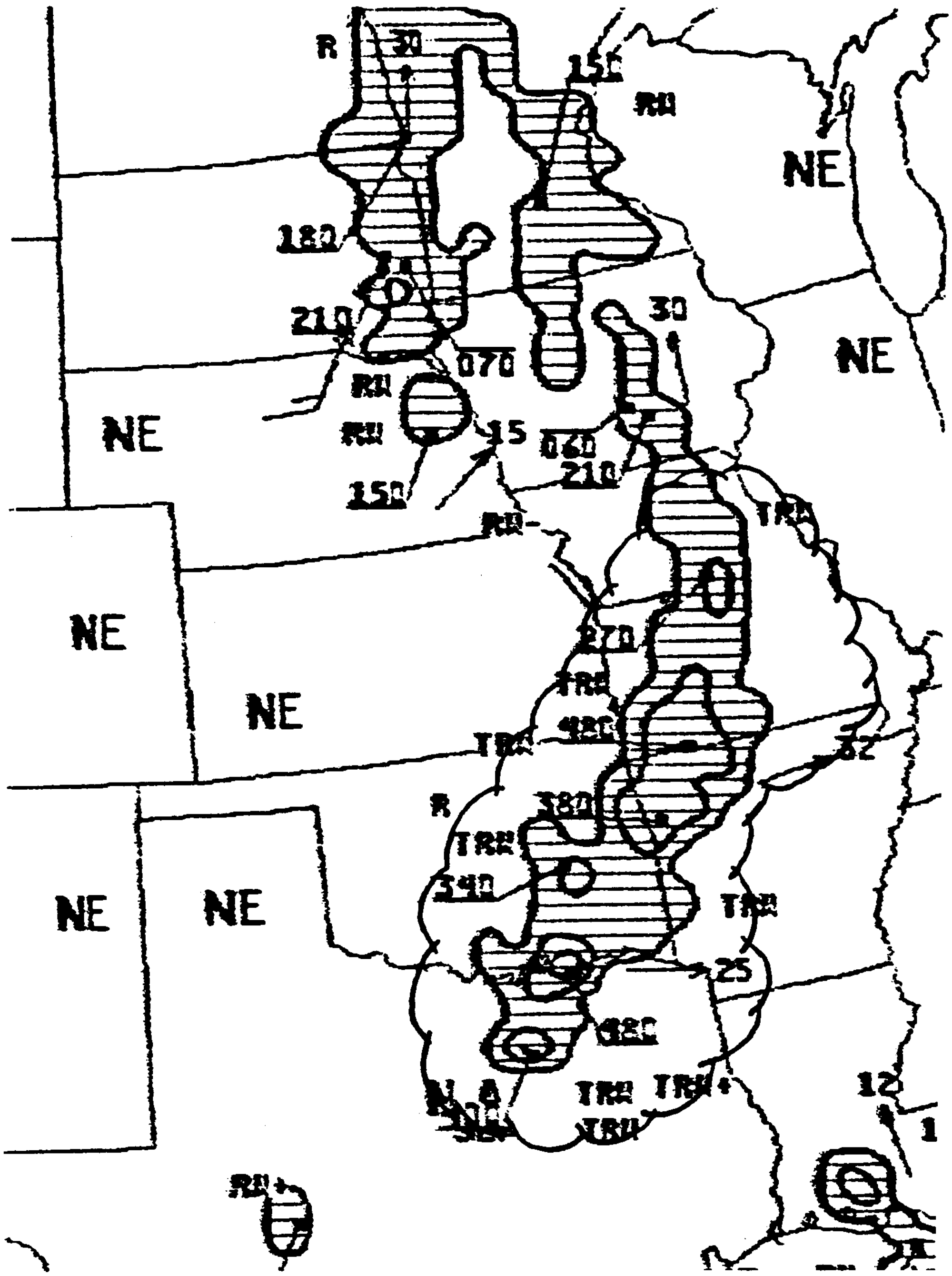

Fig. 45. Radar summary chart for 1035 GMT 14 June 1983. Shading indicates echo areas. Contours at echo intensities 1, 3, and 5; echo heights are in hundreds of feet; cell movement given at end of arrows in knots; area and line movement given by pennant with full barb = 10 kt. The scalloped area represents the approximate location of the MCC cloud shield at 1000 GMT 14 June 1983.

C-2

Table 14. Summary of significant events associated with category 1 and 2 MCSs. Time of MCS maximum extent, gust front/mesohigh first appearance in hourly surface analyses and arc cloud first appearance and termination, as determined by satellite imagery are listed.

Case number	Maximum extent (GMT)	Gust front/ mesohigh (GMT)	Arc cloud began (GMT)	Arc cloud ended (GMT)
		Category 1 MCSs		
2	0500	0500	1200	1800
3	1000	0700	1230	1800
4	0400	0200	1000	2200
7	1100	1100	1430	2200
8	0900	0800	1200	2100
10	0800	0400	1200	1800
11	0900	0800	1200	1800
		Category 2 MCSs		
1	0300	0200	none	none
5	0900	1000	1100	1600
6	0700	0500	none	none
9	0200	0000	none	none

4. The arc cloud, if any, became indistinguishable in the satellite images.

As seen in Table 14, all category 1 MCSs produced arc clouds. These MCSs, by definition, produced gust fronts that persisted for more than 6 h. In contrast, only one of the category 2 MCSs produced an arc cloud. These MCSs, by definition, produced gust fronts of shorter duration, lasting 6 h or less.

CHAPTER IV

COMPOSITE ANALYSES

To determine any differences between the MCSs of the two categories, composite analyses of the five following characteristics were accomplished:

1. Maximum hourly thunderstorm height.
2. Maximum hourly surface divergence.
3. Sum of the three largest precipitation rates.
4. Maximum hourly point precipitation rate.
5. Coldest hourly cloud top temperature.

Method of the Composite Analyses

The maximum extent of each MCS was determined by the McIDAS (see Table 2, page 19). The time of maximum extent, as defined in this research, occurred when the area, as depicted in IR satellite imagery, with temperatures less than or equal to -62°C, reached its maximum size.

For the composite analyses, the time of maximum extent was referred to as the zero (0) hour or zero (0) reference time. That is, this time was used as a reference time for all MCSs and determined when all the MCSs were at the same stage in their life-history. The hours before the maximum extent were defined as minus (-) hours and the hours after the maximum extent were defined as plus (+) hours. For example, the maximum extent time of the MCC for Case 1 was 0300 GMT 11 April 1981. Therefore, 0300 GMT was referred to as the zero (0) reference hour. 0400, 0500 and 0600 GMT were referred to as +1, +2 and +3 hours, respectively.

The MCS characteristic, "maximum hourly point precipitation," will be used as an example to demonstrate the method employed to accomplish the composite analyses. Assume the MCSs of Cases 2, 3, 4, 7, 8, 10 and 11 (category 1 MCSs) had maximum point precipitation rates of 1.10, 1.00, 0.90, 0.50, 0.50, 1.50 and 1.50 in h^{-1}, respectively, at hour +1 (1 h after maximum extent). The composite analysis, for this hour, would be the average of the precipitation rates (1.00 in h^{-1}). This procedure was applied for several hours before and after the maximum extent.

Results of the Composite Analyses

Composite analyses of the five characteristics were accomplished for the MCSs of category 1. The results of the composite analyses are displayed in the following five figures (thin solid lines). Similarly, composite analyses of the five characteristics were accomplished for the MCSs of category 2. These results are also shown in the following five figures (thick solid lines).

Fig. 46 graphically displays the results of the composite analysis for the maximum hourly thunderstorm heights. In the hours before the maximum extent time, category 1 MCSs, on average, had higher maximum thunderstorm heights, compared to the MCSs of category 2. This was especially true from -2 to -6 h (2 to 6 h before the time of maximum extent). This is the critical time period for the formation of the gust front, as the gust front and mesohigh usually form within the few hours before the maximum extent time of the MCS (see Table 14, page 88). In the hours after maximum extent, the differences in the maximum

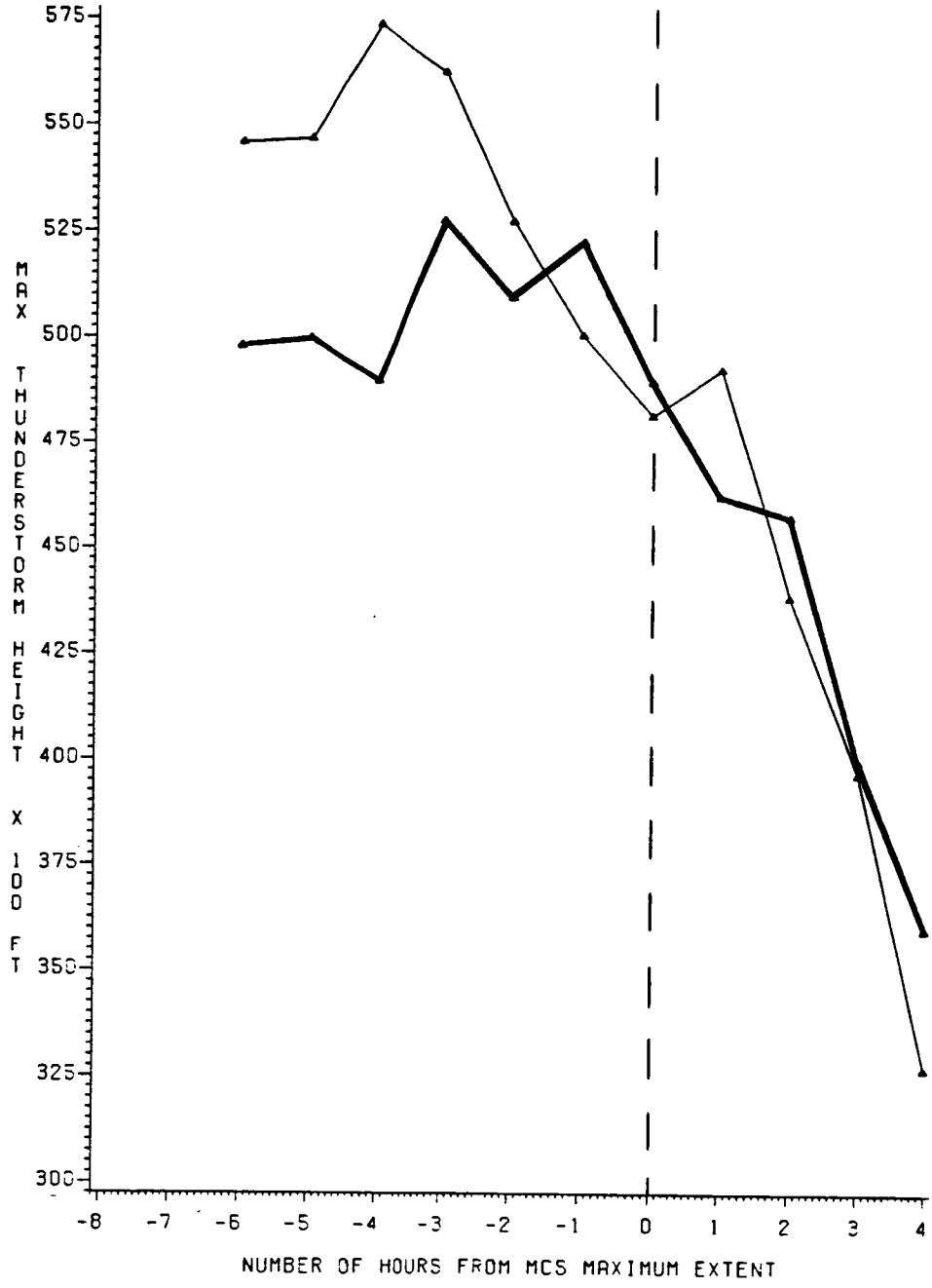

Fig. 46. Composite of the maximum hourly thunderstorm tops of category 1 (thin line) MCSs and category 2 (thick line) MCSs. Minus (-) hours are before MCS maximum extent and plus (+) hours are after MCS maximum extent.

thunderstorm heights of category 1 and 2 MCSs became negligible.

Fig. 47 depicts the results of the composite analysis of the maximum hourly surface divergence. The most striking result from the analysis occurred from hours +2 to +5. For category 2 MCSs, the divergence decreased from 2.25×10^{-5} s^{-1} at hour +2 to 1.00×10^{-5} s^{-1} at hour +5. The opposite occurred for category 1 MCSs. The divergence increased from 2.43×10^{-5} s^{-1} at hour +2 to 3.40×10^{-5} s^{-1} at hour +5. The increasing magnitude of the maximum surface divergence associated with category 1 MCSs, from hours +2 to +5, may be misleading. A possible explanation of the increase, which occurred after MCS maximum extent, is as follows. During this period, the gust front for category 1 MCSs was still well-defined and continued to propagate away from its initial formative location, thus affecting an increasing number of weather stations. Therefore, at hour +5, the surface divergence associated with the gust front/mesohigh was calculated from a greater number of reliable winds, compared to the calculation at hour +2. This could have led to an apparent increase in the magnitude of the surface divergence, as calculated by the McIDAS. Divergence values as large as 10^{-4} s^{-1} have been measured in a mesonetwork of instruments (Ulanski and Garstang, 1978). The most significant result of the composite analysis is that at hour +5, the magnitude of the maximum surface divergence associated with category 1 MCSs was much larger than the magnitude of the maximum surface divergence associated with category 2 MCSs.

Fig. 48 depicts the composite analysis of the sum of the three largest precipitation rates. There was a distinct difference between the precipitation rates of the two categories. With the exception of

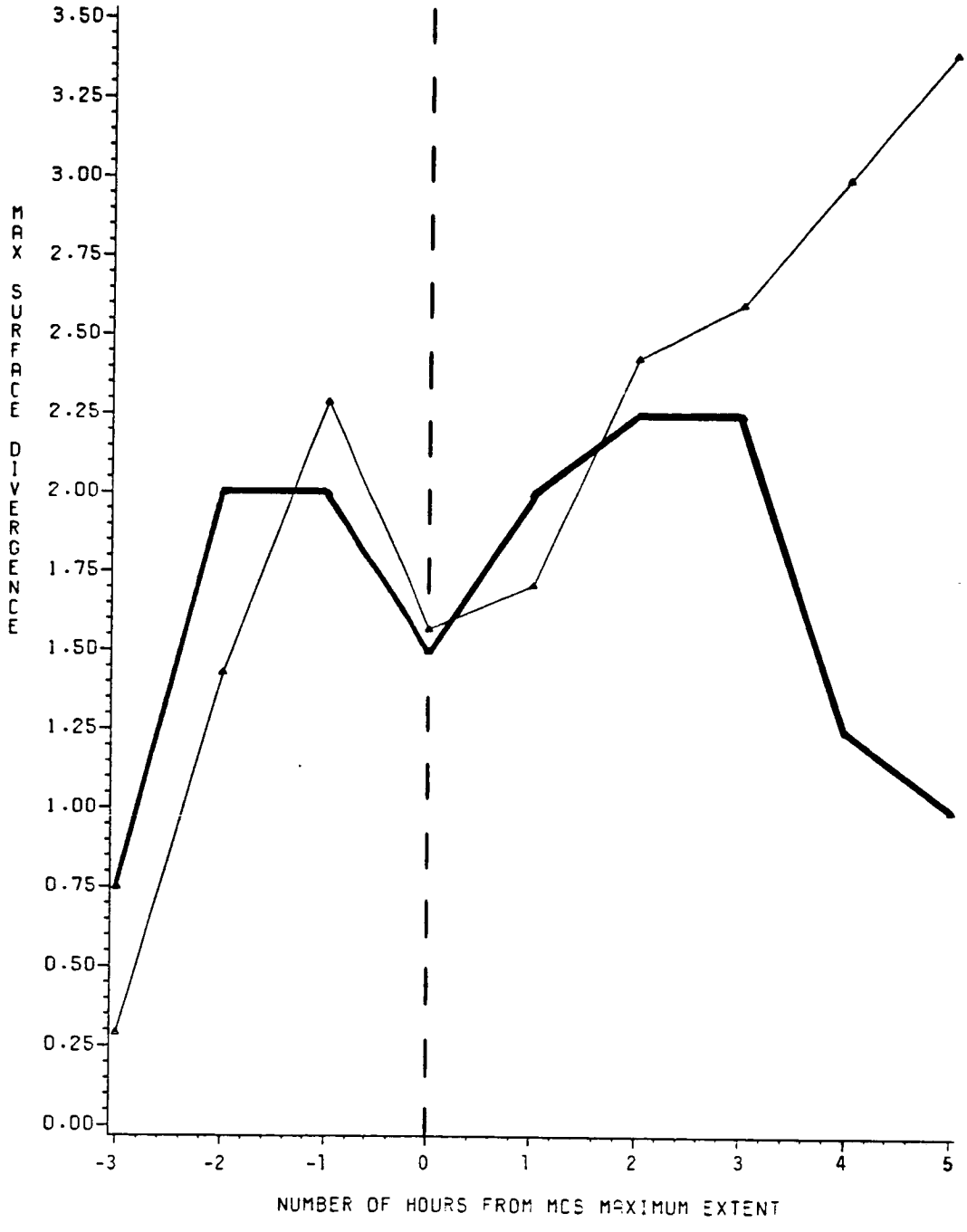

Fig. 47. Composite of the maximum hourly surface divergence of category 1 (thin line) MCSs and category 2 (thick line) MCSs. Minus (-) hours are before MCS maximum extent and plus (+) hours are after MCS maximum extent. Divergence values have units of 10^{-5} s^{-1}.

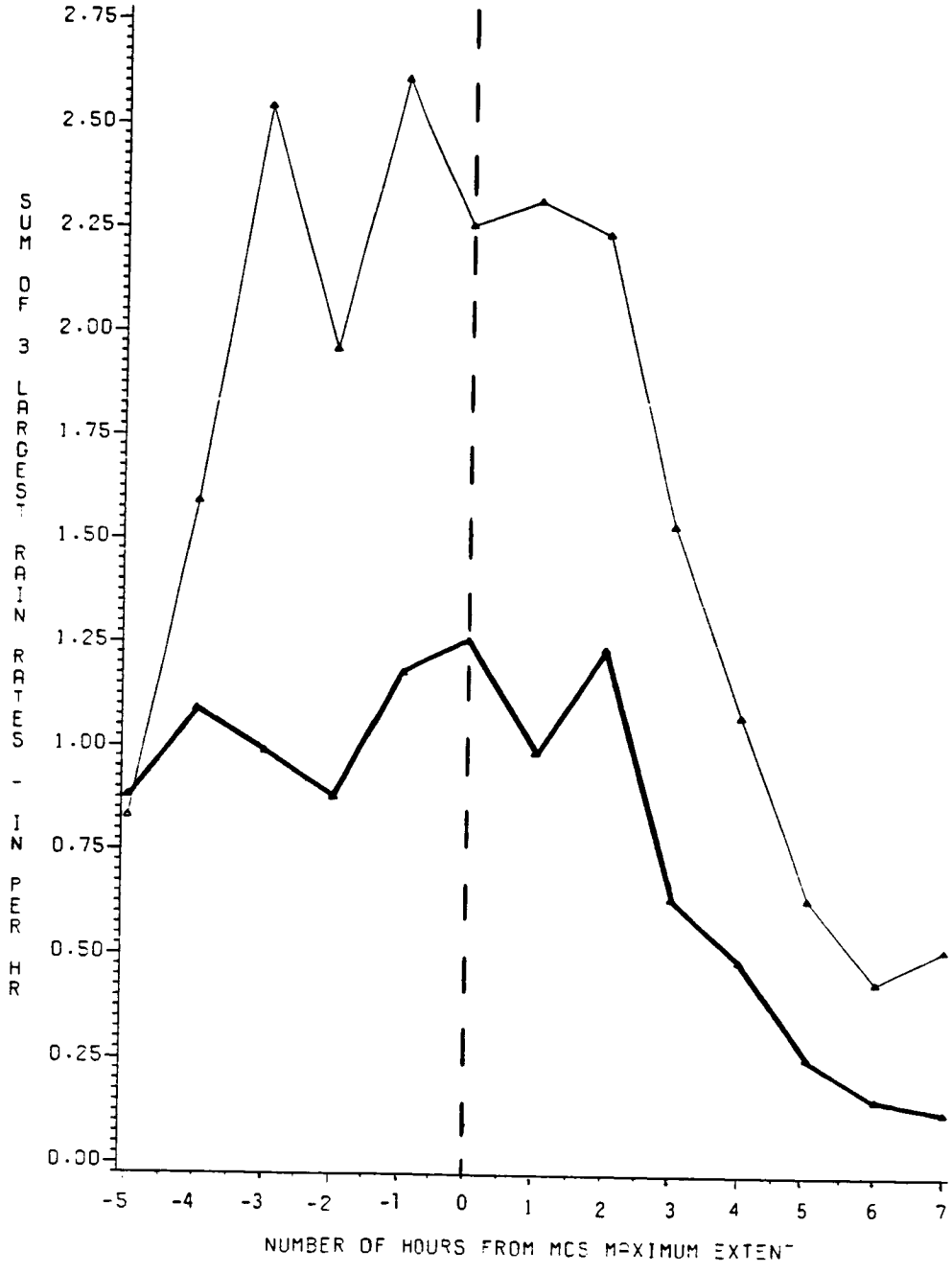

Fig. 48. Composite of the sum of the three largest precipitation rates of category 1 (thin line) MCSs and category 2 (thick line) MCSs. Minus (-) hours are before MCS maximum extent and plus (+) hours are after MCS maximum extent.

hour -5, the sum of the three largest precipitation rates was significantly higher for category 1 MCSs. In fact, in the 8 h of heaviest precipitation, from -4 to +3, the average sum of the three largest precipitation rates of category 1 MCSs was more than double that of category 2 MCSs (2.13 in h^{-1} to 1.03 in h^{-1}). This would imply that category 1 MCSs produced significantly higher rainfall rates, over an area, than the MCSs of category 2.

The intense precipitation associated with category 1 MCSs persisted for a longer period, compared to the heaviest precipitation associated with the MCSs of category 2. The sum of the three largest precipitation rates, produced by the MCSs of Cases 2, 3, 4, 7, 8, 10 and 11 (category 1 MCSs), stayed above 1.5 in h^{-1} for 8, 6, 11, 6, 7, 5 and 5 h, respectively. However, the sum of the three largest precipitation rates, produced by the MCSs of Cases 1, 5, 6 and 9 (category 2 MCSs), stayed above 1.5 in h^{-1} for 1, 1, 3 and 3 h, respectively. Thus, the sum of the three largest precipitation rates stayed above 1.5 in h^{-1} for an average of almost 7 h for category 1 MCSs and only 2 h for category 2 MCSs. Therefore, category 1 MCSs produced more intense precipitation rates over an area, for a longer period, compared to category 2 MCSs.

Fig. 49 shows the results of the composite analysis for the maximum hourly point precipitation rates. This analysis verifies that category 1 MCSs produced, on average, more intense rainfall rates than category 2 MCSs. As seen in Fig. 49, the higher precipitation rates of category 1 MCSs were maintained throughout the entire time period of the composite analysis. In the 8 h of heaviest precipitation, from -4 to +3, the average maximum point precipitation rate of category 1 MCSs was almost

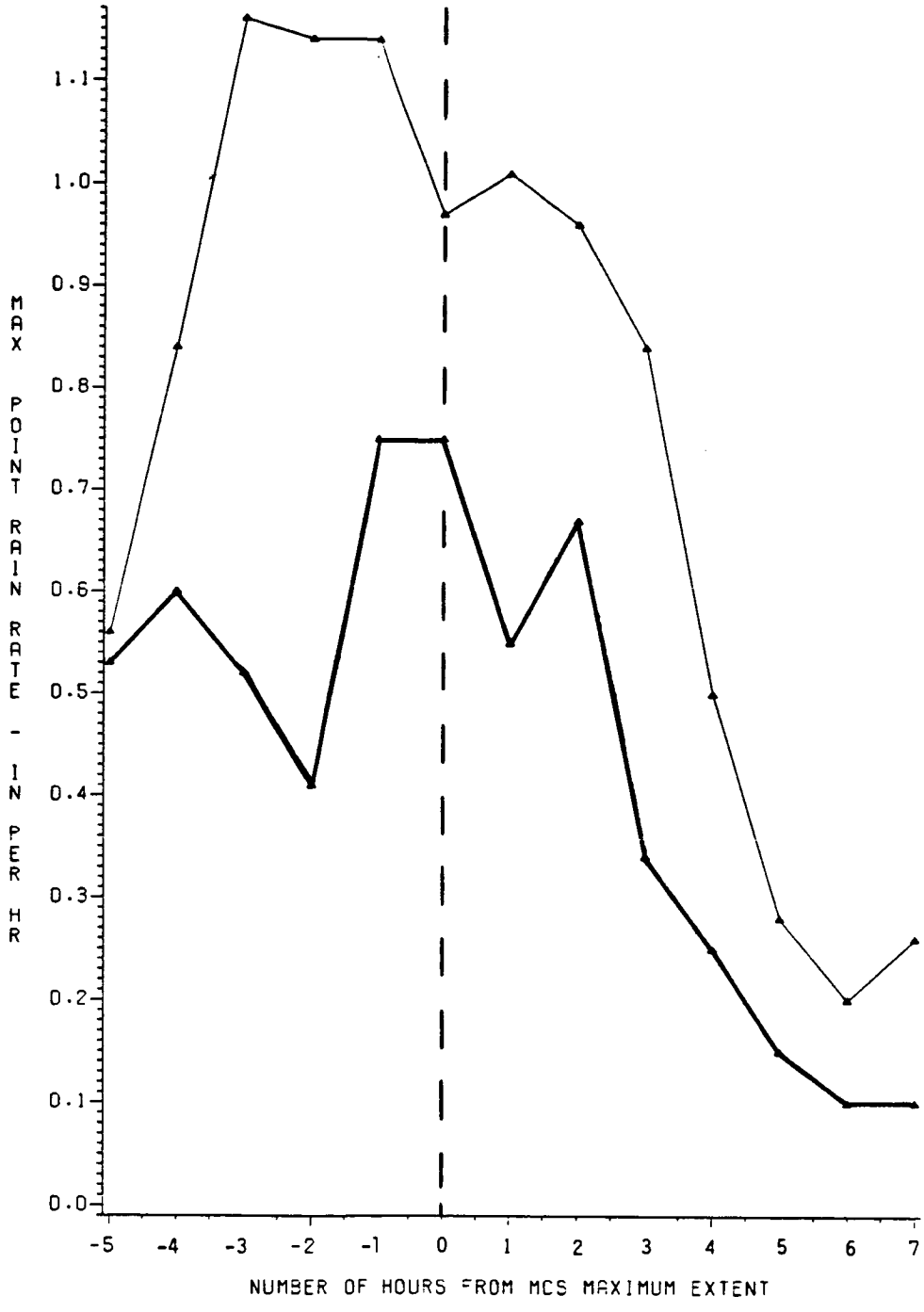

Fig. 49. Composite of the maximum hourly point precipitation rates of category 1 (thin line) MCSs and category 2 (thick line) MCSs. Minus (-) hours are before MCS maximum extent and plus (+) hours are after MCS maximum extent.

double that of category 2 MCSs (1.01 in h^{-1} to 0.57 in h^{-1}).

Fig. 50 represents the results of the composite analysis for the coldest hourly cloud top temperatures. Category 1 MCSs, on average, had colder cloud top temperatures, compared to the MCSs of category 2.

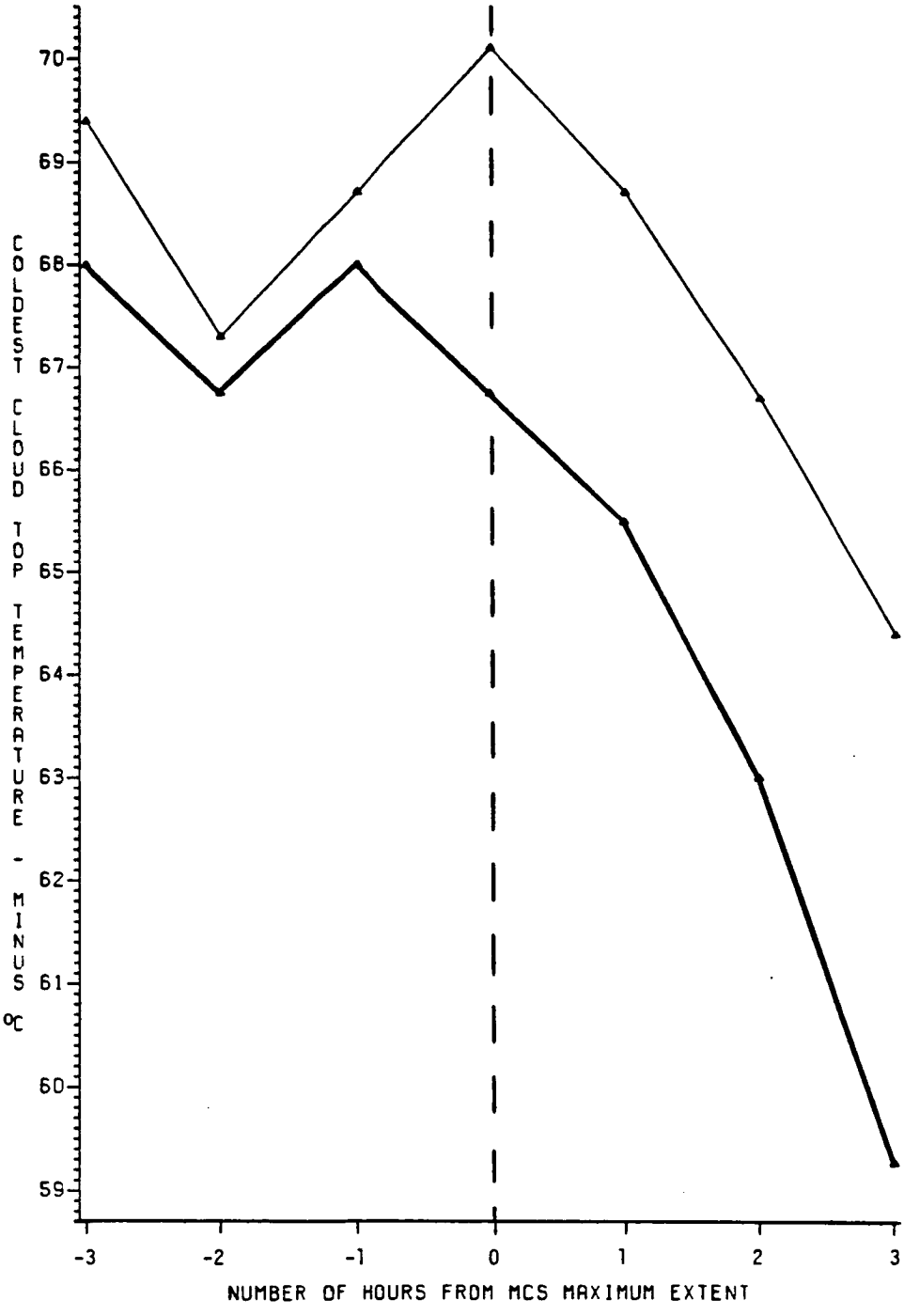

Fig. 50. Composite of the coldest hourly cloud top temperatures for category 1 (thin line) MCSs and category 2 (thick line) MCSs. Minus (-) hours are before MCS maximum extent and plus (+) hours are after MCS maximum extent.

CHAPTER V

SUMMARY

Category 1 and 2 MCSs have significant differences in their characteristics. This contention is supported by the results of the composite analyses. It appears these differences aid in producing stronger, longer-lasting gust fronts in category 1 MCSs. In turn, since all category 1 MCSs produced arc clouds and only one category 2 MCS produced an arc cloud (see Table 14, page 88), the strength and duration of the gust front seems to be an important factor in whether an arc cloud forms.

A summary of the differences in the category 1 and 2 MCSs follows:

1. Category 1 MCSs, on average, produce more intense precipitation rates than category 2 MCSs. In the hours of heaviest precipitation, the average sum of the three largest precipitation rates of category 1 MCSs is more than double that of category 2 MCSs. For this study, this average sum for category 1 and 2 MCSs was 2.13 in h^{-1} to 1.03 in h^{-1}, respectively. During this same period, the average maximum point precipitation rate of category 1 MCSs is nearly double that of category 2 MCSs. For this study, the average maximum point precipitation rate for category 1 and 2 MCSs was 1.01 in h^{-1} to 0.57 in h^{-1}, respectively. Also, the intense precipitation associated with category 1 MCSs persists for a longer period, compared to the heaviest precipitation associated with the MCSs of category 2. For instance, the sum of the three largest precipitation rates stayed above 1.5 in h^{-1} for an average of almost 7 h for category 1 MCSs and only 2 h for category 2 MCSs.

2. The maximum hourly surface divergence, on average, associated

with category 1 MCSs, is stronger than the divergence associated with category 2 MCSs, for the hours +2 to +5.

3. In the hours from -2 to -6, the critical hours for gust front formation, category 1 MCSs, on average, have higher maximum thunderstorm heights than category 2 MCSs, as determined at 35 min past each hour. During this period, the average maximum thunderstorm heights for category 1 and 2 MCSs are 55,000 and 51,000 ft, respectively.

4. The coldest hourly cloud top temperatures of category 1 MCSs, on average, are colder than those in category 2.

The gust front, on average, formed approximately 1.5 h prior to the MCS maximum extent, as determined from Table 14. Using this information, coupled with the results shown in Fig. 46-50, for category 1 MCSs, the following becomes apparent:

1. The gust front, on average, forms approximately 2 h after the maximum thunderstorm heights are reached (see Fig. 46).

2. The time of formation of the gust front corresponds to the period of maximum precipitation intensity (see Figs. 48-49).

3. The formation of the gust front takes place during a period of increasing magnitude of the surface divergence (see Fig. 47). The increasing surface divergence corresponds to the period of maximum precipitation intensity (see Figs. 48-49). This correlation (see Fig. 1) agrees with the findings of Byers and Braham (1949).

4. The formation of the gust front corresponds to a decrease in the coldest cloud top temperatures (see Fig. 50).

The arc cloud, on average, formed approximately 4 h after MCS maximum extent, as determined from Table 14. As mentioned earlier, the

appearance of the arc cloud was determined, in most cases, by inspection of the visible satellite images. Undoubtedly, some of the arc clouds formed during the period when only IR satellite images were available. During this period the arc cloud would be undetectable, in most cases, because arc clouds normally consist of low, warm clouds. Taking this into account, the arc cloud, on average, probably formed approximately 3 h after MCS maximum extent. Using this information, coupled with the results shown in Figs. 46-50, for category 1 MCSs, the following becomes apparent:

1. The arc cloud forms during a period of rapidly falling thunderstorm heights (see Fig. 46).

2. The arc cloud forms as the precipitation intensity dramatically lowers (see Figs. 48-49).

3. The arc cloud forms during a period when the magnitude of the maximum surface divergence remains large (see Fig. 47).

4. The arc cloud forms during a period of rapid warming of the cloud top temperatures (see Fig. 50).

Using the radar summary charts from the NWS, a composite analysis of the maximum hourly radar reflectivity intensity for category 1 and 2 MCSs was accomplished. The determination of intensity was done by an intensity processor known as the Digital Video Integrator and Processor (D/VIP). Contours on the radar summary charts correspond to the 1, 3 and 5 D/VIP levels. D/VIP level 1 corresponds to "light" precipitation, D/VIP level 3 corresponds to "heavy" precipitation and D/VIP level 5 corresponds to "intense" precipitation (U.S. Department of Commerce, 1980). This analysis was done because the results could be used by

operational meteorologists, since this information is readily available.

Fig. 51 depicts the results of the composite analysis of the maximum hourly radar reflectivity intensity. From hours -5 to -2, both category 1 and 2 MCSs produced D/VIP level 5 radar reflectivities. However, from hours -2 to +1, the maximum reflectivities produced by category 2 MCSs dropped below D/VIP level 4, on average, while category 1 MCSs maintained D/VIP level 5.

Using the above information, the following criteria are given as guidance, to the operational meteorologist, in forecasting the occurrence of gust fronts and arc clouds:

1. The gust front, on average, forms approximately 1.5 h before maximum extent of the MCS.

2. If the gust front persists for more than 6 h, it is likely an arc cloud will form. The arc cloud, on average, forms approximately 3 h after maximum extent of the MCS.

3. The arc cloud forms while the thunderstorm heights are rapidly falling.

4. The arc cloud forms while the coldest cloud top temperatures are rapidly warming.

5. Lastly, it seems likely that an arc cloud will form if the maximum D/VIP level remains at level 5 through hour +1 (1 h after MCS maximum extent). Caution should be used when using this criterion alone, as the MCS of Case 1, which did not produce an arc cloud, produced D/VIP level 5 reflectivities through hour +3. However, using this criterion with the other guidelines, should prove more useful. For example, even though the MCS of Case 1 produced D/VIP level 5

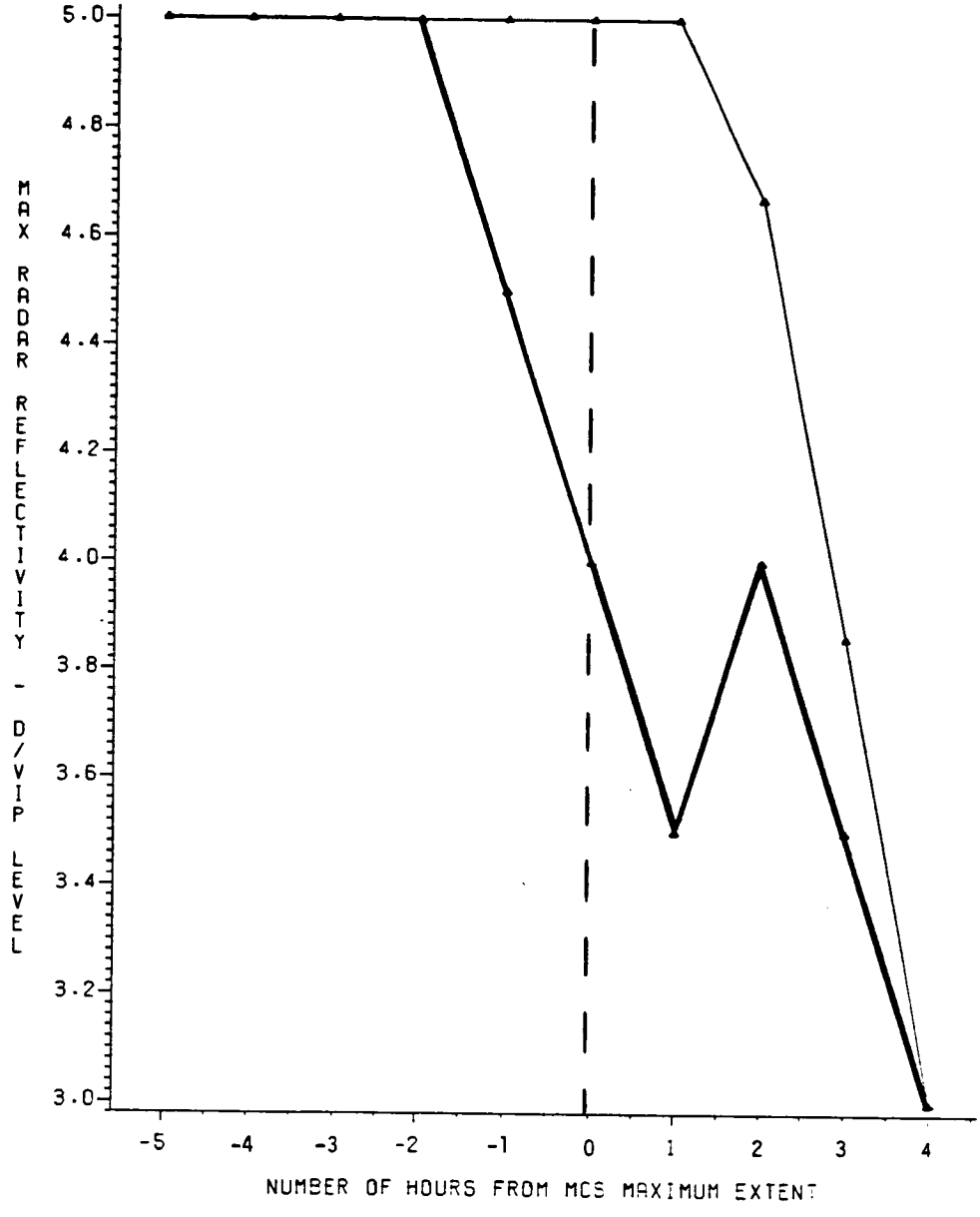

Fig. 51. Composite of the maximum hourly radar reflectivity intensity of category 1 (thin line) MCSs and category 2 (thick line) MCSs. Minus (-) hours are before MCS maximum extent and plus (+) hours are after MCS maximum extent.

reflectivities through hour +3, the gust front only lasted for 5 h, therefore, it is unlikely an arc cloud will form.

REFERENCES

Barnes, S. L., 1973: Mesoscale objective map analysis using weighted time-series observations. NOAA Tech. Memo. ERL NSSL-62, NTIS COM-73-10781, 60 pp.

Bartels, D. L., 1983: Internal structure and evolution of a dual mesoscale convective complex. Preprints, 5th Conf. on Hydrometeorology, Tulsa, OK, Amer. Meteor. Soc., 97-102.

Belville, J. D., and N. O. Stewart, 1983: Extreme rainfall events in Louisiana: The "New Orleans Type." Preprints, 5th Conf. on Hydrometeorology, Tulsa, OK, Amer. Meteor. Soc., 284-290.

Brundidge, K. C., 1983: Investigation of the arc cloud complex. Research Reports - 1983 NASA/ASEE Summer Faculty Fellowship Program, George C. Marshall Space Flight Center, Huntsville, AL, 23 pp.

_____, 1984: Precipitation factors leading to arc cloud formation. NASA Proposal, Texas A&M University, College Station, TX, 14 pp.

Byers, H. R., and R. R. Braham, Jr., 1948: Thunderstorm structure and circulation. J. Meteor., 5, 71-86.

_____, and _____, 1949: The Thunderstorm. U.S. Dept. of Commerce, Weather Bureau, Washington, D. C., 282 pp.

Fritsch, J. M., R. A. Maddox and A. B. Barnston, 1981: The character of mesoscale convective complex precipitation and its contribution to warm season rainfall in the U.S. Preprints, 4th Conf. on Hydrometeorology, Reno, NV, Amer. Meteor. Soc., 94-99.

Fujita, T., 1955: Result of detailed synoptic studies of squall lines. Tellus, 7, 405-436.

_____, 1959: Precipitation and cold air production in mesoscale thunderstorm systems. J. Meteor., 16, 454-466.

_____, 1963: Analytical mesometeorology: A review. Meteor. Monogr., 5, 77-122.

Gagin, A., D. Rosenfeld and R. E. Lopez, 1985: The relationship between height and precipitation characteristics of summertime convection cells in south Florida. J. Atmos. Sci., 42, 84-94.

Goff, R. C., 1976: Vertical structure of thunderstorm outflows. Mon. Wea. Rev., 104, 1429-1440.

Greene, G. E., 1977: Wind shear characterization. U.S. Fed. Aviation Admin., Washington, D.C., Report No. FAA-RD-77-33, 120 pp.

Howard, K., and R. A. Maddox, 1983: Precipitation characteristics of two mesoscale convective systems. Preprints, 5th Conf. on Hydrometeorology, Tulsa, OK, Amer. Meteor. Soc.

Leary, C. A., and E. N. Rappaport, 1982: Internal structure of a mesoscale convective complex. Preprints, 21st Conf. Radar Meteor., Edmonton, Alberta, Canada, Amer. Meteor. Soc., 70-77.

Maddox, R. A., 1980: Mesoscale convective complexes. Bull. Amer. Soc., 61, 1374-1387.

_____, 1981: The structure and lifecycle of midlatitude mesoscale convective complexes. Ph.D. dissertaion, Colorado State University, 171 pp.

_____, 1982: Forecasting mesoscale convective complexes over the central United States. Preprints, 12th Conf. Severe Local Storms, San Antonio, TX, Amer. Meteor. Soc., 180-183.

_____, 1983: Large-scale meteorological conditions associated with midlatitude, mesoscale convective complexes. Mon. Wea. Rev., 111, 1475-1493.

_____, D. M. Rodgers and K. W. Howard, 1982: Mesoscale convective complexes over the United States during 1981. Mon. Wea. Rev., 110, 1501-1514.

Miller, R. C., 1972: Notes on Analysis and Severe-Storm Forecasting Procedures of the Air Force Global Weather Service, Tech. Rep. 200 (Rev.), Air Weather Service, Scott Air Force Base, IL, 190 pp.

Miller, R. L., 1984: The arc cloud complex: A case study. Masters Thesis, Texas A&M Univ., College Station, TX, 101 pp.

Orlanski, I., 1975: A rational subdivision of scales of atmospheric processes. Bull. Amer. Meteor. Soc., 56, 527-530.

Purdom, J. F. W., 1973: Picture of the month: Mesohigh and satellite imagery. Mon. Wea. Rev., 101, 180-181.

_____, 1974: Satellite imagery applied to the mesoscale surface analysis and forecast. Preprints, 5th Conf. Weather Forecasting and Analysis, St. Louis, MO, Amer. Meteor. Soc., 63-68.

_____, 1976: Some uses of high-resolution GOES imagery in the mesoscale forecasting of convection and its behavior. Mon. Wea. Rev., 104, 1474-1483.

Purdom, J. F. W., 1979: The development and evolution of deep convection. Preprints, 11th Conf. Severe Local Storms, Kansas City, MO, Amer. Meteor. Soc., 143-150.

Rodgers, D. M., K. W. Howard and E. C. Johnston, 1983: Mesoscale convective complexes over the United States during 1982. Mon. Wea. Rev., 111, 2363-2369.

_____, M. J. Magnano and J. H. Arns, 1985: Mesoscale convective complexes over the United States during 1983.. Mon. Wea. Rev., 113, 888-901.

Schnapf, A., 1982: The development of the TIROS global environmental satellite system. NASA Conf. Pub. 2227, Meteorological Satellites-Past, Present, and Future, 20th Aerospace Sciences Meeting, AIAA, Orlando, FL, Jan., 1982, 7-16.

Sinclair, P. C., and J. F. W. Purdom, 1982: Integration of research aircraft data and 3 minute interval GOES data to study the genesis and development of deep convective storms. Preprints, 12th Conf. Severe Local Storms, San Antonio, TX, Amer. Meteor. Soc., 269-271.

_____, and _____, 1984: Aircraft penetrations of arc cloud lines. Preprints, Satellite Meteorology/Remote Sensing and Applications, Clearwater Beach, FL, Amer. Meteor. Soc., 160-163.

Tepper, M., 1950a: A proposed mechanism of squall lines: The pressure jump line. J. Meteor., 7, 21-29.

_____, 1950b: On the origins of tornadoes. Bull. Amer. Meteor. Soc., 31, 311-314.

Ulanski, S. L., and M. Garstang, 1978: The role of surface divergence and vorticity in the life cycle of convective rainfall. Part I: Observation and analysis. J. Atmos. Sci., 35, 1047-1062.

U. S. Department of Commerce, 1980: National Weather Service Radar Code User's Guide, NOAA, National Weather Service publication, Silver Spring, Maryland, 179 pp.

Wetzel, P. J., W. R. Cotton and R. L. McAnelly, 1983: A long-lived mesoscale convective complex. Part I: The mountain generated component. Mon. Wea. Rev., 111, 1893-1918.

Woodley, W. L., B. Sancho and A. H. Miller, 1972: Rainfall Estimation from Satellite Cloud Photographs. NOAA Tech. Memo. ERL OD-11, 43 pp.

Zipser, E. J., 1969: The role of organized unsaturated convective downdrafts in the structure and rapid decay of an equitorial disturbance. J. Appl. Meteor., 8, 799-814.